Supporting Information

$ZnCl_2$ catalysed transfer hydrogenation of carbonyls and chemoselective reduction of C=C bond in α,β-unsaturated ketones

Sonu Sheokand, Sunita Sharma, Manali A. Mohite, Gopalan Rajaraman* and Maravanji S. Balakrishna*

Phosphorus Laboratory, Department of Chemistry, Indian Institute of Technology Bombay, Powai, Mumbai 400076, India.

Table of Contents

---

*Author to whom correspondence should be addressed. E-mail: krishna@chem.iitb.ac.in, msb_krishna@iitb.ac.in (M. S. Balakrishna); Fax: +91-22-5172-3480/2576-7152 and *Email:* rajaraman@chem.iitb.ac.in (G. Rajaraman)

Experimental details

General Procedures. All reactions were performed under a nitrogen atmosphere. All the solvents used in this study were dried by conventional methods, and distilled prior to use. $[(C_5H_4N)(C_2HN_3C_6H_5)]$[1] (**L3**), $[2,6\text{-}\{H_2N(C_5H_3N)(C_2HN_3C_6H_5)\}]$[2] (**L4**) and $[2,6\text{-}\{(PPh_2)\text{-}N(H)(C_5H_3N)(C_2HN_3C_6H_5)\}]$[2] (**L5**) were prepared according to the published procedures. Other regents and metal salts were purchased from Aldrich chemicals, and other local chemical suppliers and purified prior to use.

Instrumental methods

The solution NMR spectra were recorded on Bruker FT spectrometers (Avance-400 or -500) MHz at ambient probe temperatures (298 K). $^{13}C\{^1H\}$ and $^{31}P\{^1H\}$ NMR spectra were acquired using a broad-band decoupling method. The spectra were recorded in $CDCl_3$ and DMSO-d_6 solutions. Chemical shifts of ^1H and $^{13}C\{^1H\}$ NMR spectra are reported in ppm downfield from TMS. The chemical shifts of $^{31}P\{^1H\}$ NMR spectra are referred to 85% H_3PO_4 as an external standard. Positive values indicate downfield shifts. Mass spectra were recorded using a Bruker Maxis Impact LC-q-TOF Mass Spectrometer. GC-MS analyses were carried out using an Agilent 7890A GC system with an FID detector using a J & amp; WDB-1 column (10 m, 0.1 mm ID). Catalytical reactions were monitored by thin-layer chromatography (TLC) using Merck Silica Gel 60 F_{254} plates.

Crystal structure determination of compound Cf

Single crystals of all complexes were mounted on a Cryoloop with a drop of paratone oil and positioned in the cold nitrogen stream on a Bruker D8 Venture diffractometer. The data collections were performed at 100 K to 150 K using Bruker D8 Venture diffractometer with a graphite monochromated Mo Kα radiation source (λ = 0.71073 Å) with the ω-scan technique. The data were reduced using CrysalisPro Red 171.41_64.93a software.[3] The structures were solved using Olex2 1.5[4] with the ShelXT[5] structure solution program using intrinsic phasing and refined with SHELXL[5] refinement package using least-squares minimization. All non-hydrogen atoms were refined anisotropically. Hydrogen atoms were placed in calculated positions and included as riding contributions with isotropic displacement parameters tied to those of the attached non-hydrogen atoms. The given chemical formula and other crystal data do not take count the unknown solvent molecule(s). The reflections with error/esd more than 10 were excluded in order to avoid problems related to better refinement of the data. The data completeness is more than 99.8% in most of the cases, which is enough to guarantee a very

good refinement of data. Crystallographic data for the structures reported in this paper have been deposited with the Cambridge Crystallographic Data Centre as supplementary publication no. CCDC: 2330701.

General procedure for the catalytic transfer hydrogenation of carbonyl compounds: KOH (1 equiv.), ^{i}PrOH (1 mL), acetophenone derivative, $ZnCl_2$ (0.5 mol%) and **L5** (0.5 mol%) were added to a reaction tube, degassed and purged with nitrogen gas and heated to the desired temperature with stirring. After 5 h, the reaction mixture was allowed to cool to room temperature, diluted with EtOAc (10 mL), and washed with saturated brine solution. The organic layer was dried over Na_2SO_4 and the solvent was removed under reduced pressure. The product was purified by column chromatography using a mixture of petroleum ether and ethyl acetate as an eluent.

Table S1. Optimized reaction condition for transfer hydrogenation of acetophenone[a]

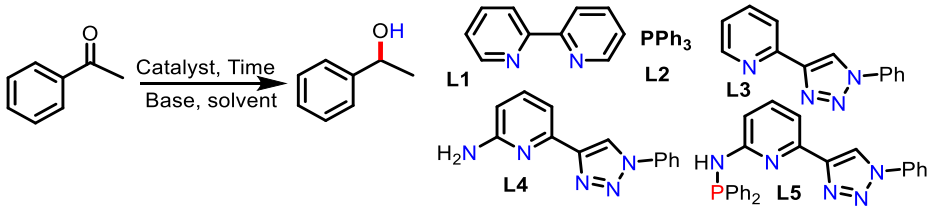

Entry	Catalyst (mol %)	Ligand (mol %)	Solvent	Time	Yield[b] (%)
1	$ZnCl_2$	L1(0.5)	^{i}PrOH	3 h	49
2	$ZnCl_2$	L2(0.5)	^{i}PrOH	3 h	nrc
3	$ZnCl_2$	L3(0.5)	^{i}PrOH	3 h	39
4	$ZnCl_2$	L4(0.5)	^{i}PrOH	3 h	58
5	$ZnCl_2$	L5(0.5)	^{i}PrOH	3 h	85
6	**$ZnCl_2$**	**L5(0.5)**	**^{i}PrOH**	**5 h**	**100**
7	$ZnCl_2$	L5(0.5)	EtOH	5 h	nr
8	$ZnCl_2$	L5(0.5)	MeOH	5 h	nr
9[c]	No catalyst	L5(0.5)	^{i}PrOH	5 h	nr
10	$ZnCl_2$	No ligand	^{i}PrOH	5 h	nr
11[d]	$ZnCl_2$	L5(0.5)	^{i}PrOH	5 h	nr
12[e]	$ZnCl_2$	L5(0.5)	^{i}PrOH	5 h	96
13[f]	$ZnCl_2$	L5(0.5)	^{i}PrOH	5 h	94

[a]acetophenone (1 mmol), isopropanol (1 mL). The reaction was carried out at 80 °C, Catalyst (0.5 mol%), Ligand (L) (0.5 mol%), KOH (1 equiv); [b]Yields were determined by NMR spectroscopy with 1,3,5-Trimethoxybenzene as the internal standard. 0.5 mol% catalyst used, [c]nr: no reaction. [d]no KOH, [e]in presence of Hg (5 equiv), [f]in presence of TEMPO (5 equiv).

1. NMR spectral data of catalytic products

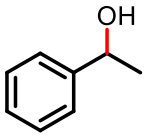

*1-phenylethan-1-ol (**Aa**)*. Purified by column chromatography on silica gel using petroleum ether and ethyl acetate as eluenets, 98% (117 mg) yield as colourless liquid. ^{1}H NMR (400 MHz, $CDCl_3$) δ 7.41 – 7.34 (m, 4H), 7.33 – 7.27 (m, 1H), 4.87 (q, *J* = 6.4 Hz, 1H), 2.62 (s, 1H), 1.51 (d, *J* = 6.6 Hz, 3H). ^{13}C{^{1}H} NMR (101 MHz, $CDCl_3$) δ 145.92, 128.49, 127.43, 125.46, 70.30, 25.17.

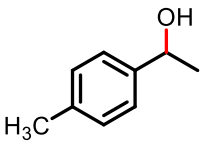

1-(p-tolyl)ethan-1-ol (***Ab***). Purified by column chromatography on silica gel using petroleum ether and ethyl acetate as eluents, 96% (131 mg) yield as colourless liquid. ^{1}H NMR (400 MHz, $CDCl_3$) δ 7.36 (d, J = 8.3 Hz, 2H), 7.25 (d, J = 7.9 Hz, 2H), 4.96 (q, J = 6.5 Hz, 1H), 2.43 (s, 3H), 1.57 (d, J = 6.4 Hz, 3H). ^{13}C{^{1}H} NMR (101 MHz, $CDCl_3$) δ 143.02, 137.32, 129.32, 125.49, 70.42, 25.23, 21.24.

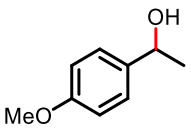

*1-(4-methoxyphenyl)ethan-1-ol (**Ac**).* Purified by column chromatography on silica gel using petroleum ether and ethyl acetate as eluents, 94% (143 mg) yield as colourless liquid. ^{1}H NMR (400 MHz, $CDCl_3$) δ 7.26 (d, *J* = 7.3 Hz, 2H), 6.85 (d, *J* = 8.4 Hz, 2H), 4.79 (q, *J* = 6.6 Hz, 1H), 3.77 (s, 3H), 2.70 (s, 1H), 1.43 (d, *J* = 6.4 Hz, 3H).^{13}C{^{1}H} NMR (101 MHz, $CDCl_3$) δ 158.86, 138.15, 126.70, 113.79, 69.78, 55.26, 25.04.

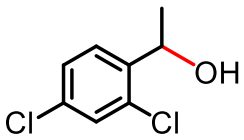

(2,4-dichlorophenyl)methanol (**Ad**). Purified by column chromatography on silica gel using petroleum ether and ethyl acetate as eluents, 88% (168 mg) yield as white solid. ^{1}H NMR (400 MHz, $CDCl_3$) δ 7.45 (dd, J = 8.4, 4.5 Hz, 1H), 7.27 (m, 1H), 7.21-7.18 (m, 1H), 5.19 – 5.12 (m, 1H), 1.39 – 1.37 (m, 3H). ^{13}C{^{1}H} NMR (101 MHz, $CDCl_3$) δ 141.82, 133.45, 132.23, 129.18, 127.60, 127.54, 66.66, 23.69.

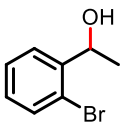

*1-(2-bromophenyl)ethan-1-ol (**Ae**).* Purified by column chromatography on silica gel using petroleum ether and ethyl acetate as eluents, 90% (181 mg) yield as white solid. ^{1}H NMR (400 MHz, $CDCl_3$) δ 7.50 (s, 1H), 7.37 (d, J = 7.8 Hz, 1H), 7.25 (d, J = 7.7 Hz, 1H), 7.18 (t, J = 7.8 Hz, 1H), 4.82 (q, J = 6.4 Hz, 1H), 1.44 (d, J = 6.4 Hz, 3H). ^{13}C{^{1}H} NMR (101 MHz, $CDCl_3$) δ 148.23, 130.56, 130.20, 128.68, 124.13, 122.70, 69.83, 25.34

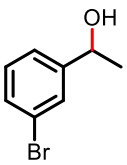

1-(3-bromophenyl)ethan-1-ol (***Af***). Purified by column chromatography on silica gel using petroleum ether and ethyl acetate as eluents, 88% (177 mg) yield as yellowish liquid. ^{1}H NMR (400 MHz, $CDCl_3$) δ 7.54 (d, *J* = 1.9 Hz, 1H), 7.40 (d, *J* = 7.9 Hz, 1H), 7.29 (d, *J* = 7.8 Hz, 1H), 7.21 (t, *J* = 7.8 Hz, 1H), 4.87 (m, 1H), 1.49 (d, *J* = 6.5 Hz, 3H). ^{13}C NMR (101 MHz, $CDCl_3$) δ 148.26, 130.63, 130.25, 128.72, 124.15, 122.77, 69.92, 25.42.

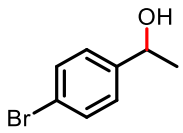

1-(4-bromophenyl)ethan-1-ol (***Ag***). Purified by column chromatography on silica gel using petroleum ether and ethyl acetate as eluents, 79% (159 mg) yield as yellowish liquid ^{1}H NMR (400 MHz, $CDCl_3$) δ 7.48 (d, J = 8.4 Hz, 2H), 7.25 (d, J = 8.4 Hz, 2H), 4.86 (q, J = 6.4 Hz, 1H), 1.47 (d, J = 6.5 Hz, 3H). ^{13}C{^{1}H} NMR (101 MHz, $CDCl_3$) δ 144.88, 131.65, 127.27, 121.25, 69.86, 25.34.

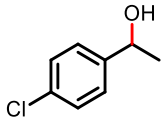

1-(4-cholrophenyl)ethan-1-ol (***Ah***). Purified by column chromatography on silica gel using petroleum ether and ethyl acetate as eluents, 85% (133 mg) yield as yellowish liquid. ^{1}H NMR (400 MHz, $CDCl_3$) δ 7.28 (s, 4H), 4.85 (q, J = 6.6 Hz, 1H), 1.45 (d, J = 2.3 Hz, 3H). ^{13}C{^{1}H} NMR (101 MHz, $CDCl_3$) δ 144.39, 133.20, 128.73, 126.92, 69.86, 25.38.

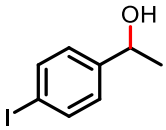

1-(4-iodophenyl)ethan-1-ol (***Ai***). Purified by column chromatography on silica gel using petroleum ether and ethyl acetate as eluents, 83% (206 mg) yield as yellow liquid. ^{1}H NMR (400 MHz, $CDCl_3$) δ 7.80 (d, *J* = 8.3 Hz, 2H), 7.25 (d, *J* = 8.3 Hz, 2H), 4.98 (q, *J* = 6.5 Hz, 1H), 1.59 (d, *J* = 6.5 Hz, 3H). ^{13}C{^{1}H} NMR (101 MHz, $CDCl_3$) δ 145.60, 137.68, 127.55, 92.85, 70.00, 25.38.

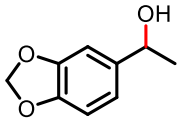

1-(benzo[d][1,3]dioxol-5-yl)ethan-1-ol (***Aj***). Purified by column chromatography on silica gel using petroleum ether and ethyl acetate as eluents, 84% (140 mg) yield as colourless liquid. ^{1}H NMR (500 MHz, $CDCl_3$) δ 6.89 (d, *J* = 1.7 Hz, 1H), 6.83 – 6.79 (m, 1H), 6.76 (d, *J* = 8.0 Hz, 1H), 5.94 (s, 2H), 4.81 (q, *J* = 6.4 Hz, 1H), 1.45 (d, *J* = 6.4 Hz, 3H). ^{13}C{^{1}H} NMR (126 MHz, $CDCl_3$) δ 147.77, 146.84, 140.00, 118.70, 108.09, 106.07, 100.98, 70.24, 25.16.

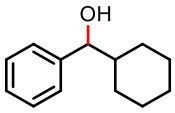

cyclohexyl(phenyl)methanol (***Ak***). Purified by column chromatography on silica gel using petroleum ether and ethyl acetate as eluents, 90% (171 mg) yield as colourless liquid. ^{1}H NMR (400 MHz, $CDCl_3$) δ 7.36 – 7.25 (m, 5H), 4.35 (d, J = 7.3 Hz, 1H), 2.01 – 1.96 (m, 2H), 1.80 – 1.77 (m, 1H), 1.71 – 1.57 (m, 3H), 1.38 (d, J = 11.3 Hz, 1H), 1.30 – 1.20 (m, 1H), 1.20 – 1.12 (m, 2H), 1.00 – 0.91 (m, 1H). ^{13}C{^{1}H} NMR (101 MHz, $CDCl_3$) δ 143.66, 128.19, 127.40, 126.67, 79.38, 44.96, 29.32, 28.86, 26.45, 26.12, 26.04.

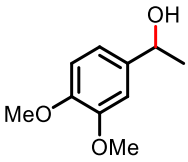

1-(3,4-dimethoxyphenyl)ethan-1-ol (***Al***). Purified by column chromatography on silica gel using petroleum ether and ethyl acetate as eluents, 94% (171 mg) yield as colourless liquid. ^{1}H NMR (400 MHz, $CDCl_3$) δ 6.92 (d, J = 2.1 Hz, 1H), 6.87 (dd, J = 7.9, 2.3 Hz, 1H), 6.81 (d, J = 8.2 Hz, 1H), 4.82 (q, J = 6.5 Hz, 1H), 3.87 (s, 3H), 3.85 (s, 3H), 1.46 (d, J = 6.4 Hz, 3H). ^{13}C{^{1}H} NMR (101 MHz, $CDCl_3$) δ 149.13, 148.42, 138.68, 117.61, 111.10, 108.77, 108.75, 70.26, 56.02, 55.92, 25.17.

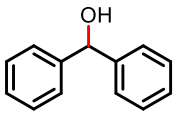

*Diphenylmethanol (**Am**).* Purified by column chromatography on silica gel using petroleum ether and ethyl acetate as eluents, 93% (171 mg) yield as white solid. ^{1}H NMR (400 MHz, $CDCl_3$) δ 7.41 (dd, *J* = 7.8, 2.1 Hz, 4H), 7.37 (t, *J* = 8.0 Hz, 4H), 7.30 (t, *J* = 7.1 Hz, 2H), 5.87 (br, 1H), 2.35 (s, 1H). ^{13}C{^{1}H} NMR (101 MHz, $CDCl_3$) δ 143.83, 128.53, 127.60, 126.57, 76.28.

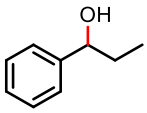

1-phenylpropan-1-ol (***An***). Purified by column chromatography on silica gel using petroleum ether and ethyl acetate as eluents, 90% (123 mg) yield as colourless liquid. ^{1}H NMR (500 MHz, $CDCl_3$) δ 7.30 – 7.17 (m, 5H), 4.50 (t, J = 6.6 Hz, 1H), 1.77 – 1.67 (m, 2H), 0.84 (t, J = 7.5 Hz, 3H). ^{13}C{^{1}H} NMR (126 MHz, $CDCl_3$) δ 144.71, 128.50, 127.59, 126.09, 76.11, 31.98, 10.25.

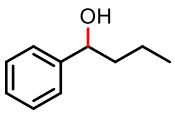

*1-phenylbutan-1-ol (**Ao**).* Purified by column chromatography on silica gel using petroleum ether and ethyl acetate as eluents, 95% (143 mg) yield as colourless liquid. ^{1}H NMR (500 MHz, $CDCl_3$) δ 7.31 – 7.18 (m, 5H), 4.58 (q, *J* = 6.6 Hz, 1H), 1.75 – 1.56 (m, 2H), 1.39 – 1.22 (m, 2H), 0.86 (t, *J* = 7.4 Hz, 3H). ^{13}C{^{1}H} NMR (126 MHz, $CDCl_3$) δ 145.04, 128.47, 127.51, 126.01, 74.47, 41.30, 19.12, 14.06.

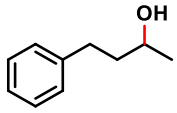

4-phenylbutan-2-ol (***Ap***). Purified by column chromatography on silica gel using petroleum ether and ethyl acetate as eluents, 92% (138 mg) yield as colourless liquid. ^{1}H NMR (400 MHz, $CDCl_3$) δ 7.32 – 7.28 (m, 2H), 7.23-7.18 (m, 3H), 3.84 (h, J = 6.1 Hz, 1H), 2.83 – 2.64 (m, 2H), 1.85 – 1.73 (m, 2H), 1.24 (d, J = 6.1 Hz, 3H). ^{13}C{^{1}H} NMR (101 MHz, $CDCl_3$) δ 142.18, 128.50, 125.92, 67.59, 40.95, 32.24, 23.72.

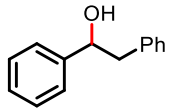

*1,2-diphenylethan-1-ol (**Aq**).* Purified by column chromatography on silica gel using petroleum ether and ethyl acetate as eluents, 86% (171 mg) yield as yellowish liquid. ^{1}H NMR (500 MHz, $CDCl_3$) δ 7.41 (d, *J* = 4.4 Hz, 4H), 7.36 (dq, *J* = 6.3, 2.3 Hz, 3H), 7.33 – 7.28 (m, 1H), 7.27 – 7.23 (m, 2H), 4.93 (dd, *J* = 8.3, 5.1 Hz, 1H), 3.12 – 3.01 (m, 2H). ^{13}C{^{1}H} NMR (126 MHz, $CDCl_3$) δ 143.90, 138.14, 129.61, 128.56, 128.47, 127.67, 126.66, 126.00, 75.40, 46.13.

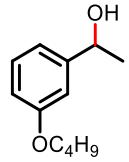

*1-(4-butoxyphenyl)ethan-1-ol (**As**).* Purified by column chromatography on silica gel using petroleum ether and ethyl acetate as eluents, 86% (155 mg) yield as colourless ^{1}H NMR (500 MHz, $CDCl_3$) δ 7.24 (t, *J* = 7.8 Hz, 1H), 6.92 (d, *J* = 8.5 Hz, 2H), 6.81 (d, *J* = 8.2 Hz, 1H), 4.83 (q, *J* = 6.4 Hz, 1H), 3.97 (t, *J* = 6.5 Hz, 2H), 1.78 (p, *J* = 6.6 Hz, 2H), 1.55 – 1.46 (m, 5H), 1.00 (t, *J* = 7.4 Hz, 3H). ^{13}C{^{1}H} NMR (126 MHz, $CDCl_3$) δ 159.34, 147.61, 129.47, 117.53, 113.37, 111.56, 70.29, 67.65, 31.39, 25.13, 19.29, 13.91.

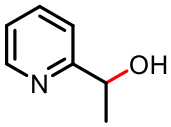

*1-(pyridin-2-yl)ethan-1-ol (**At**).* Purified by column chromatography on silica gel using petroleum ether and ethyl acetate as eluents, 72% (88 mg) yield as colourless liquid. ^{1}H NMR (400 MHz, $CDCl_3$) δ 8.45 (d, *J* = 5.3 Hz, 1H), 7.66 – 7.59 (m, 1H), 7.27 (d, *J* = 7.9 Hz, 1H), 7.17 – 7.10 (m, 1H), 4.84 (q, *J* = 6.7 Hz, 1H), 1.45 (d, *J* = 6.5 Hz, 3H). ^{13}C{^{1}H} NMR (101 MHz, $CDCl_3$) δ 163.39, 148.13, 136.91, 122.25, 119.86, 69.11, 24.22.

EXPERIMENTAL DETAILS FOR ALDEHYDE

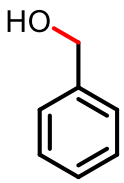

*penylmethanol (**Ba**).* Purified by column chromatography on silica gel using petroleum ether and ethyl acetate as eluents, 96% (104 mg) yielded as colourless liquid. ^{1}H NMR (500 MHz, $CDCl_3$): δ 7.26 (d, J = 4.6 Hz, 4H), 7.19 (dq, J = 9.0, 4.5 Hz, 1H), 4.59 (s, 2H). ^{13}C{^{1}H} (126 MHz, $CDCl_3$): δ 141.05, 128.65, 127.72, 127.10, 65.37.

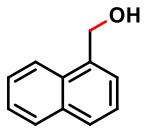

naphthalen-1-ylmethanol (***Bb***). Purified by column chromatography on silica gel using petroleum ether and ethyl acetate as eluents, 88% (139 mg) yield as colourless liquid. ^{1}H NMR (400 MHz, $CDCl_3$) δ 8.13 (d, *J* = 8.2 Hz, 1H), 7.89 (d, *J* = 9.6 Hz, 1H), 7.82 (d, *J* = 8.2 Hz, 1H), 7.58 – 7.49 (m, 3H), 7.45 (dd, *J* = 8.2, 7.0 Hz, 1H), 5.14 (s, 2H). ^{13}C{^{1}H} NMR (101 MHz, $CDCl_3$) δ 136.39, 133.92, 131.35, 128.79, 128.71, 126.47, 126.00, 125.53, 125.46, 123.77, 63.80.

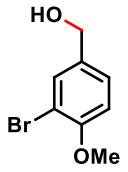

(3-bromo-4-methoxyphenyl)methanol (***Bc***). Purified by column chromatography on silica gel using petroleum ether and ethyl acetate as eluents, 86% (187 mg) yield as colourless liquid. ^{1}H NMR (500 MHz, $CDCl_3$) δ 7.47 (d, *J* = 12.4 Hz, 1H), 7.16 (d, *J* = 8.5 Hz, 1H), 6.78 (d, *J* = 8.4 Hz, 1H), 4.49 (s, 2H), 3.80 (s, 3H). ^{13}C{^{1}H} NMR (126 MHz, $CDCl_3$) δ 155.41, 134.62, 132.32, 127.43, 111.72, 111.19, 64.26, 56.40.

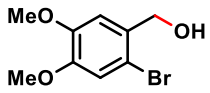

(2-bromo-4,5-dimethoxyphenyl)methanol (***Bd***). Purified by column chromatography on silica gel using petroleum ether and ethyl acetate as eluents, 96% (237 mg) yield as colourless liquid. ^{1}H NMR (500 MHz, $CDCl_3$) δ 7.02 (s, 2H), 4.68 (s, 2H), 3.88 (s, 3H), 3.87 (s, 3H). ^{13}C{^{1}H} NMR (126 MHz, $CDCl_3$) δ 149.00, 148.65, 131.98, 115.50, 112.54, 111.98, 64.85, 56.31, 56.15.

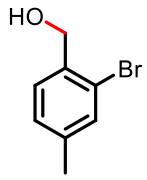

(2-bromo-4-methylphenyl)methanol (***Be***). Purified by column chromatography on silica gel using petroleum ether and ethyl acetate as eluents, 97% (195 mg) yielded as white solid. ^{1}H NMR (400 MHz, $CDCl_3$): δ 7.40 (s, 1H), 7.36 (d, J = 7.8 Hz, 1H), 7.15 (d, J = 5.7 Hz, 1H), 4.72 (s, 2H), 2.35 (s, 3H). ^{13}C{^{1}H} NMR (101 MHz, $CDCl_3$): δ 139.52, 136.80, 133.21, 129.06, 128.53, 122.66, 65.06, 20.87.

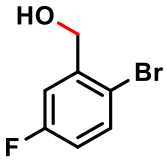

(2-bromo-5-fluorophenyl)methanol (***Bf***). Purified by column chromatography on silica gel using petroleum ether and ethyl acetate as eluents, 88% (180 mg) yield as colourless liquid. ^{1}H NMR (400 MHz, $CDCl_3$) δ 7.46 (dd, J = 8.8, 5.1 Hz, 1H), 7.25 (d, J = 7.5 Hz, 1H), 6.89 – 6.85 (m, 1H), 4.70 (s, 2H). ^{13}C{^{1}H} NMR (101 MHz, CDCl3) δ 163.68, 161.23, 142.23, 133.81, 116.11, 115.88, 64.62.

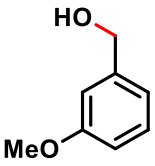

(3-methoxyphenyl)methanol (***Bg***). Purified by column chromatography on silica gel using petroleum ether and ethyl acetate as eluents, 92% (127 mg) yield as colourless liquid. ^{1}H NMR (400 MHz, $CDCl_3$) δ 7.28 (d, J = 14.6 Hz, 1H), 6.94

(d, J = 5.6 Hz, 2H), 6.84 (d, J = 10.0 Hz, 1H), 4.66 (s, 2H), 3.82 (s, 3H). $^{13}C\{^{1}H\}$ NMR (101 MHz, $CDCl_3$) δ 159.90, 142.66, 129.68, 119.21, 113.33, 112.34, 65.25, 55.31.

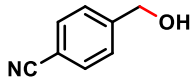

*4-(hydroxymethyl)benzonitrile (**Bh**).* Purified by column chromatography on silica gel using petroleum ether and ethyl acetate as eluents, 95% (126 mg) yield as colourless liquid. ^{1}H NMR (400 MHz, $CDCl_3$) δ 7.41 (d, *J* = 6.4 Hz, 2H), 7.25 (d, *J* = 8.0 Hz, 2H), 4.54 (s, 2H). $^{13}C\{^{1}H\}$ NMR (101 MHz, $CDCl_3$) δ 146.57, 132.36, 127.10, 119.01, 111.05, 64.15.

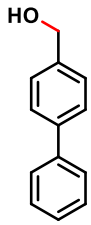

*[1,1'-biphenyl]-4-ylmethanol (**Bi**).* Purified by column chromatography on silica gel using petroleum ether and ethyl acetate as eluents, 81% (149 mg) yield as colourless liquid. ^{1}H NMR (400 MHz, $CDCl_3$) δ 7.62 – 7.58 (m, 4H), 7.48 – 7.42 (m, 4H), 7.38 – 7.33 (m, 1H), 4.75 (s, 2H). $^{13}C\{^{1}H\}$ NMR (101 MHz, $CDCl_3$) δ 140.96, 140.81, 140.01, 128.93, 127.61, 127.49, 127.48, 127.24, 65.28.

*(2-bromophenyl)methanol (**Bj**).* Purified by column chromatography on silica gel using petroleum ether and ethyl acetate as eluents, 89% (166 mg) yield as colourless liquid. ^{1}H NMR (500 MHz, $CDCl_3$) δ 7.62 (d, *J* = 8.0 Hz, 1H), 7.55 (d, *J* = 9.3 Hz, 1H), 7.40 (t, *J* = 7.4 Hz, 1H), 7.23 (t, *J* = 7.7 Hz, 1H), 4.81 (s, 2H). $^{13}C\{^{1}H\}$ NMR (126 MHz, $CDCl_3$) δ 139.75, 132.56, 129.07, 128.84, 127.65, 122.51, 64.93.

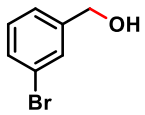

*(3-bromophenyl)methanol (**Bk**).* Purified by column chromatography on silica gel using petroleum ether and ethyl acetate as eluents, 85% (159 mg) yield as colourless liquid. ^{1}H NMR (500 MHz, $CDCl_3$) δ 7.54 (s, 1H), 7.43 (d, *J* = 7.8 Hz, 1H), 7.29 (d, *J* = 7.8 Hz, 1H), 7.24 (t, *J* = 7.7 Hz, 1H), 4.67 (s, 2H). $^{13}C\{^{1}H\}$ NMR (126 MHz, $CDCl_3$) δ 143.13, 130.62, 130.12, 129.90, 125.36, 122.64, 64.39.

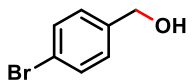

*(4-bromophenyl)methanol (**Bl**).* Purified by column chromatography on silica gel using petroleum ether and ethyl acetate as eluents, 82% (153 mg) yield as colourless liquid. ^{1}H NMR (500 MHz, $CDCl_3$) δ 7.51 (d, J = 8.0 Hz, 2H), 7.27 (d, J = 8.1 Hz, 2H), 4.68 (s, 2H). $^{13}C\{^{1}H\}$ NMR (126 MHz, $CDCl_3$) δ 139.89, 131.75, 128.72, 121.57, 64.69.

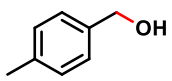

*p-tolylmethanol (**Bm**).* Purified by column chromatography on silica gel using petroleum ether and ethyl acetate as eluents, 82% (100 mg) yield as colourless liquid. ^{1}H NMR (400 MHz, $CDCl_3$) δ 7.26 (d, *J* = 8.0 Hz, 2H), 7.18 (d, *J* = 7.8 Hz, 2H), 4.65

(s, 2H), 2.35 (s, 3H). $^{13}C\{^{1}H\}$ NMR (101 MHz, $CDCl_3$) δ 137.91, 137.43, 129.26, 127.13, 65.32, 21.16.

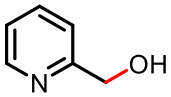

*pyridin-2-ylmethanol (**Bn**).* Purified by column chromatography on silica gel using petroleum ether and ethyl acetate as eluents, 76% (83 mg) yield as colourless liquid. ^{1}H NMR (400 MHz, $CDCl_3$) δ 8.49 (d, *J* = 5.0 Hz, 1H), 7.65 (t, *J* = 6.8 Hz, 1H), 7.28 (d, *J* = 7.9 Hz, 1H), 7.16 (t, *J* = 6.2 Hz, 1H), 4.73 (s, 2H). $^{13}C\{^{1}H\}$ NMR (101 MHz, $CDCl_3$) δ 159.53, 148.50, 136.81, 122.32, 120.72, 64.29.

NMR spectral data of catalytic products

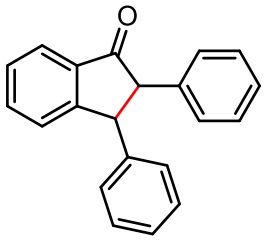

*2,3-diphenyl-2,3-dihydro-1H-inden-1-one (**Ca**).* Purified by column chromatography on silica gel using petroleum ether and ethyl acetate as eluents, 97% (69 mg) yielded colourless oil. ^{1}H NMR (500 MHz, $CDCl_3$) δ 7.94 (d, J = 7.6 Hz, 1H), 7.68 (t, J = 7.6 Hz, 1H), 7.53 (t, J = 7.5 Hz, 1H), 7.40 – 7.29 (m, 7H), 7.18 – 7.11 (m, 4H), 4.62 (d, J = 5.0 Hz, 1H), 3.86 (d, J = 4.9 Hz, 1H). $^{13}C\{^{1}H\}$ NMR (126 MHz, $CDCl_3$) δ 205.39, 156.25, 142.60, 138.63, 136.29, 135.55, 129.03, 128.97, 128.48, 128.41, 128.02, 127.32, 127.31, 126.81, 124.15, 64.74, 54.99.

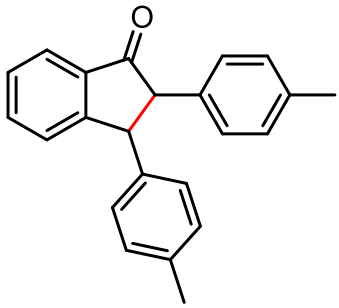

*2,3-di-p-tolyl-2,3-dihydro-1H-inden-1-one (**Cb**).* Purified by column chromatography on silica gel using petroleum ether and ethyl acetate as eluents, 91% (71 mg) yielded colourless oil. ^{1}H NMR (400 MHz, $CDCl_3$) δ 7.88 (d, J = 7.6 Hz, 1H), 7.65 – 7.60 (m, 1H), 7.50 – 7.45 (m, 1H), 7.30 (d, J = 7.8 Hz, 1H), 7.11-7.13 (m, 4H), 6.96-7.01 (m, 4H), 4.52 (d, J = 4.9 Hz, 1H), 3.75 (d, J = 4.9 Hz, 1H), 2.34 (s, 3H), 2.33 (s, 3H). $^{13}C\{^{1}H\}$ NMR (101 MHz, $CDCl_3$) δ 205.80, 156.52, 139.70, 136.91, 136.32, 135.66, 135.46, 129.70, 129.67, 128.37, 128.30, 127.92, 126.79, 124.11, 64.54, 54.69, 21.25, 21.22.

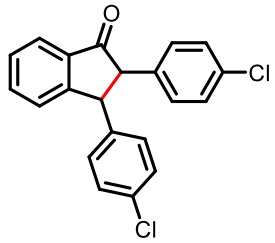

*2,3-bis(4-chlorophenyl)-2,3-dihydro-1H-inden-1-one (**Cc**).* Purified by column chromatography on silica gel using petroleum ether and ethyl acetate as eluents, 88% (78 mg) yielded yellow oil. ^{1}H NMR (400 MHz, $CDCl_3$) δ 7.91 (dt, J = 7.7, 1.0 Hz, 1H), 7.69 (t, J = 7.5 Hz, 1H), 7.54 (t, J = 7.5 Hz, 1H), 7.34 – 7.28 (m, 5H), 7.04 (dd, J = 8.4, 2.0 Hz, 4H), 4.50 (d, J = 5.2 Hz, 1H), 3.74 (d, J = 5.3 Hz, 1H). ^{13}C{^{1}H} NMR (101 MHz, $CDCl_3$) δ 204.30, 155.28, 140.66, 136.59, 136.11, 135.85, 133.47, 133.41, 129.91, 129.37, 129.35, 129.25, 128.81, 126.65, 124.35, 64.22, 54.39.

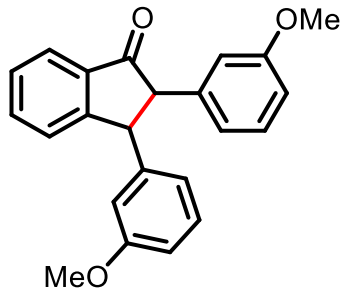

*2,3-bis(3-methoxyphenyl)-2,3-dihydro-1H-inden-1-one (**Cd**).* Purified by column chromatography on silica gel using petroleum ether and ethyl acetate as eluents, 85% (73 mg) yielded colourless oil. ^{1}H NMR (400 MHz, $CDCl_3$) δ 7.91 (d, J = 7.7 Hz, 1H), 7.70 – 7.64 (m, 1H), 7.51 (t, J = 7.0 Hz, 1H), 7.35 (d, J = 6.8 Hz, 1H), 7.26 (t, J = 7.9 Hz, 2H), 6.84 (d, J = 8.3 Hz, 2H), 6.71 (t, J = 6.6 Hz, 2H), 6.66 (dd, J = 13.6, 2.1 Hz, 2H), 4.58 (d, J = 4.8 Hz, 1H), 3.81 (d, J = 4.8 Hz, 1H), 3.78 (s, 6H). ^{13}C{^{1}H} NMR (101 MHz, $CDCl_3$) δ 205.13, 159.96, 159.85, 156.02, 144.13, 140.05, 136.12, 135.48, 129.94, 129.87, 128.35, 126.75, 124.09, 120.65, 120.29, 114.19, 113.83, 112.62, 112.23, 64.38, 55.22, 54.79.

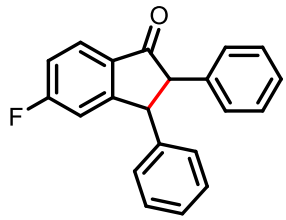

*5-fluoro-2,3-diphenyl-1H-inden-1-one (**Ce**).* Purified by column chromatography on silica gel using petroleum ether and ethyl acetate as eluents, 88% (66 mg) yielded yellow oil. ^{1}H NMR (400 MHz, $CDCl_3$) δ 7.55 (dd, J = 7.5, 2.5 Hz, 1H), 7.41 – 7.29 (m, 8H), 7.13 – 7.09 (m, 4H), 4.57 (d, J = 3.4 Hz, 1H), 3.88 (d, J = 4.7 Hz, 1H). ^{13}C{^{1}H} NMR (126 MHz, $CDCl_3$) δ 204.23, 163.86, 161.88, 151.63, 142.12, 138.06, 129.04, 128.94, 128.35, 128.33, 128.28, 127.82, 127.39, 123.09, 109.84, 65.36, 54.31. ^{19}F NMR (376 MHz, CDCl3) δ -112.87.

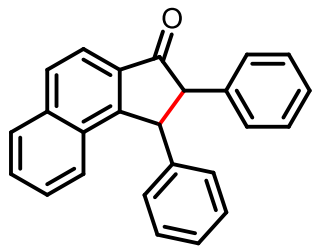

*1,2-diphenyl-1,2-dihydro-3H-cyclopenta[a]naphthalen-3-one (**Cf**).* Purified by column chromatography on silica gel using petroleum ether and ethyl acetate as eluents, 84% (70 mg) yielded white solid. 1H NMR (500 MHz, $CDCl_3$) δ 7.99 – 7.95 (m, 2H), 7.90 (d, J = 8.4 Hz, 1H), 7.68 (d, J = 8.4 Hz, 1H), 7.65 – 7.59 (m, 1H), 7.41 (t, J = 7.7 Hz, 1H), 7.35 – 7.24 (m, 6H), 7.13 (d, J = 6.7

Hz, 2H), 7.07 (d, J = 6.4 Hz, 2H), 5.00 (d, J = 3.1 Hz, 1H), 3.86 (d, J = 3.1 Hz, 1H). 13C NMR (126 MHz, $CDCl_3$) δ 205.46, 156.24, 143.59, 139.40, 137.73, 135.05, 130.22, 130.15, 129.27, 129.26, 129.22, 129.12, 128.10, 127.49, 127.38, 127.22, 126.20, 119.80, 65.42, 54.53.

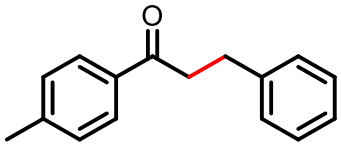

1-(4-bromophenyl) 3-phenyl-1-(p-tolyl)propan-1-one (***Cg***). Purified by column chromatography on silica gel using petroleum ether and ethyl acetate as eluents, 78% (44 mg) yielded brown solid. ^{1}H NMR (400 MHz, $CDCl_3$) δ 7.87 (d, *J* = 8.4 Hz, 2H), 7.32 – 7.28 (m, 2H), 7.27 – 7.18 (m, 5H), 3.30 – 3.26 (m, 2H), 3.08 – 3.04 (m, 2H), 2.41 (s, 3H). ^{13}C{^{1}H} NMR (101 MHz, $CDCl_3$) δ 198.94, 143.87, 141.43, 134.40, 129.31, 128.54, 128.46, 128.19, 126.13, 40.38, 30.24, 21.66.

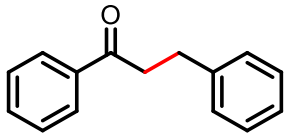

1,3-diphenylpropan-1-one (***Ch***). Purified by column chromatography on silica gel using petroleum ether and ethyl acetate as eluents, 75% (39 mg) yielded white solid. ^{1}H NMR (400 MHz, $CDCl_3$) δ 7.99 – 7.95 (m, 2H), 7.57 (t, *J* = 7.4 Hz, 1H), 7.46 (t, *J* = 7.5 Hz, 2H), 7.35 – 7.29 (m, 2H), 7.29 – 7.20 (m, 3H), 3.34 – 3.30 (m, 2H), 3.111 – 3.07 (m, 2H). ^{13}C{^{1}H} NMR (101 MHz, $CDCl_3$) δ 199.25, 141.32, 136.89, 133.09, 128.63, 128.56, 128.46, 128.07, 126.16, 40.47, 30.16.

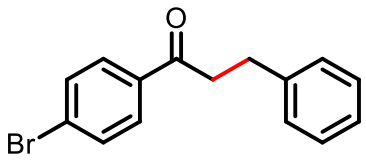

1-(4-bromophenyl)-3-phenylpropan-1-one (***Ci***). Purified by column chromatography on silica gel using petroleum ether and ethyl acetate as eluents, 82% (59 mg) yielded white solid. ^{1}H NMR (500 MHz, $CDCl_3$) δ 7.85 (d, *J* = 8.7 Hz, 2H), 7.62 (d, *J* = 8.7 Hz, 2H), 7.33 (t, *J* = 7.5 Hz, 2H), 7.26 (dd, *J* = 12.6, 8.0 Hz, 3H), 3.30 (t, *J* = 7.7 Hz, 2H), 3.09 (t, *J* = 7.6 Hz, 2H). ^{13}C{^{1}H} NMR (126 MHz, $CDCl_3$) δ 198.22, 141.05, 135.56, 131.94, 129.59, 128.60, 128.43, 128.26, 126.26, 40.44, 30.04.

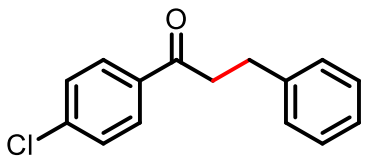

1-(4-chlorophenyl)-3-phenylpropan-1-one (***Cj***). Purified by column chromatography on silica gel using petroleum ether and ethyl acetate as eluents, 81% (50 mg) yielded yellow solid. ^{1}H NMR (400 MHz, $CDCl_3$) δ 7.53 – 7.51 (m, 1H), 7.47 (d, *J* = 7.7 Hz, 1H), 7.30 – 7.25 (m, 3H), 7.22 – 7.16 (m, 3H), 7.06 (dd, *J* = 8.0, 3.6 Hz, 1H), 3.26 (t, *J* = 7.8 Hz, 2H), 3.02 (t, *J* = 7.7 Hz,). ^{13}C{^{1}H} NMR (101 MHz, $CDCl_3$) δ 200.23, 156.41, 141.04, 138.12, 130.24, 128.42, 126.21, 120.75, 114.60, 40.60, 30.18.

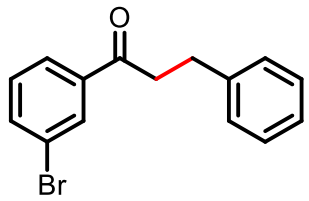

1-(3-bromophenyl)-3-phenylpropan-1-one ***(Ck)***. Purified by column chromatography on silica gel using petroleum ether and ethyl acetate as eluents, 80% (58 mg) yielded white solid. ^{1}H NMR (500 MHz, $CDCl_3$) δ 8.11 (s, 1H), 7.90 (d, *J* = 7.8 Hz, 1H), 7.71 (d, *J* = 10.5 Hz, 1H), 7.37 – 7.32 (m, 3H), 7.30 – 7.24 (m, 3H), 3.30 (t, *J* = 7.7 Hz, 2H), 3.09 (t, *J* = 7.6 Hz, 2H).^{13}C{^{1}H} NMR (126 MHz, $CDCl_3$) δ 197.80, 140.98, 138.60, 135.92, 131.17, 130.23, 128.60, 128.43, 126.55, 126.27, 123.01, 40.54, 29.98.

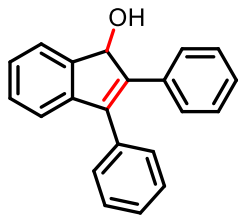

2,3-diphenyl-1H-inden-1-ol ***(Da)***. Purified by column chromatography on silica gel using petroleum ether and ethyl acetate as eluents, 51% (36 mg) yielded an yellow oil. ^{1}H NMR (400 MHz, $CDCl_3$) δ 7.65 (d, *J* = 6.2 Hz, 1H), 7.44 (q, *J* = 5.6 Hz, 3H), 7.40 – 7.32 (m, 5H), 7.29 – 7.27 (m, 2H), 7.25 – 7.21 (m, 3H), 5.68 (s, 1H), 2.13 (s, 1H). ^{13}C{^{1}H} NMR (101 MHz, $CDCl_3$) δ 144.36, 143.92, 143.86, 139.73, 134.82, 134.11, 129.35, 129.18, 128.93, 128.78, 128.40, 127.91, 127.41, 126.45, 123.84, 120.74, 77.35. HRMS (ESI): [M + H]$^{+}$ calcd for $C_{21}H_{17}O$, 285.1779; found, 285.1775.

NMR spectra of catalytic products of acetophenone derivatives reduction

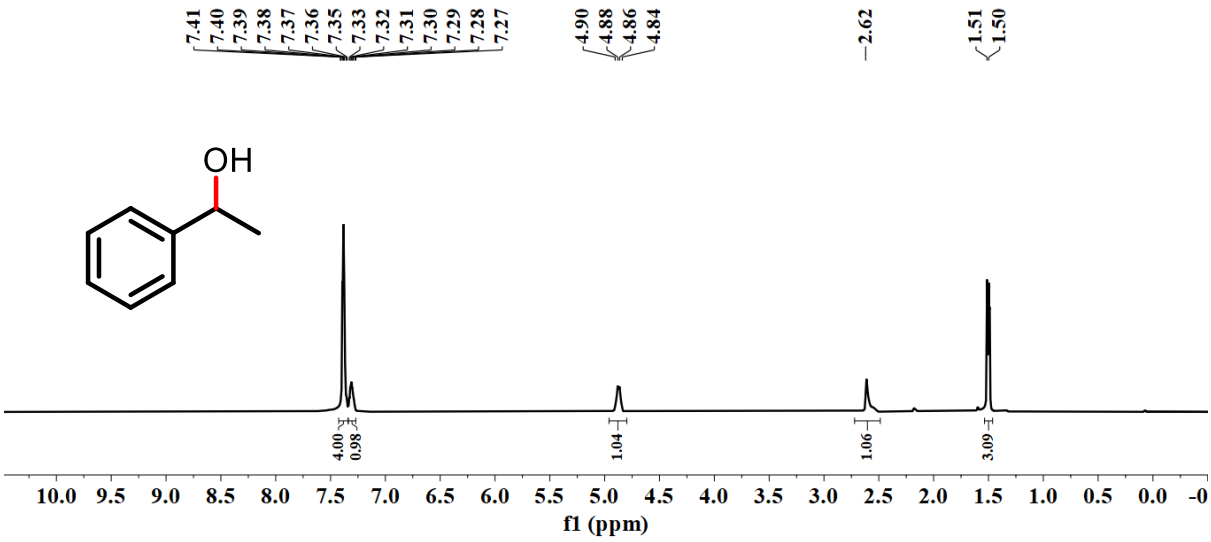

Figure S1. ^{1}H NMR spectrum of **Aa** in $CDCl_3$ (400 MHz).

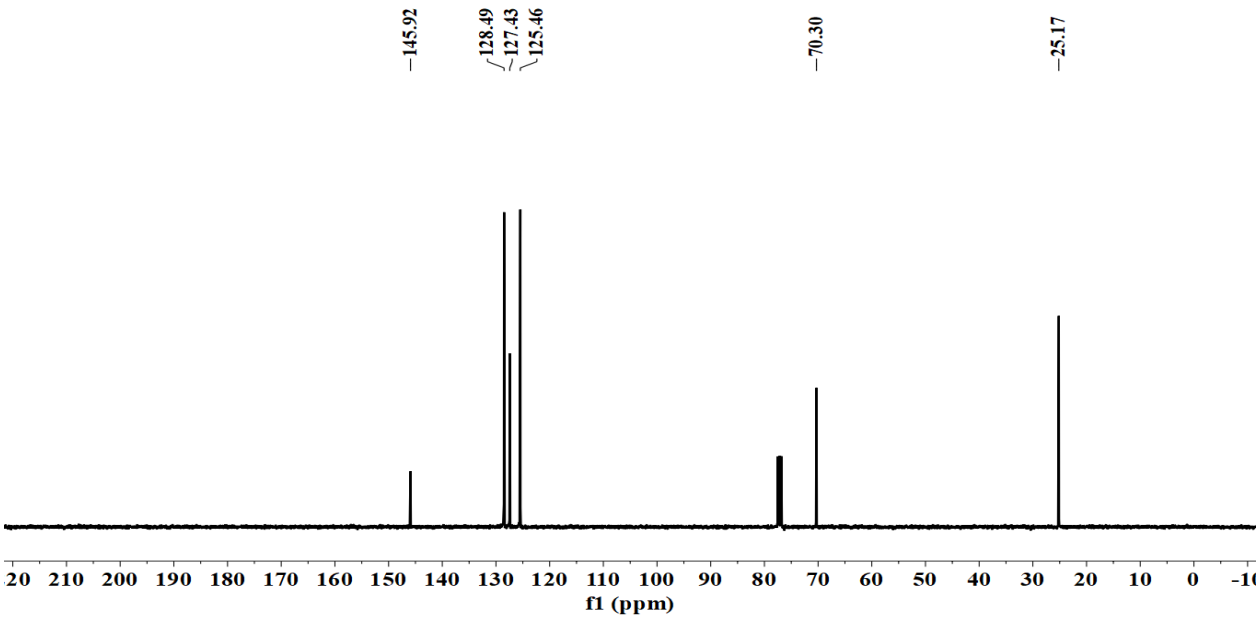

Figure S2. $^{13}C\{^{1}H\}$ NMR spectrum of **Aa** in $CDCl_3$ (101 MHz).

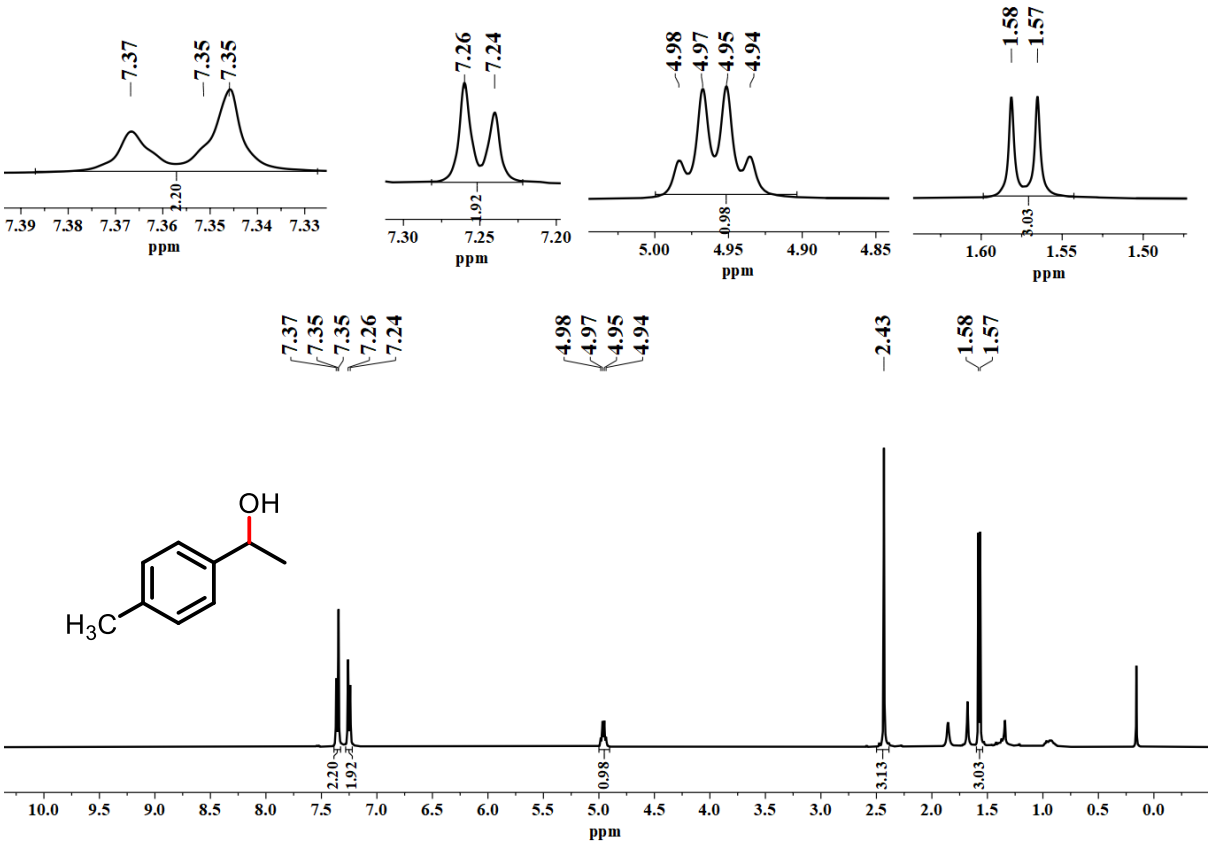

Figure S3. ^{1}H NMR spectrum of **Ab** in $CDCl_3$ (400 MHz).

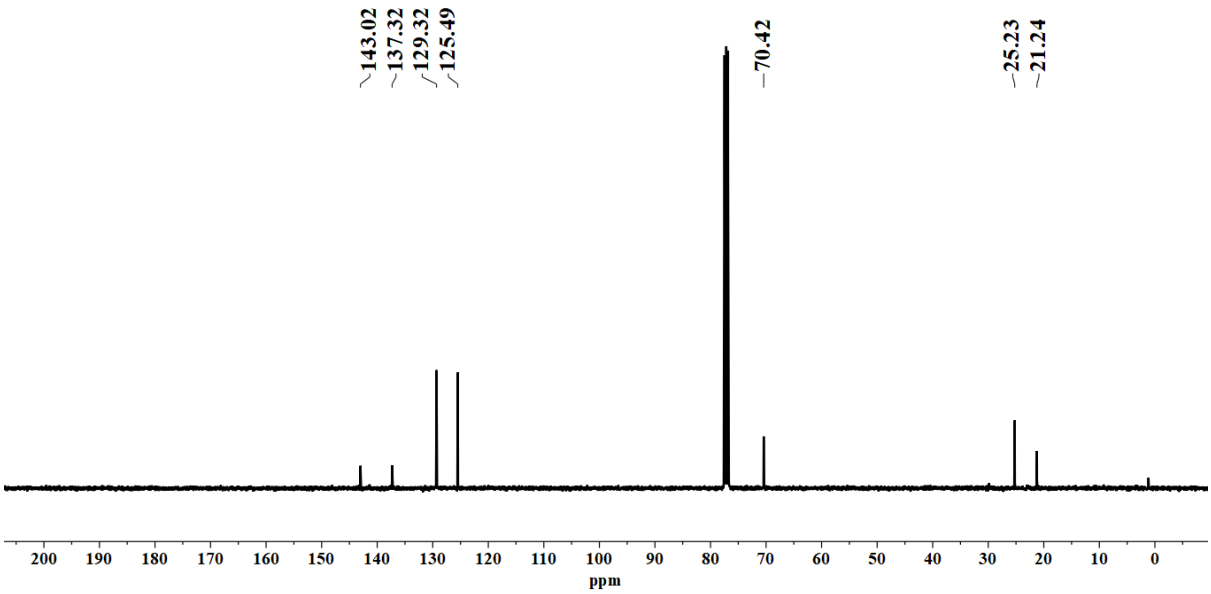

Figure S4. $^{13}C\{^{1}H\}$ NMR spectrum of **Ab** in $CDCl_3$ (101 MHz).

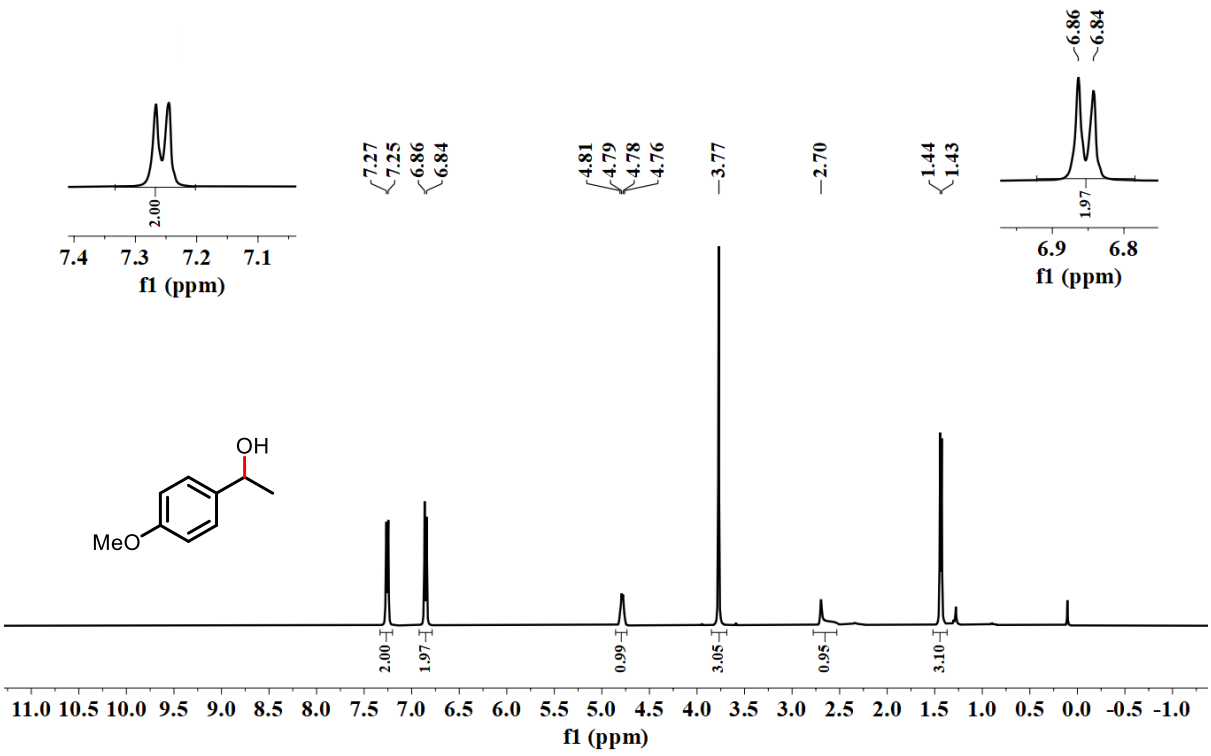

Figure S5. ^{1}H NMR spectrum of **Ac** in $CDCl_3$ (400 MHz).

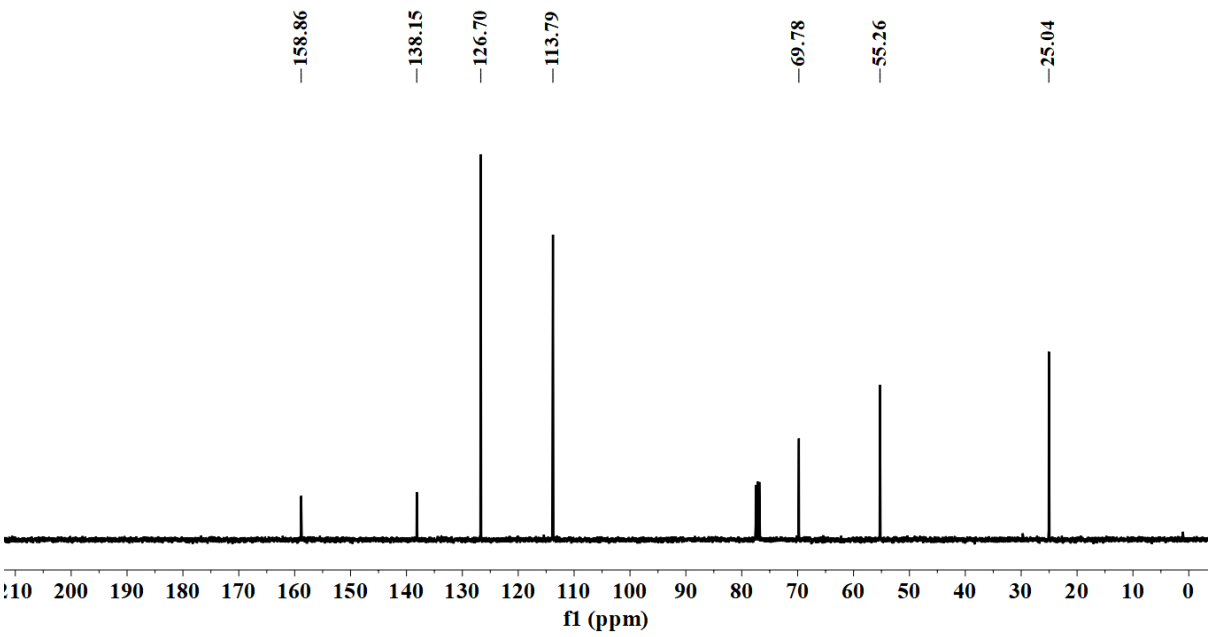

Figure S6. $^{13}C\{^{1}H\}$ NMR spectrum of **Ac** in $CDCl_3$ (101 MHz).

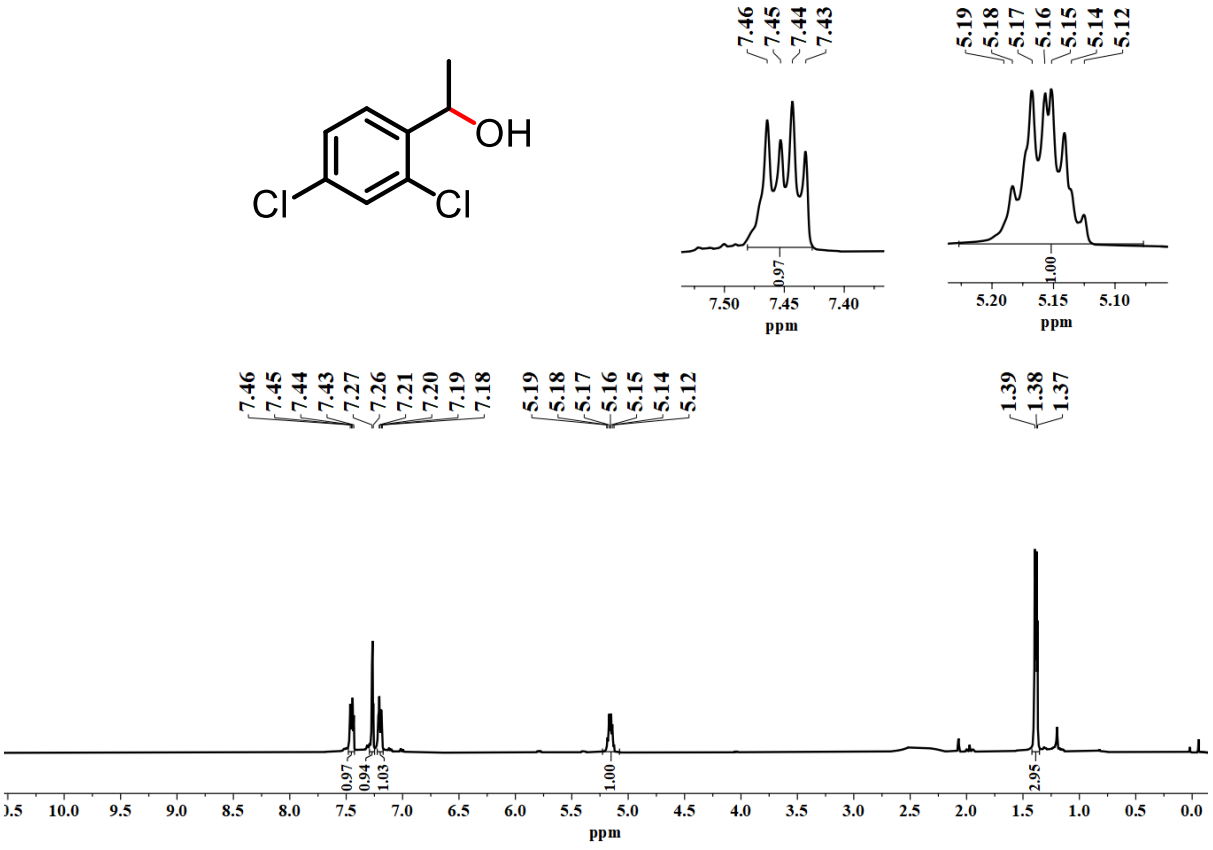

Figure S7. ^{1}H NMR spectrum of **Ad** in $CDCl_3$ (400 MHz).

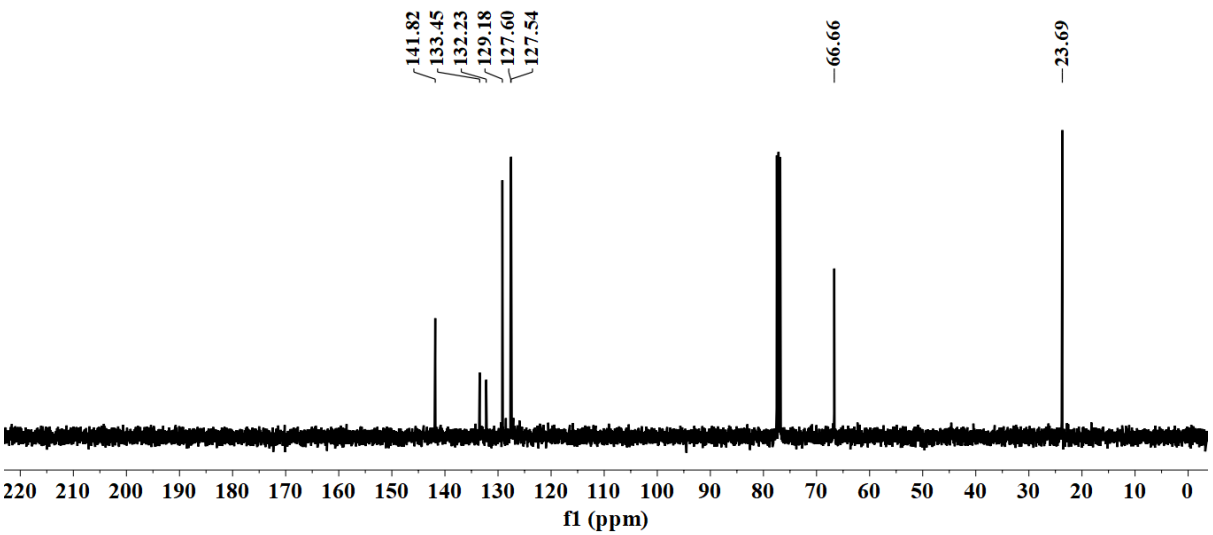

Figure S8. $^{13}C\{^{1}H\}$ NMR spectrum of **Ad** in $CDCl_3$ (101 MHz).

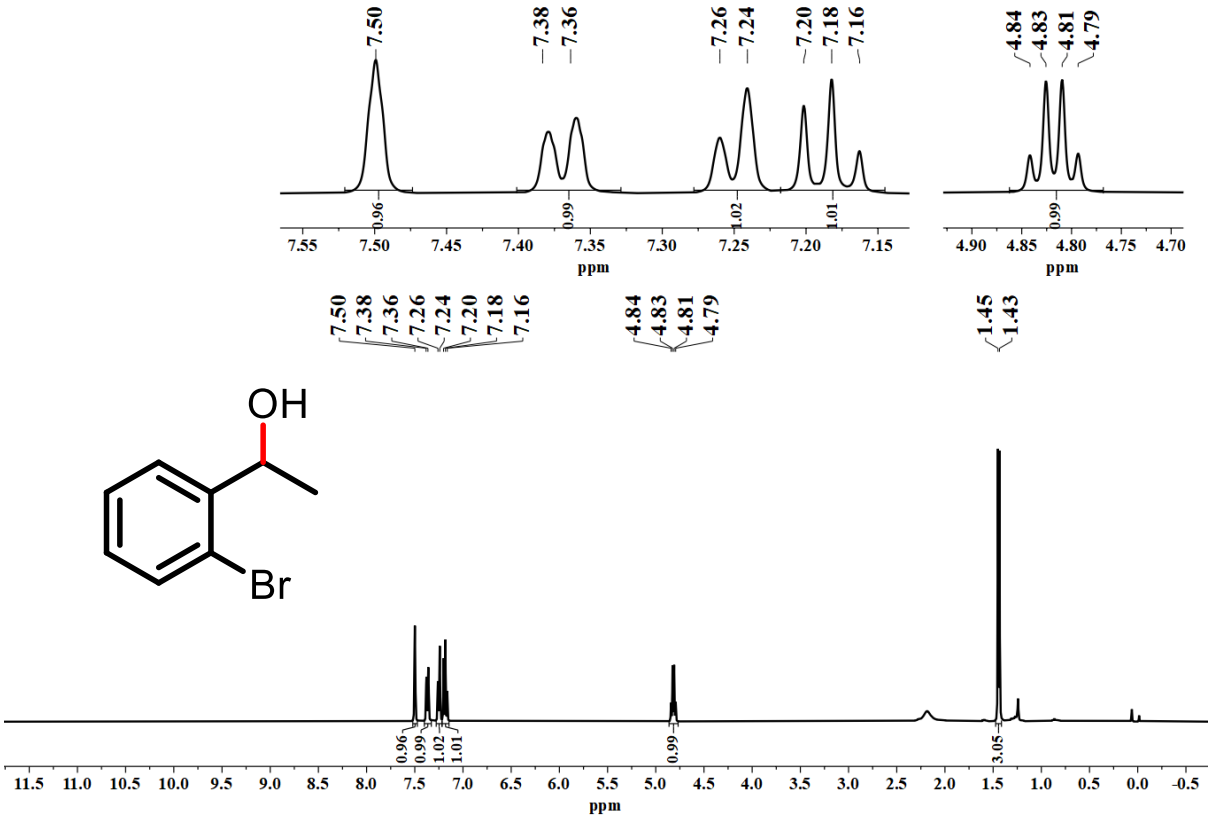

Figure S9. ^{1}H NMR spectrum of **Ae** in $CDCl_3$ (400 MHz).

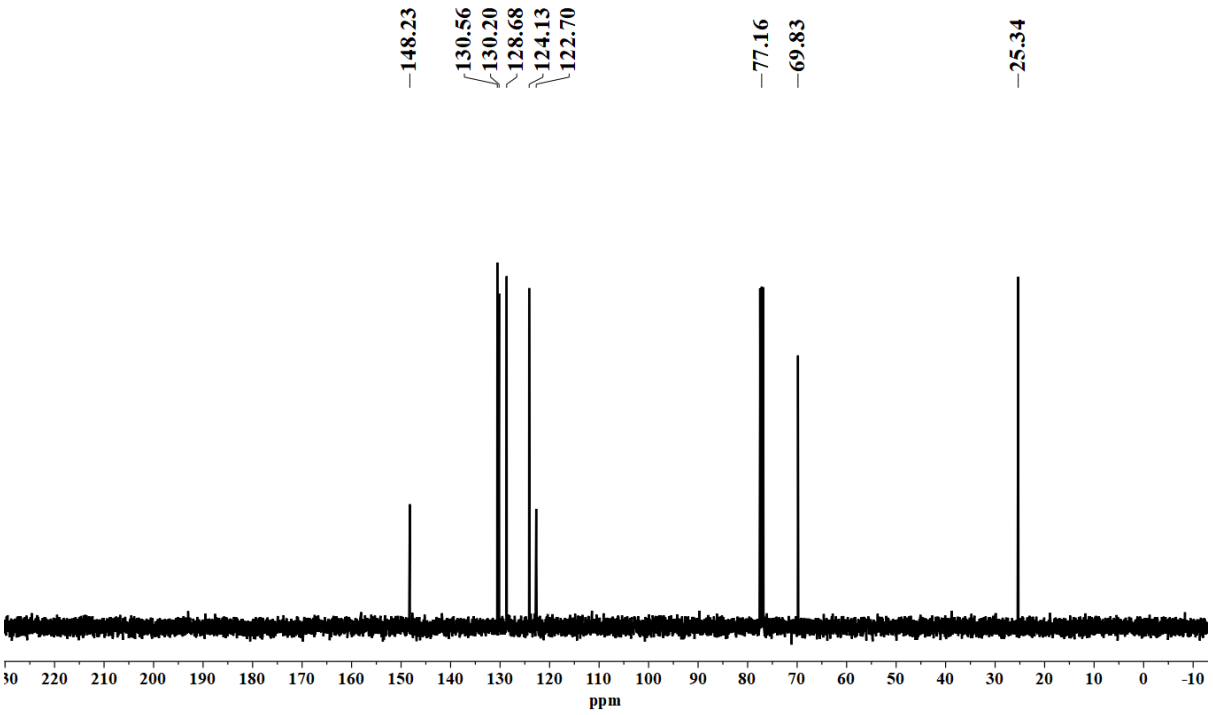

Figure S10. $^{13}C\{^{1}H\}$ NMR spectrum of **Ae** in $CDCl_3$ (101 MHz).

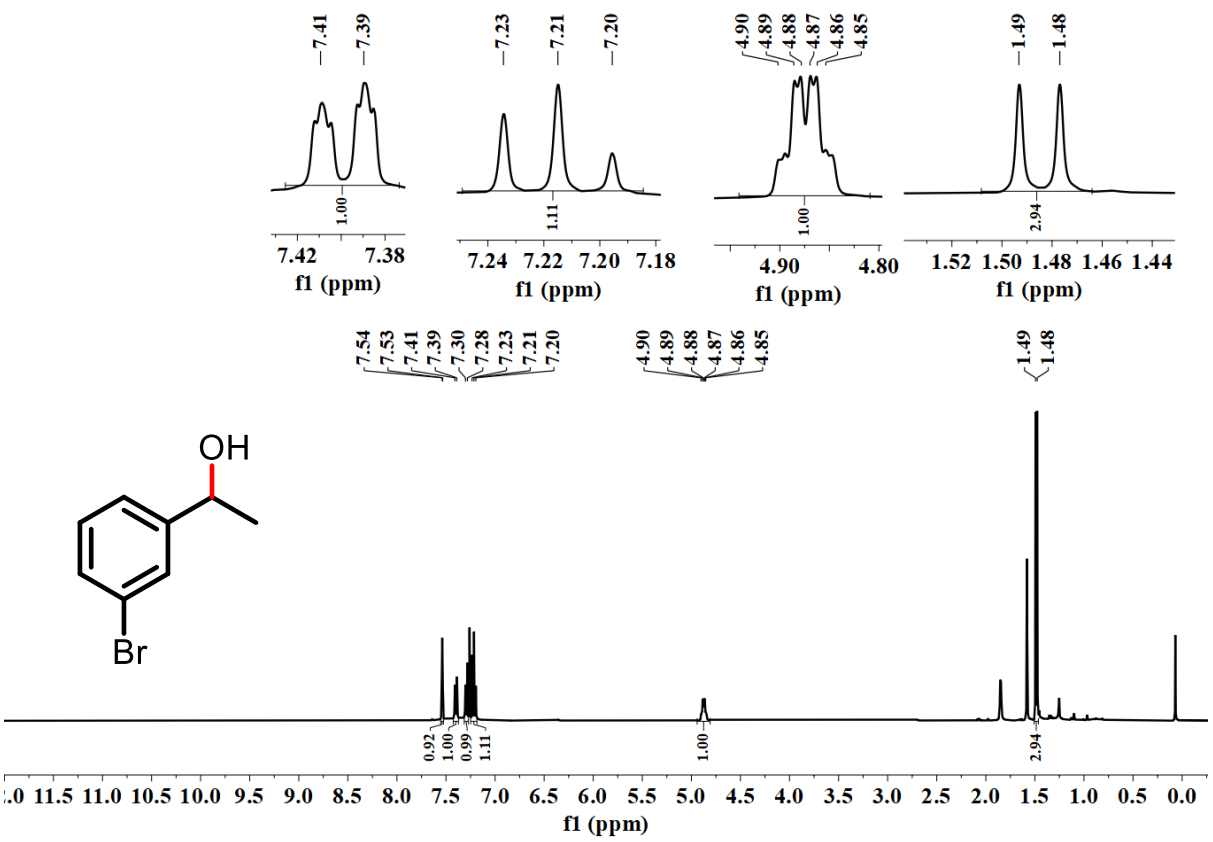

Figure S11. ^{1}H NMR spectrum of **Af** in $CDCl_3$ (400 MHz).

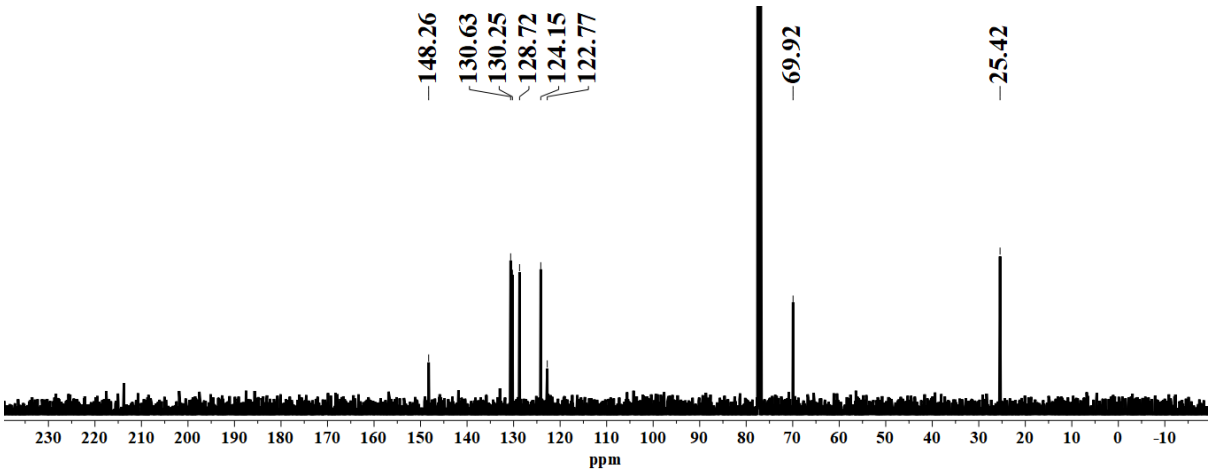

Figure S12. $^{13}C\{^{1}H\}$ NMR spectrum of **Af** in $CDCl_3$ (101 MHz).

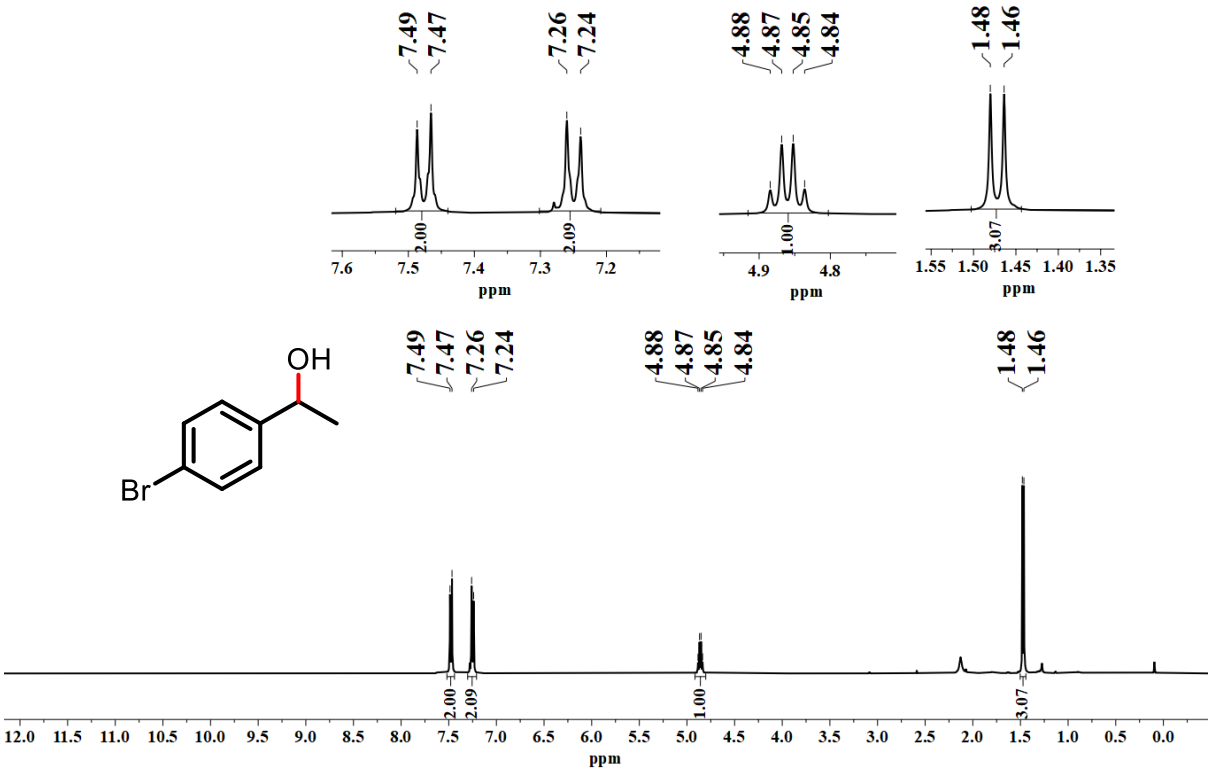

Figure S13. ^{1}H NMR spectrum of **Ag** in $CDCl_3$ (400 MHz).

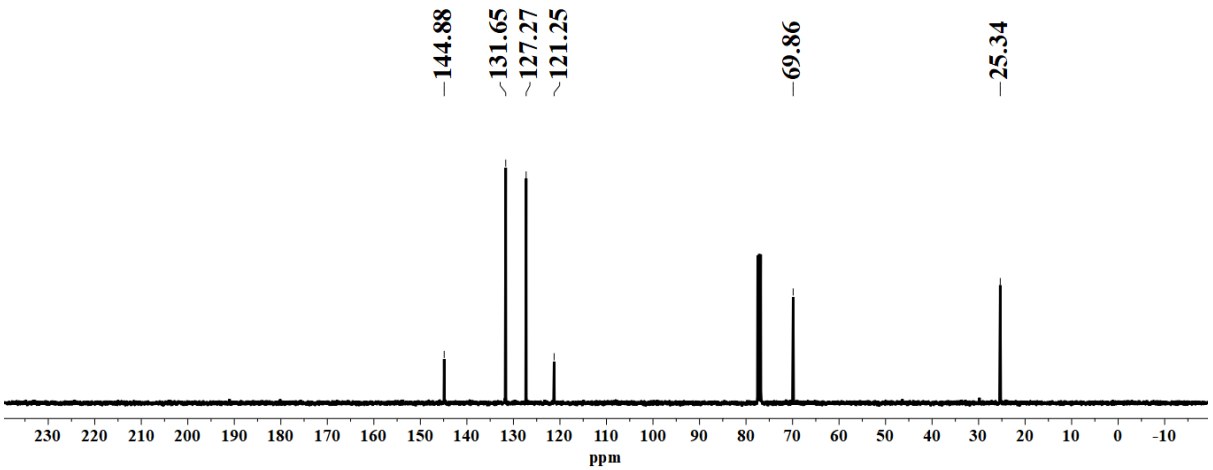

Figure S14. $^{13}C\{^{1}H\}$ NMR spectrum of **Ag** in $CDCl_3$ (101 MHz).

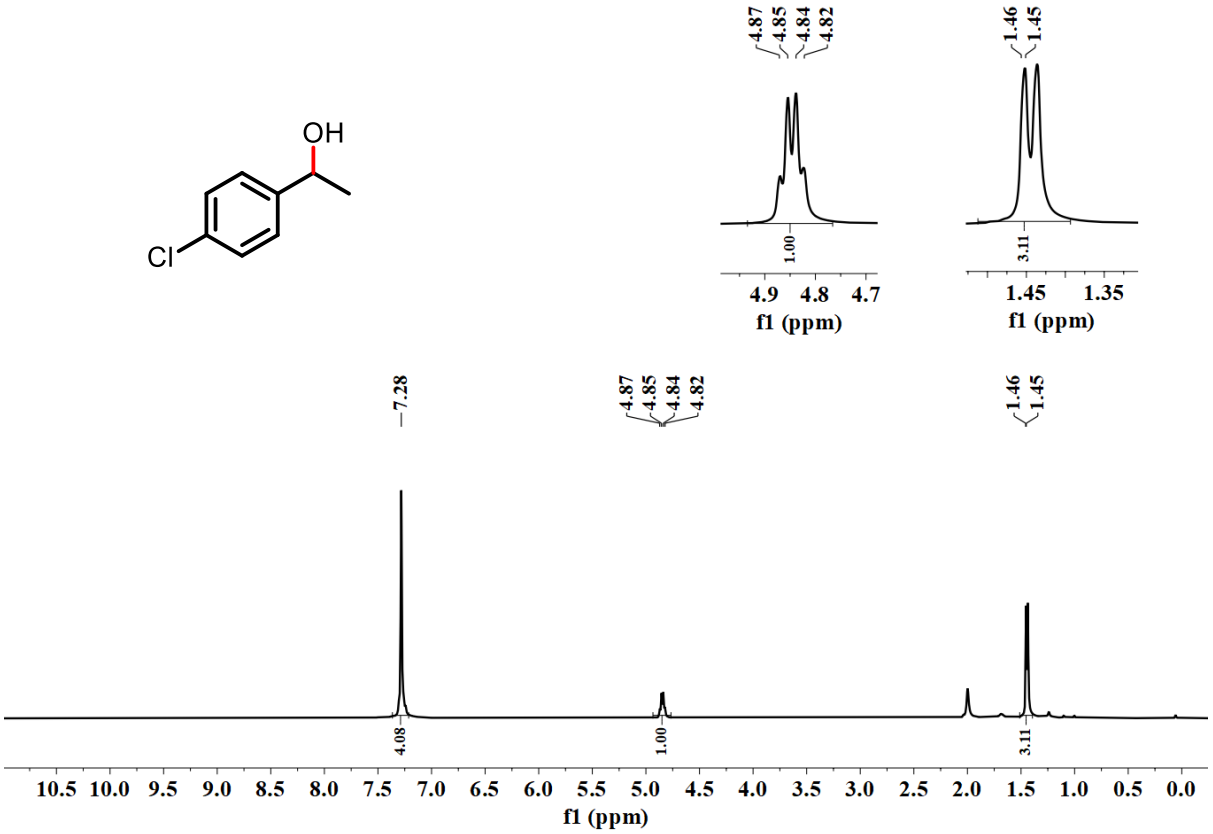

Figure S15. ^{1}H NMR spectrum of **Ah** in $CDCl_3$ (400 MHz).

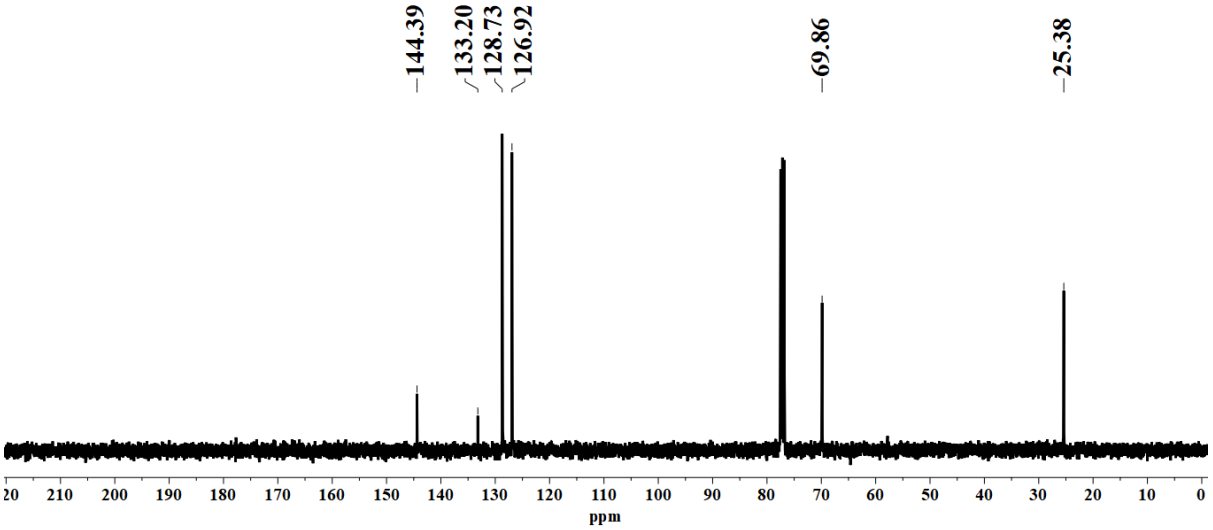

Figure S16. $^{13}C\{^{1}H\}$ NMR spectrum of **Ah** in $CDCl_3$ (101 MHz).

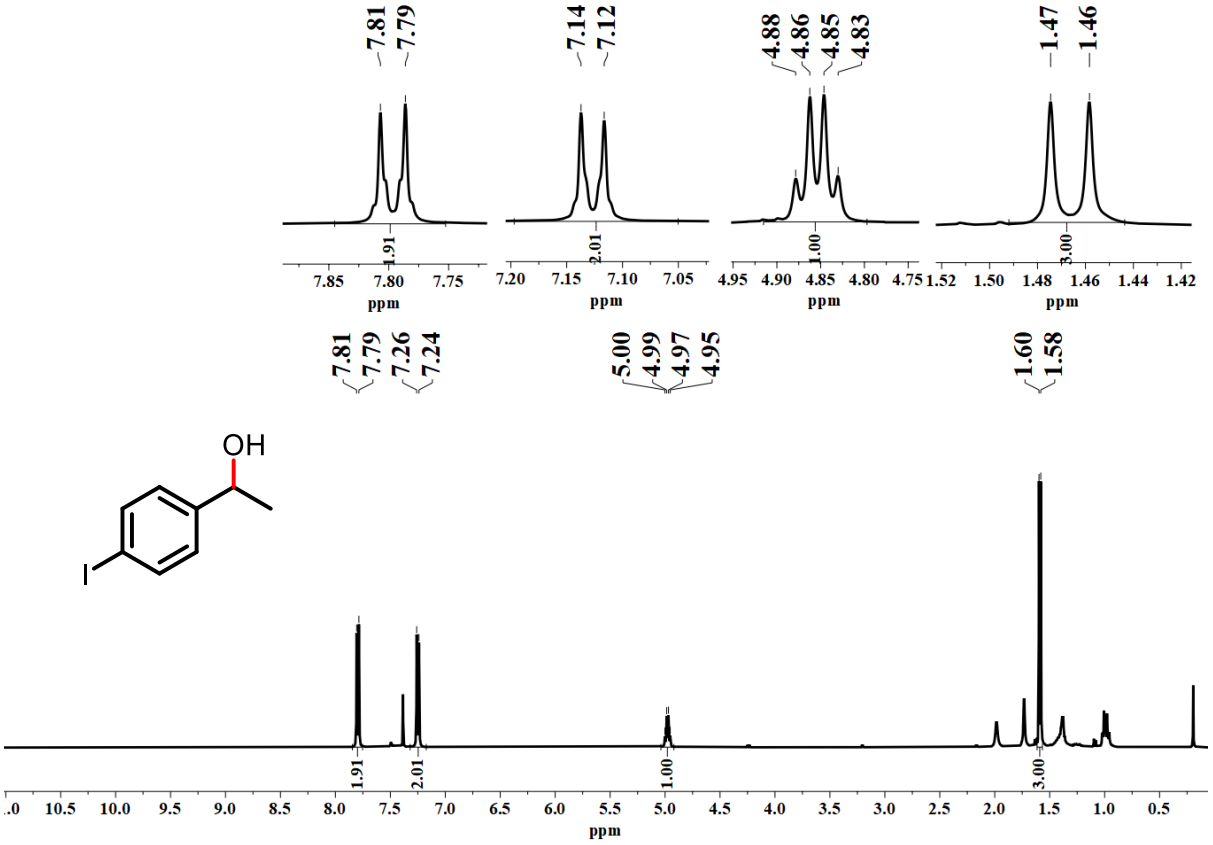

Figure S17. ^{1}H NMR spectrum of **Ai** in $CDCl_3$ (400 MHz).

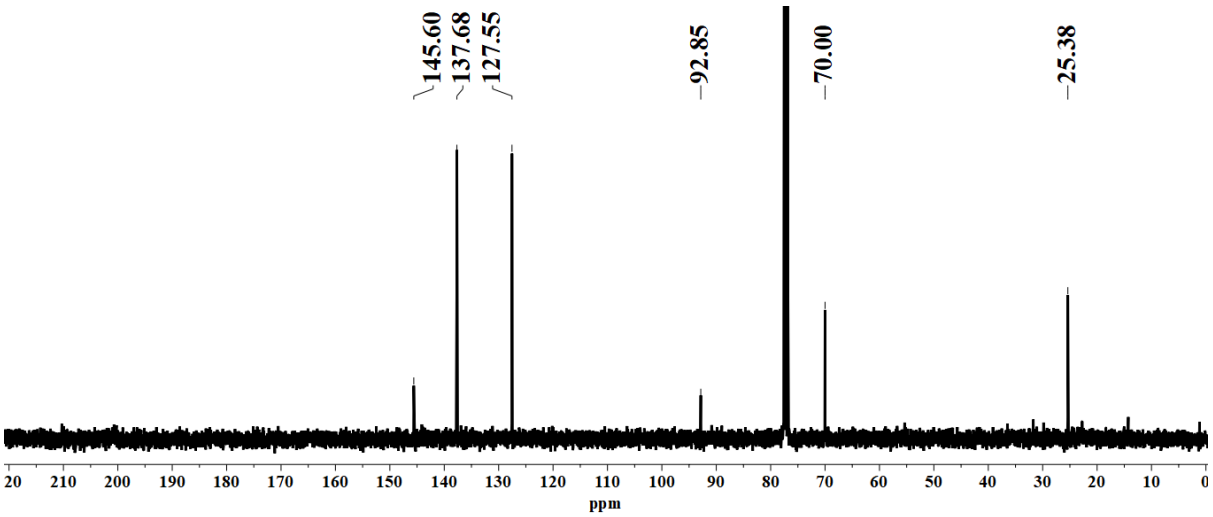

Figure S18. $^{13}C\{^{1}H\}$ NMR spectrum of **Ai** in $CDCl_3$ (101 MHz).

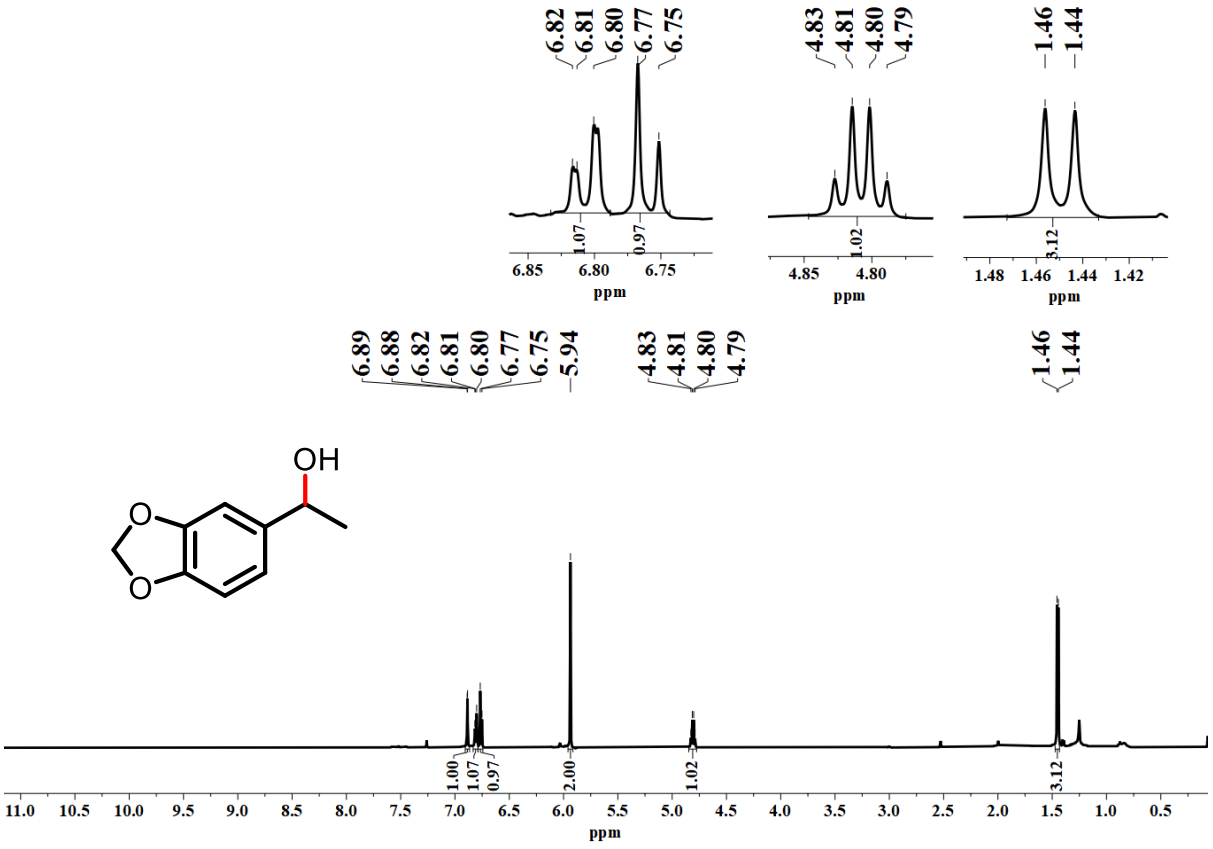

Figure S19. ^{1}H NMR spectrum of **Aj** in $CDCl_3$ (500 MHz).

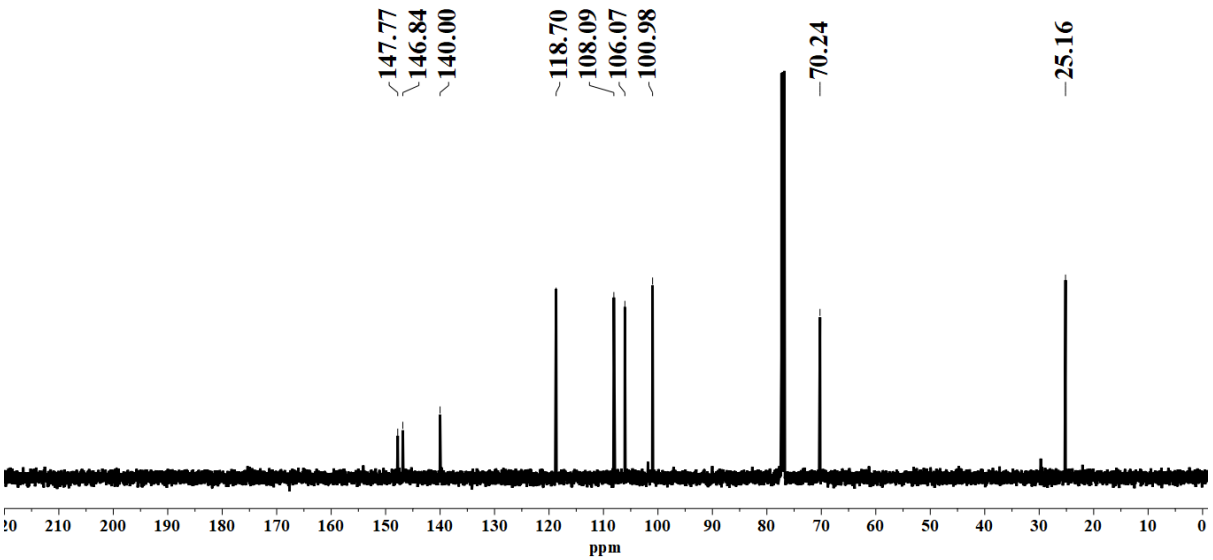

Figure S20. $^{13}C\{^{1}H\}$ NMR spectrum of **Aj** in $CDCl_3$ (126 MHz).

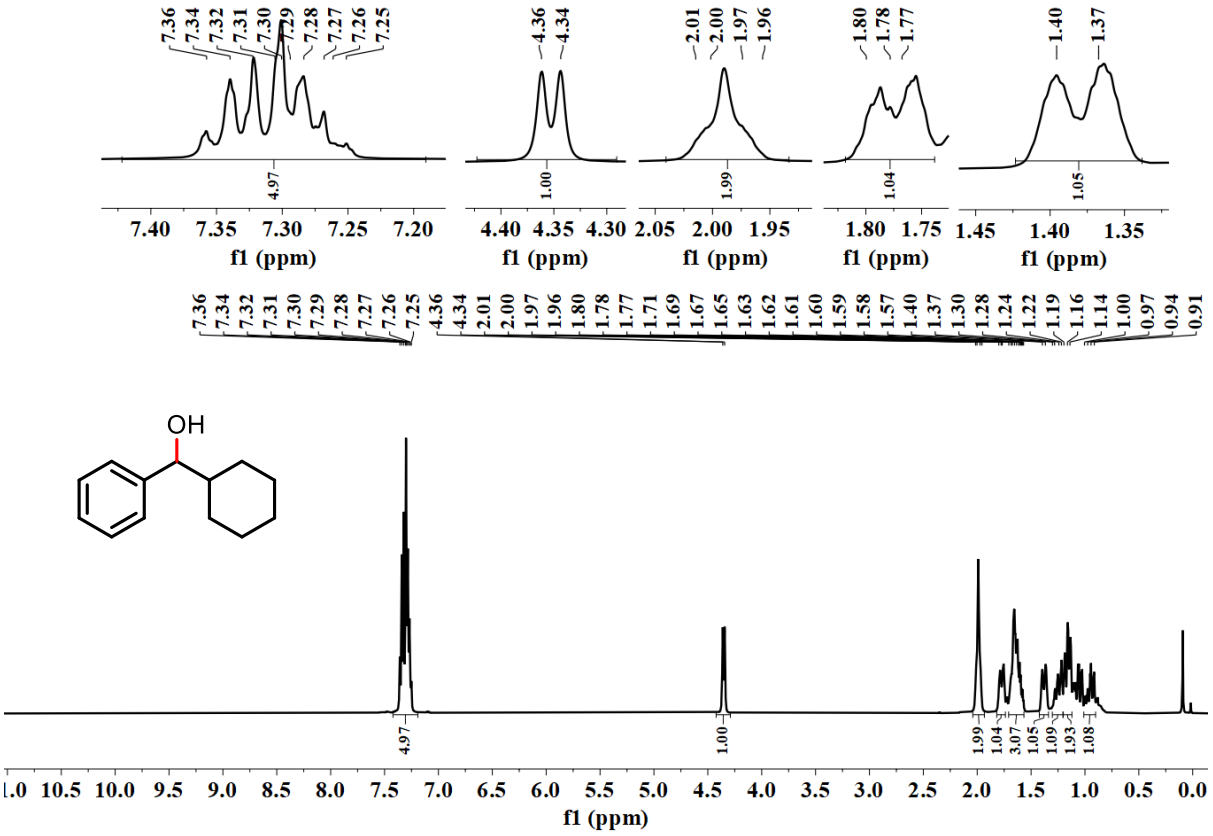

Figure S21. ^{1}H NMR spectrum of **Ak** in $CDCl_3$ (400 MHz).

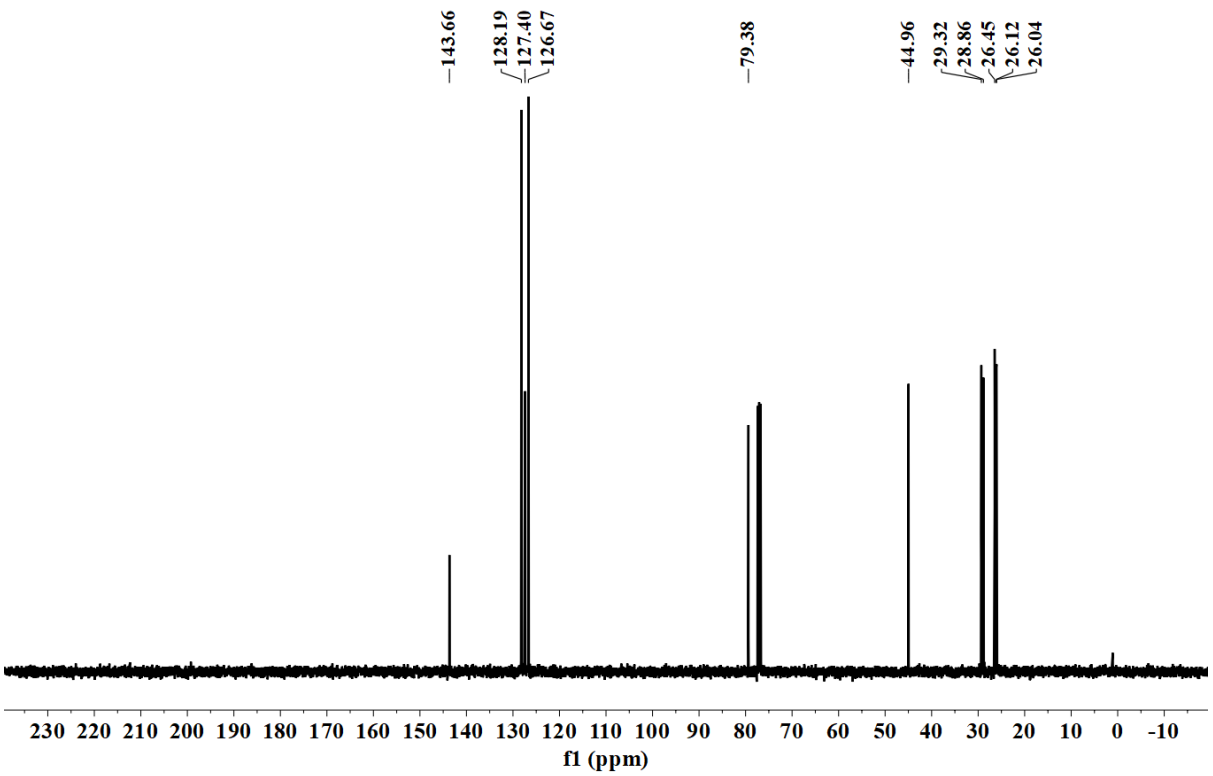

Figure S22. $^{13}C\{^{1}H\}$ NMR spectrum of **Ak** in $CDCl_3$ (101 MHz).

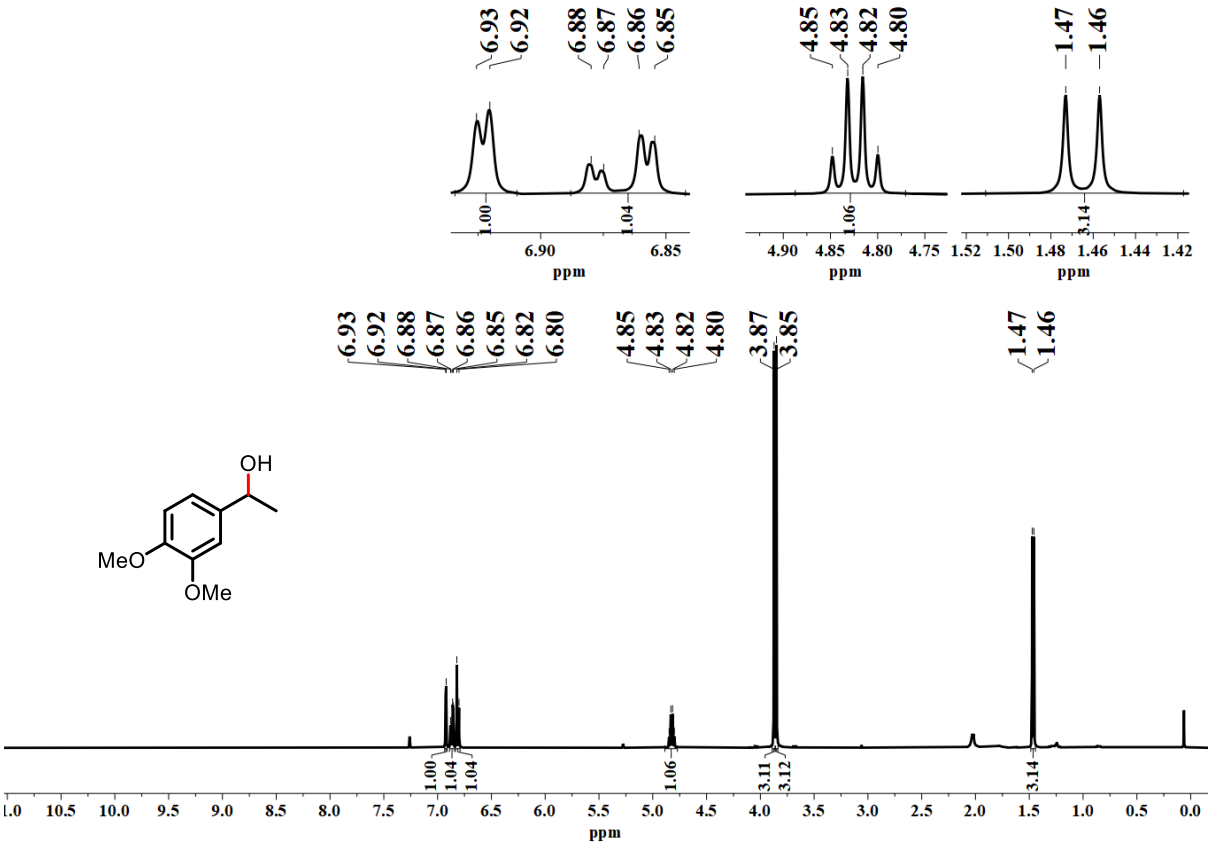

Figure S23. ^{1}H NMR spectrum of **Al** in $CDCl_3$ (400 MHz).

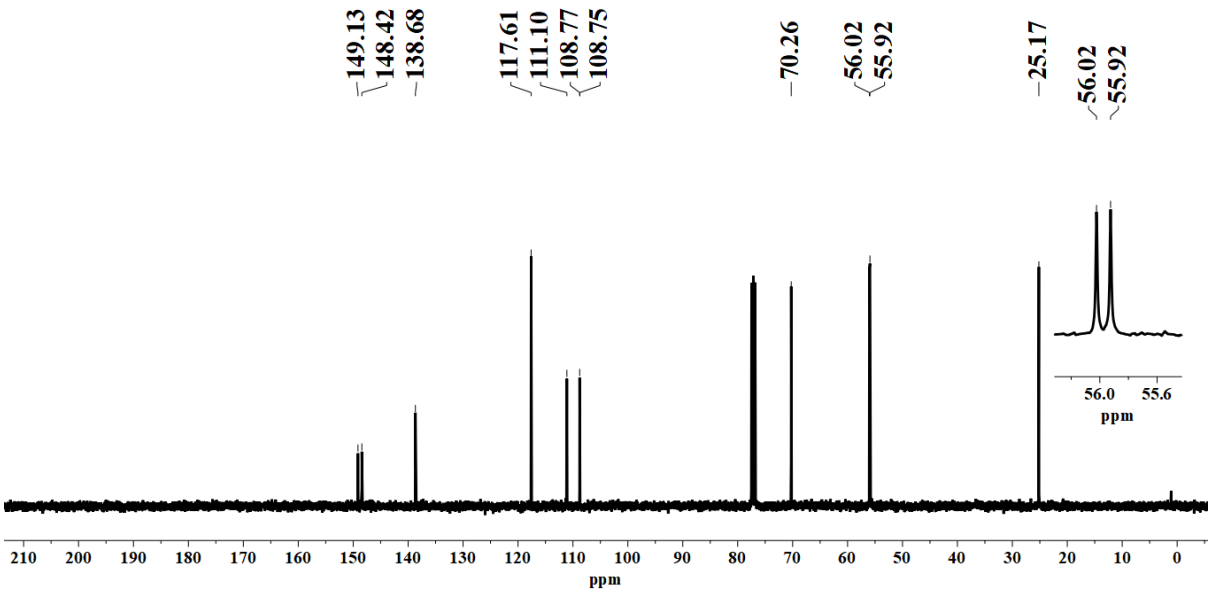

Figure S24. $^{13}C\{^{1}H\}$ NMR spectrum of **Al** in $CDCl_3$ (101 MHz).

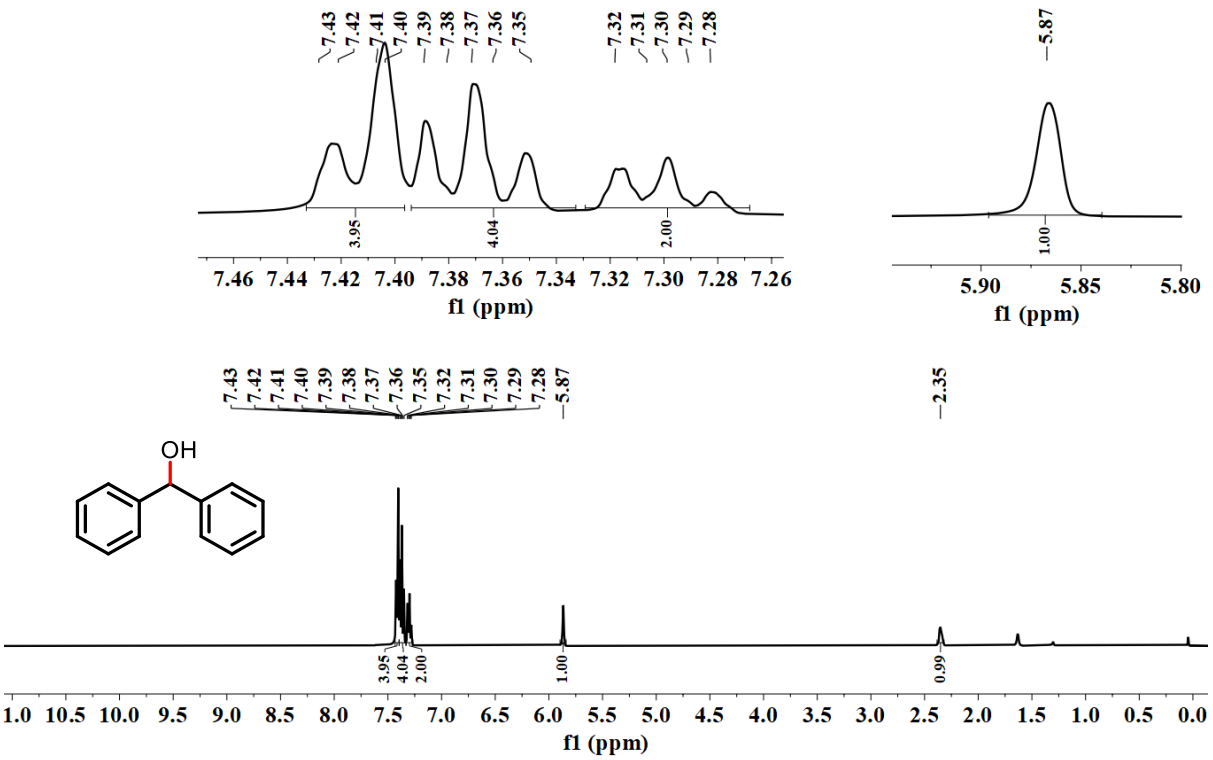

Figure S25. ^{1}H NMR spectrum of **Am** in $CDCl_3$ (400 MHz).

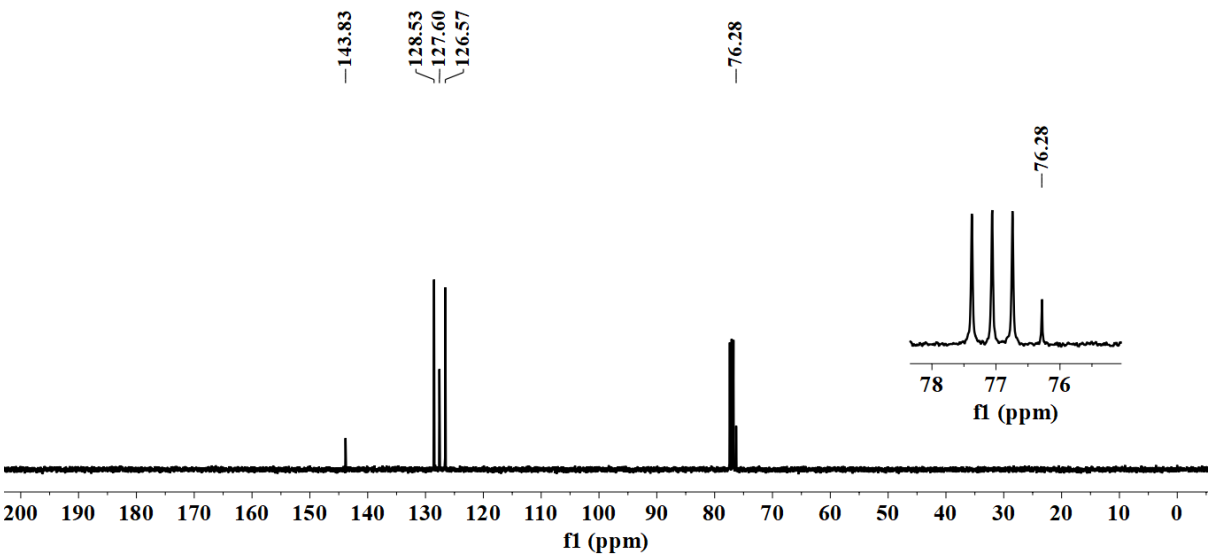

Figure S26. $^{13}C\{^{1}H\}$ NMR spectrum of **Am** in $CDCl_3$ (101 MHz).

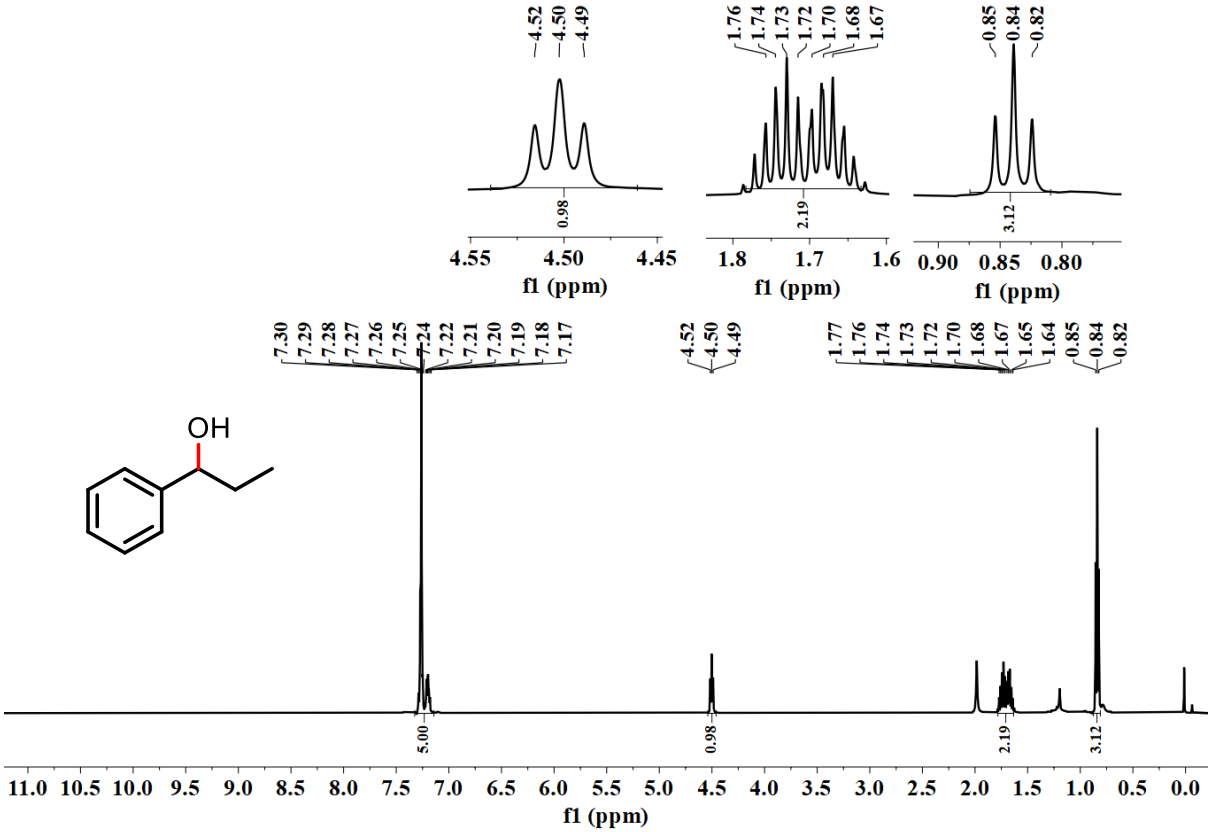

Figure S27. ^{1}H NMR spectrum of **An** in $CDCl_3$ (500 MHz).

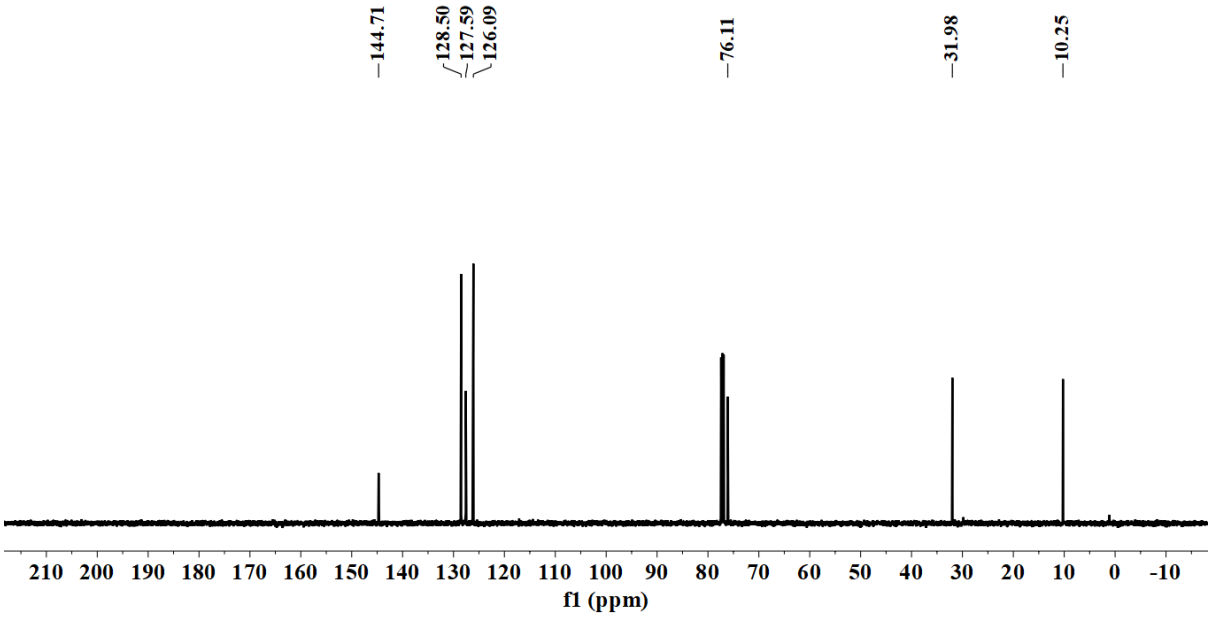

Figure S28. $^{13}C\{^{1}H\}$ NMR spectrum of **An** in $CDCl_3$ (126 MHz).

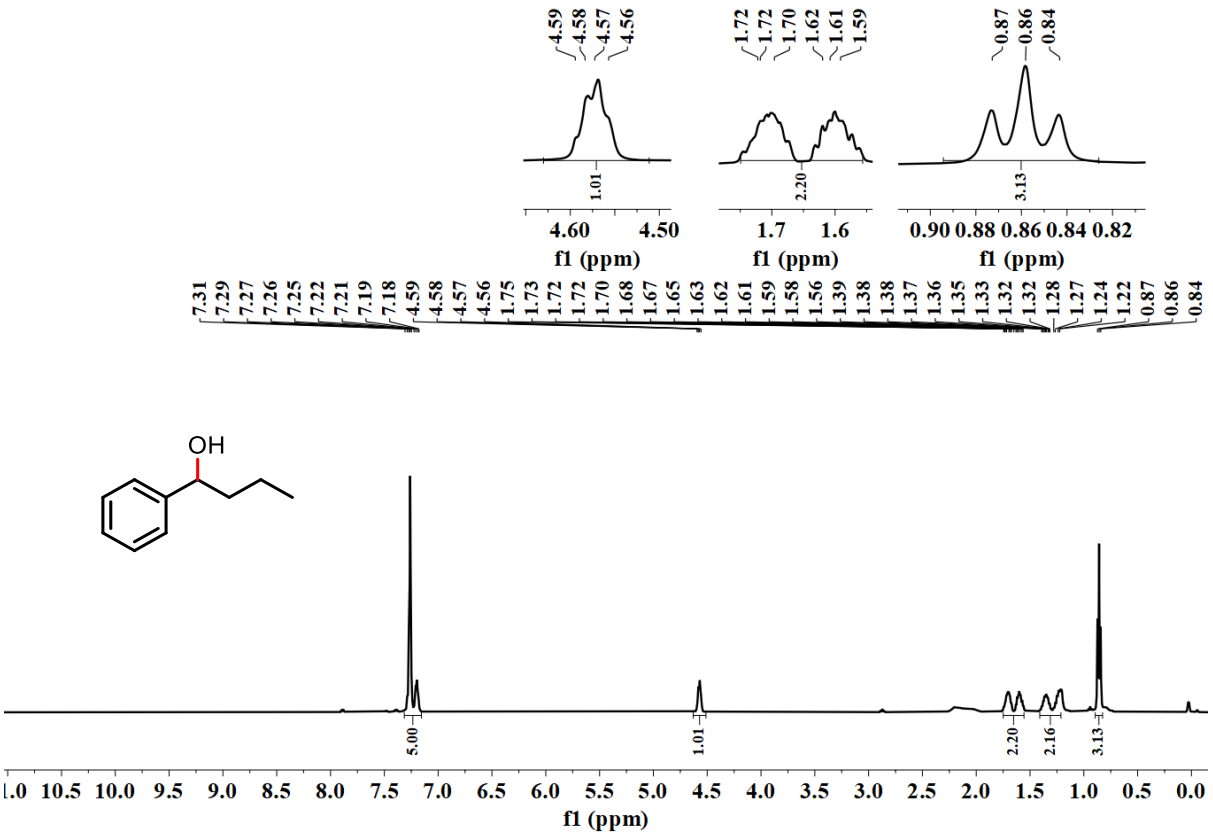

Figure S29. ^{1}H NMR spectrum of **Ao** in $CDCl_3$ (500 MHz).

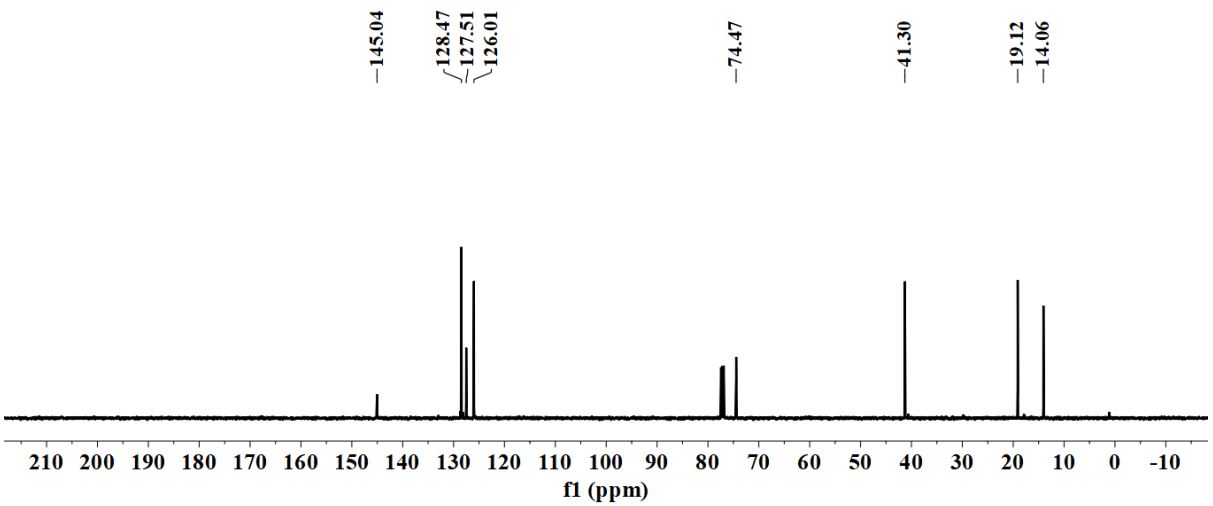

Figure S30. $^{13}C\{^{1}H\}$ NMR spectrum of **Ao** in $CDCl_3$ (126 MHz).

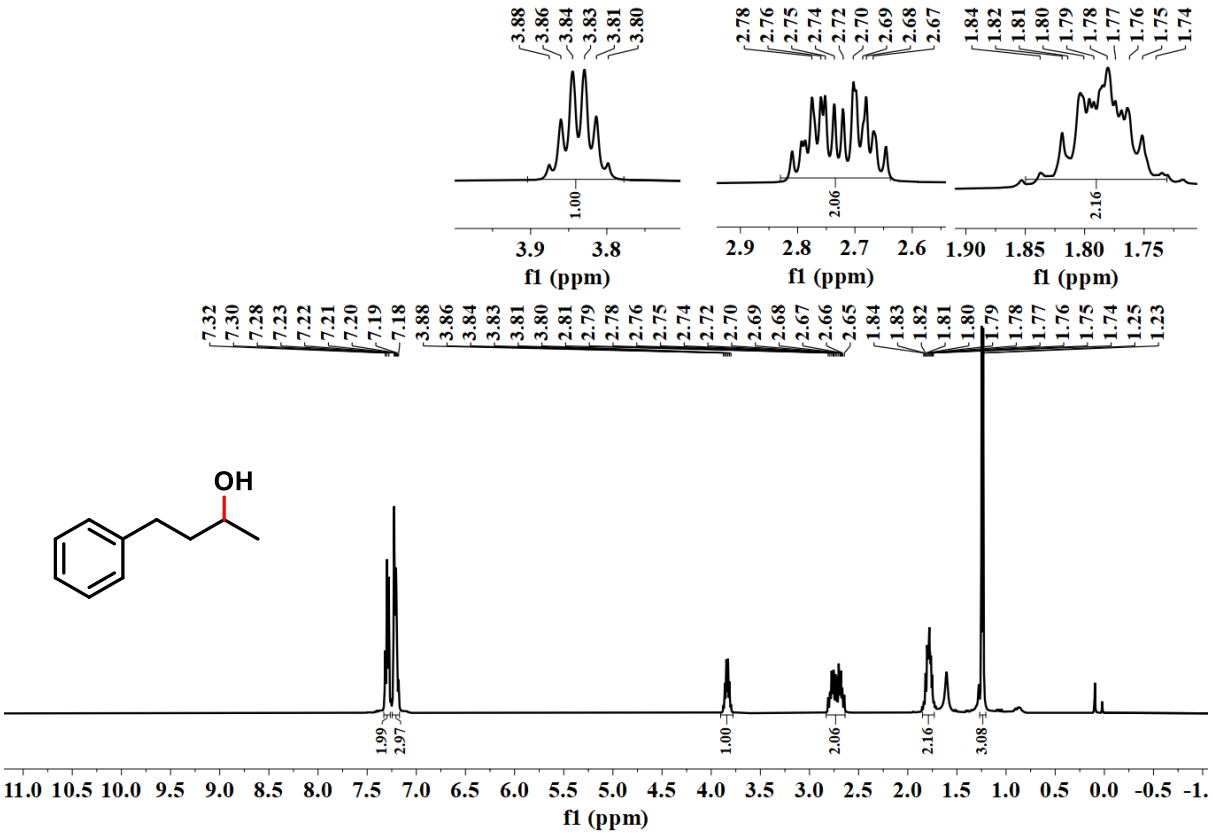

Figure S31. ^{1}H NMR spectrum of **Ap** in $CDCl_3$ (400 MHz).

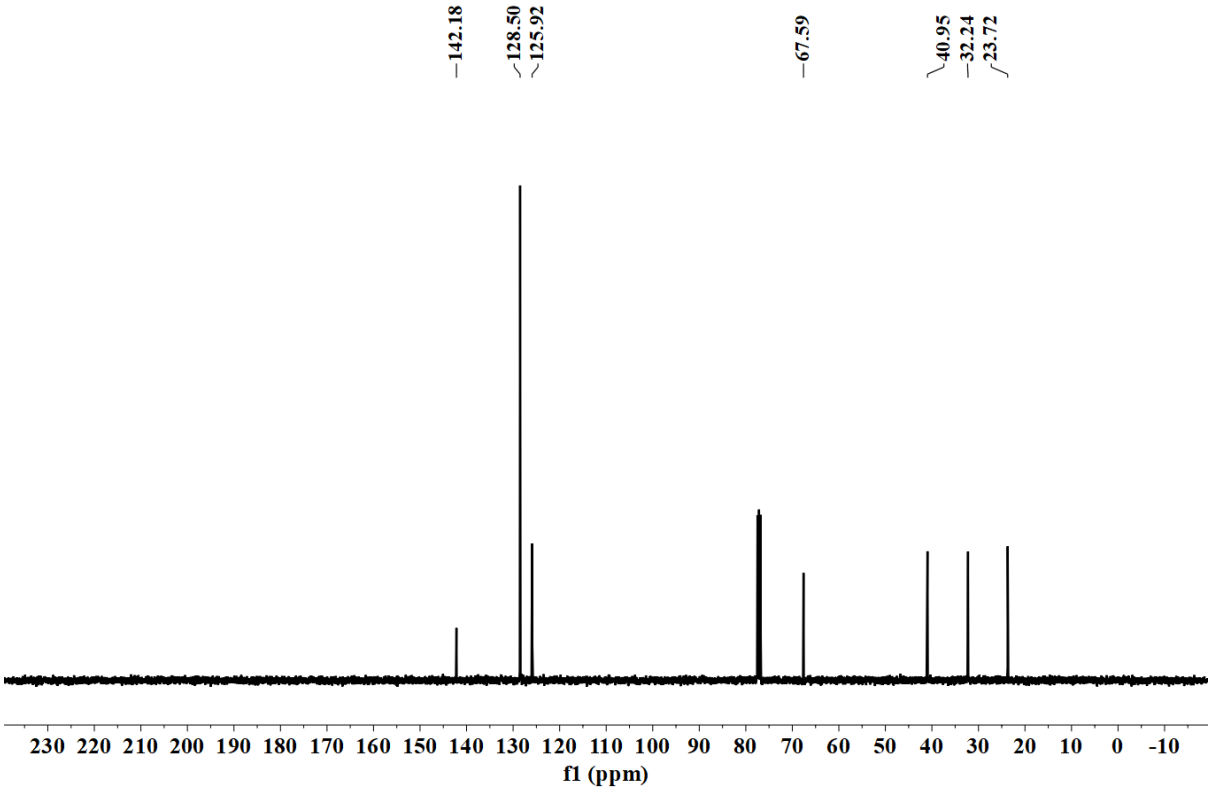

Figure S32. $^{13}C\{^{1}H\}$ NMR spectrum of **Ap** in $CDCl_3$ (101 MHz).

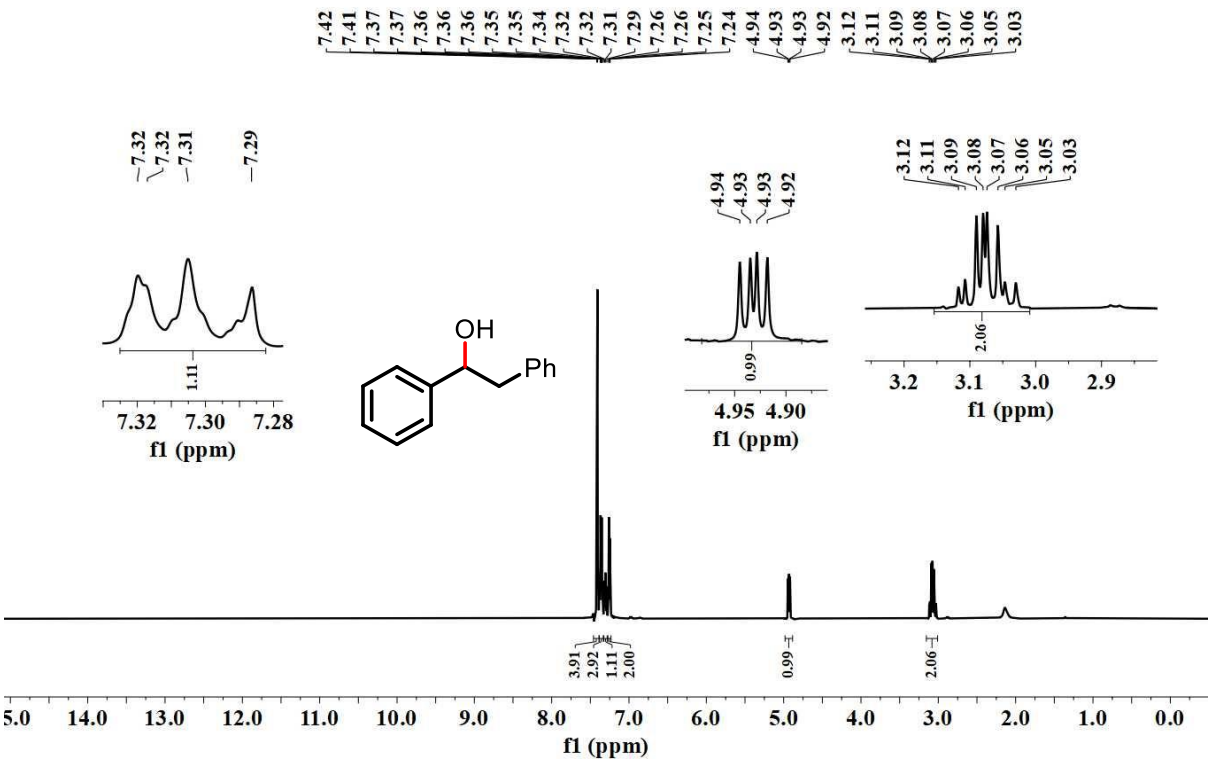

Figure S33. ^{1}H NMR spectrum of **Aq** in $CDCl_3$ (500 MHz).

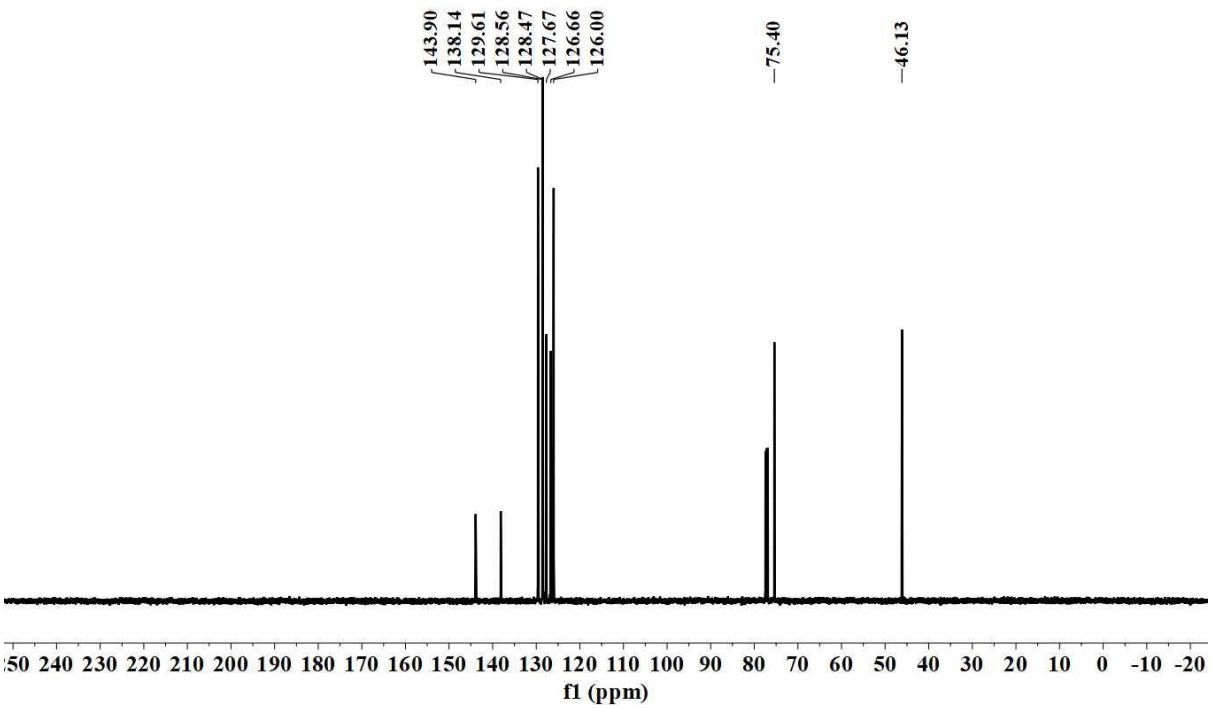

Figure S34. $^{13}C\{^{1}H\}$ NMR spectrum of **Aq** in $CDCl_3$ (126 MHz).

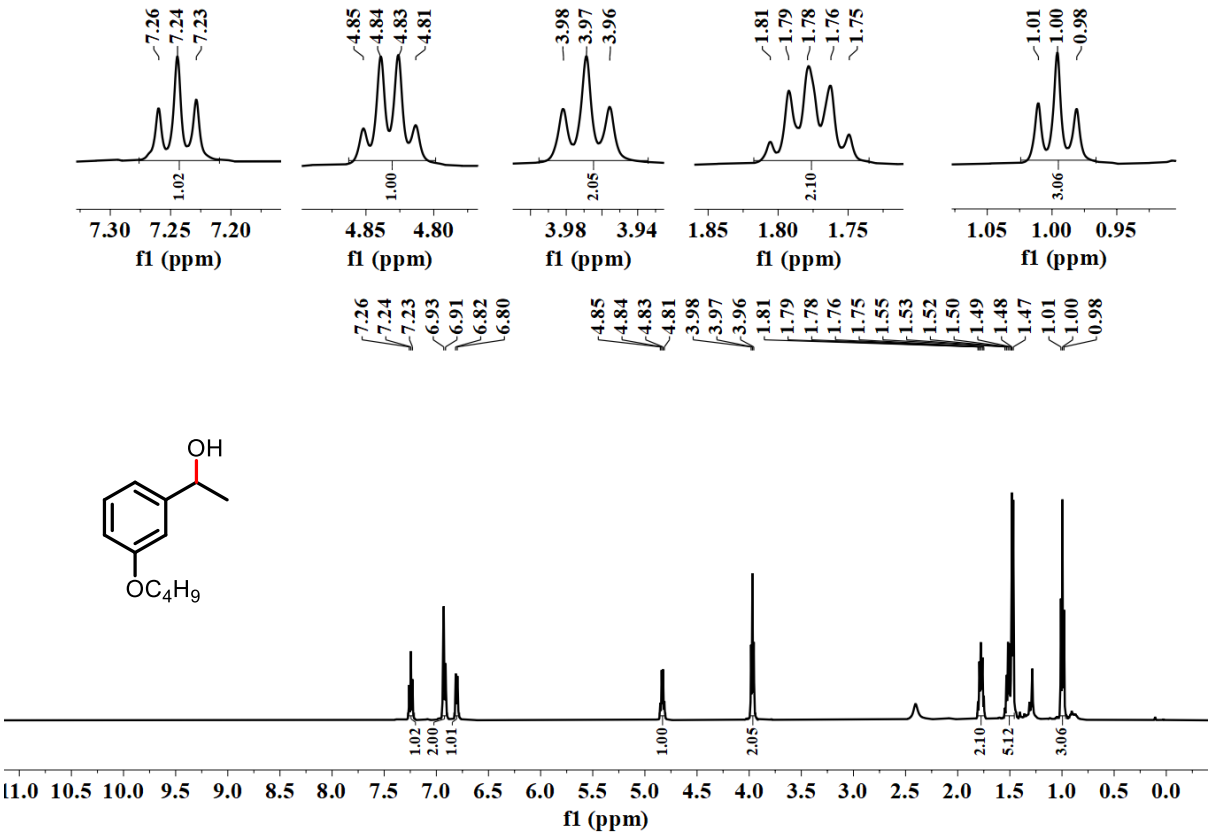

Figure S35. ^{1}H NMR spectrum of **As** in $CDCl_3$ (500 MHz).

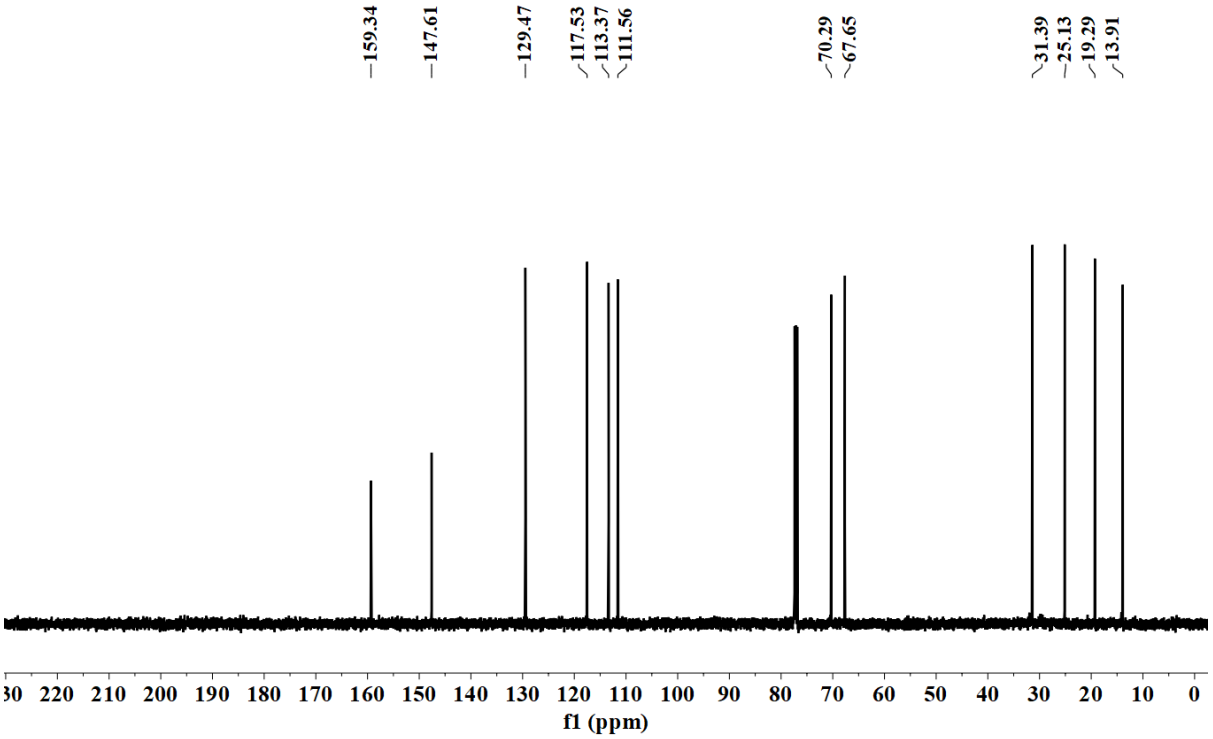

Figure S36. $^{13}C\{^{1}H\}$ NMR spectrum of **As** in $CDCl_3$ (126 MHz).

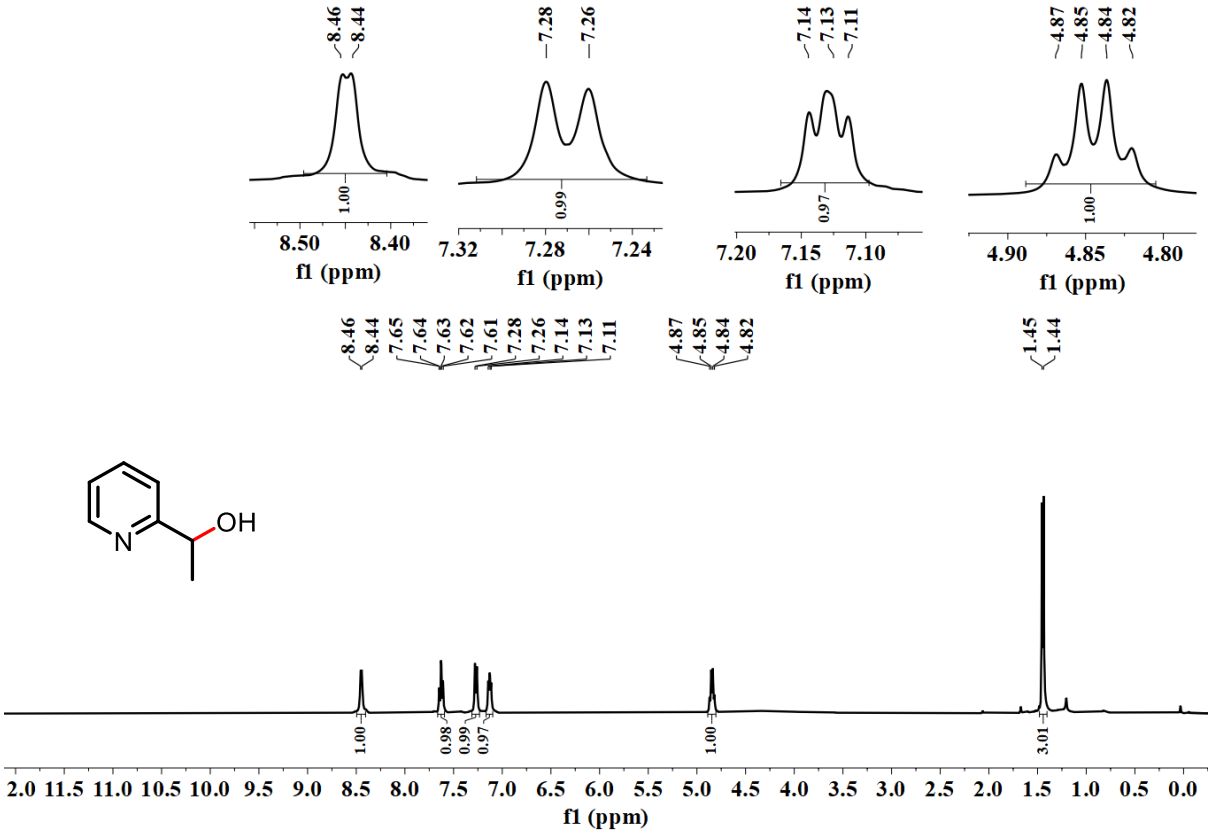

Figure S37. ^{1}H NMR spectrum of **At** in $CDCl_3$ (400 MHz).

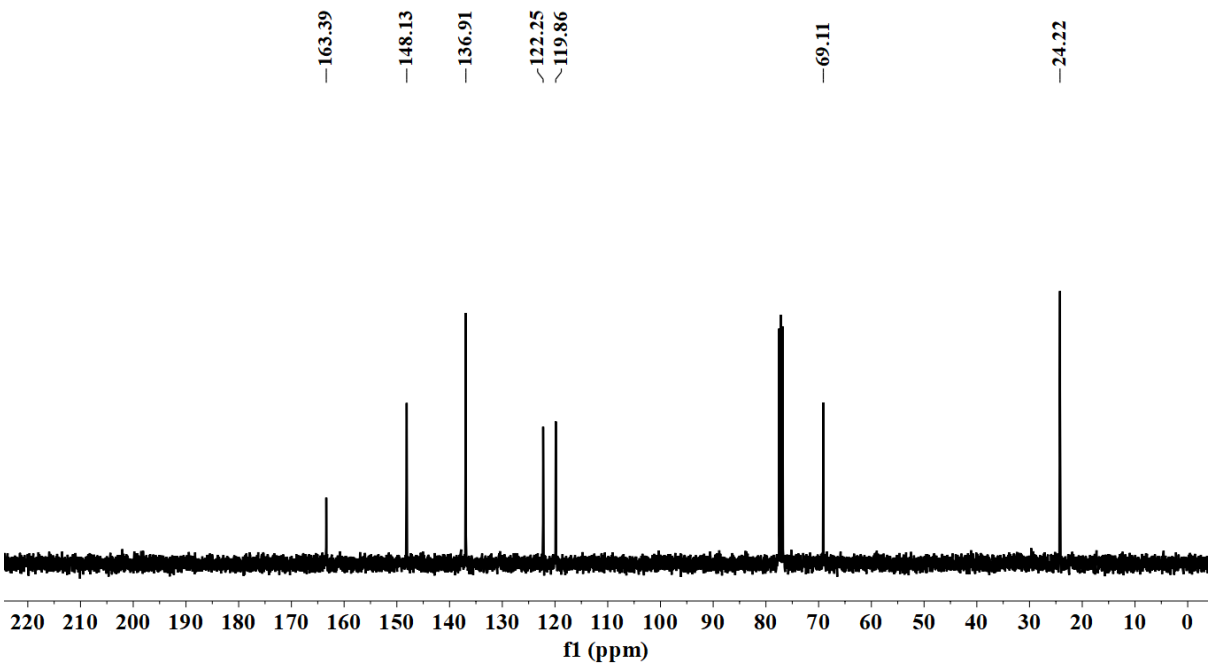

Figure S38. $^{13}C\{^{1}H\}$ NMR spectrum of **At** in $CDCl_3$ (101 MHz).

NMR spectra of catalytic products of acetophenone derivatives reduction

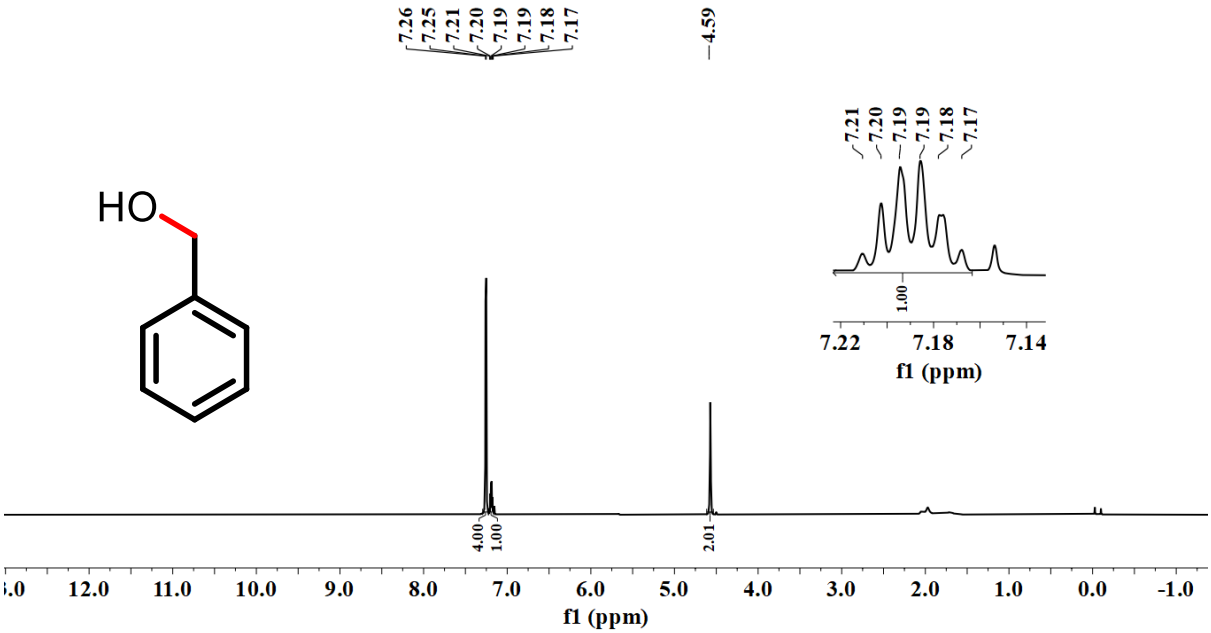

Figure S39. ^{1}H NMR spectrum of **Ba** in $CDCl_3$ (400 MHz).

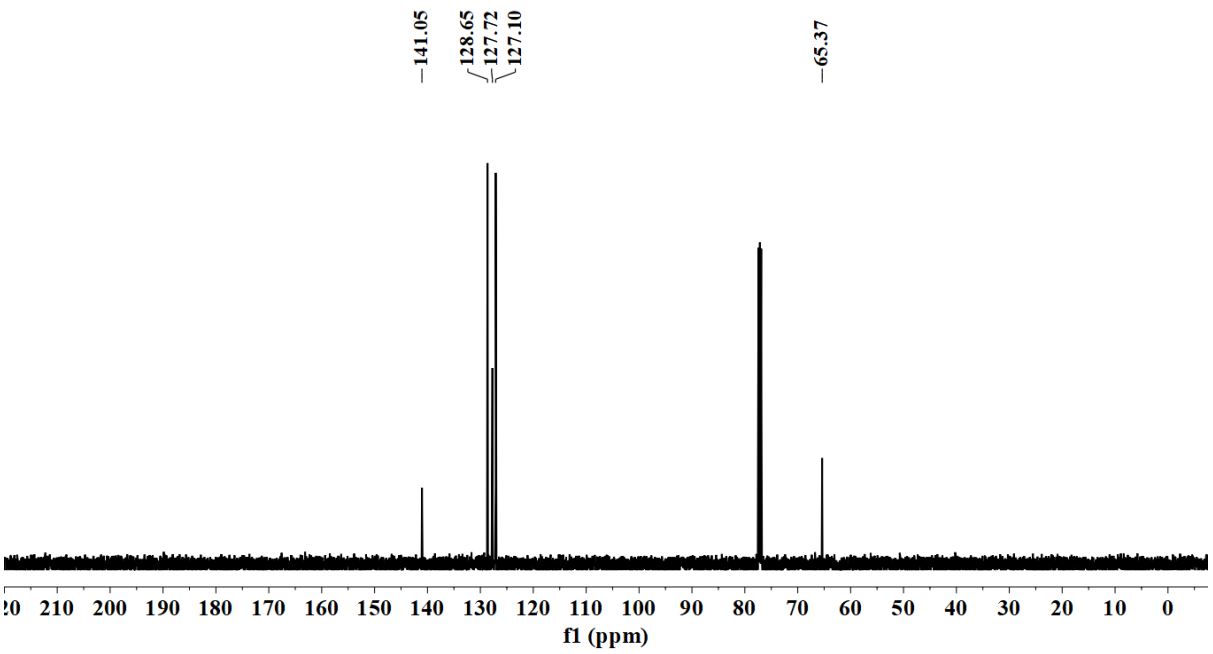

Figure S40. $^{13}C\{^{1}H\}$ NMR spectrum of **Ba** in $CDCl_3$ (101 MHz).

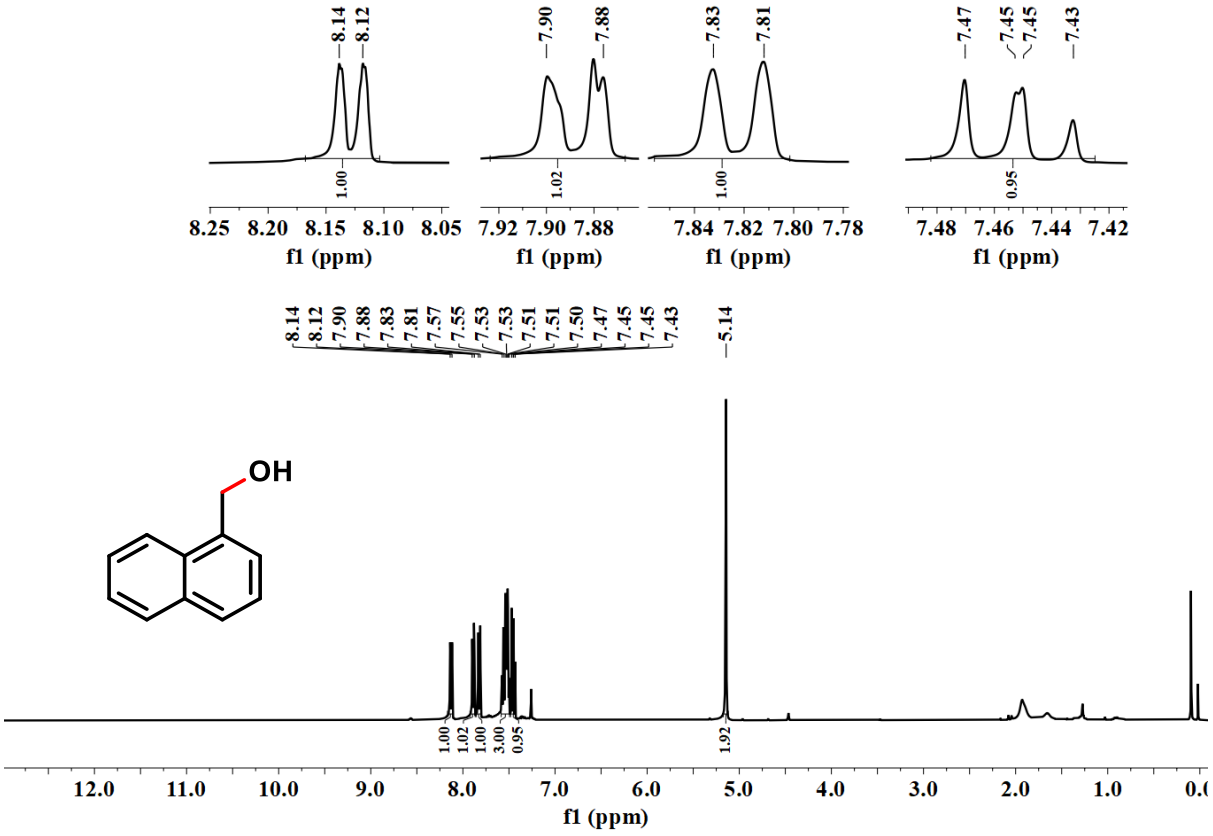

Figure S41. ^{1}H NMR spectrum of **Bb** in $CDCl_3$ (400 MHz).

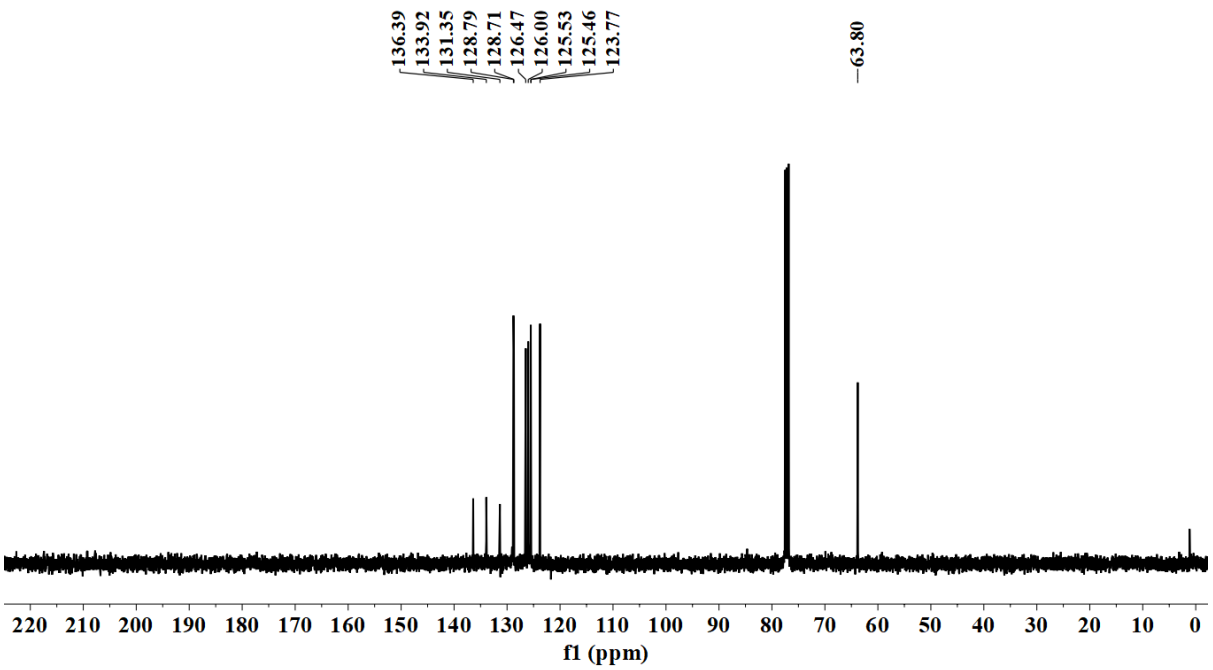

Figure S42. $^{13}C\{^{1}H\}$ NMR spectrum of **Bb** in $CDCl_3$ (101 MHz).

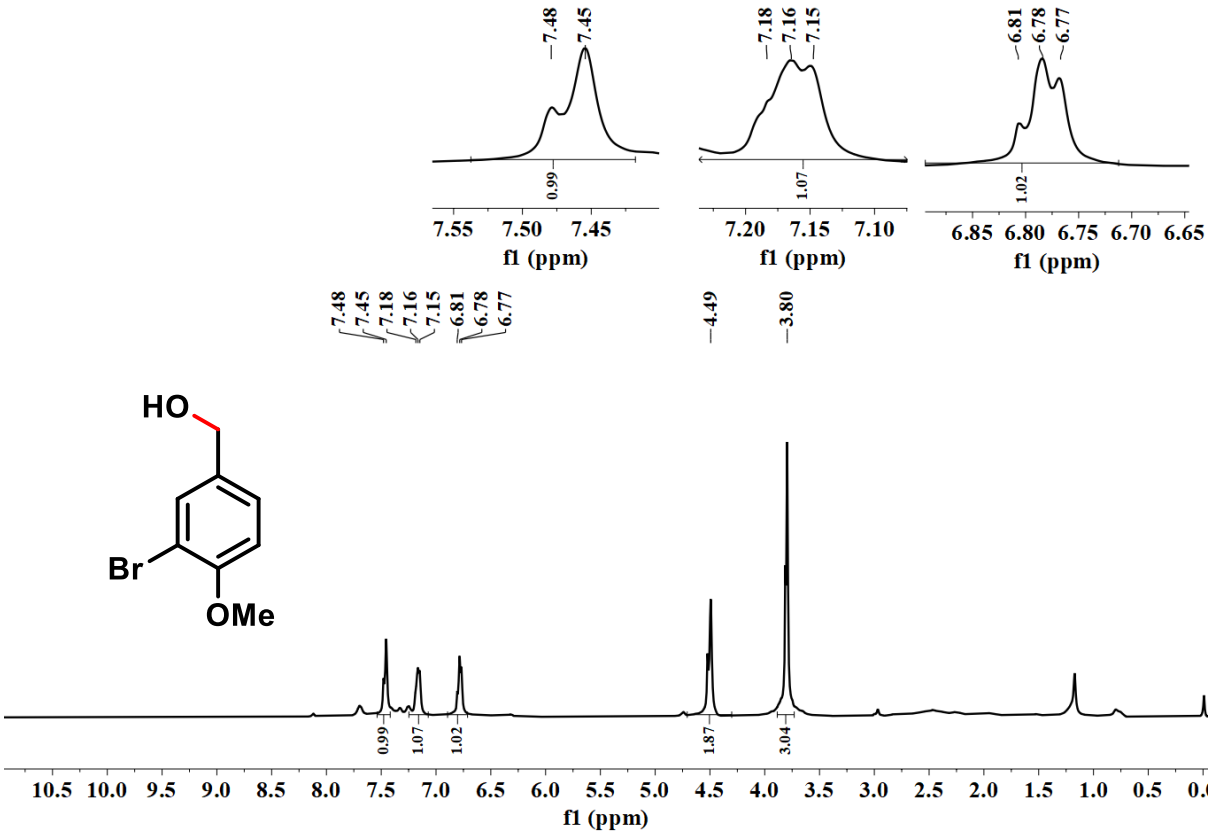

Figure S43. ^{1}H NMR spectrum of **Bc** in $CDCl_3$ (500 MHz).

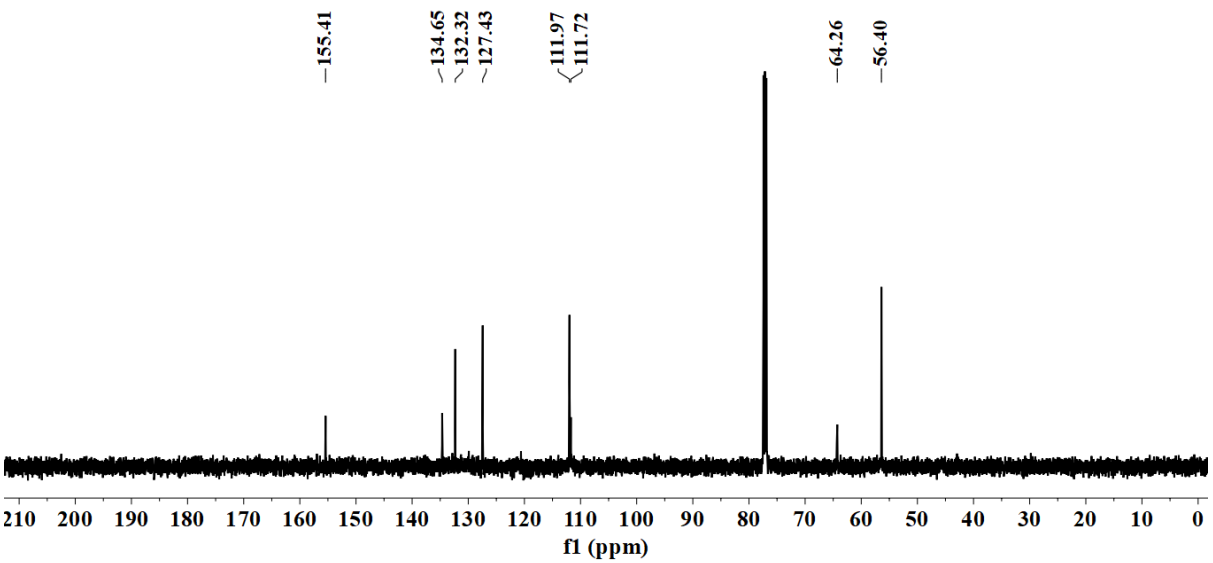

Figure S44. $^{13}C\{^{1}H\}$ NMR spectrum of **Bc** in $CDCl_3$ (126 MHz).

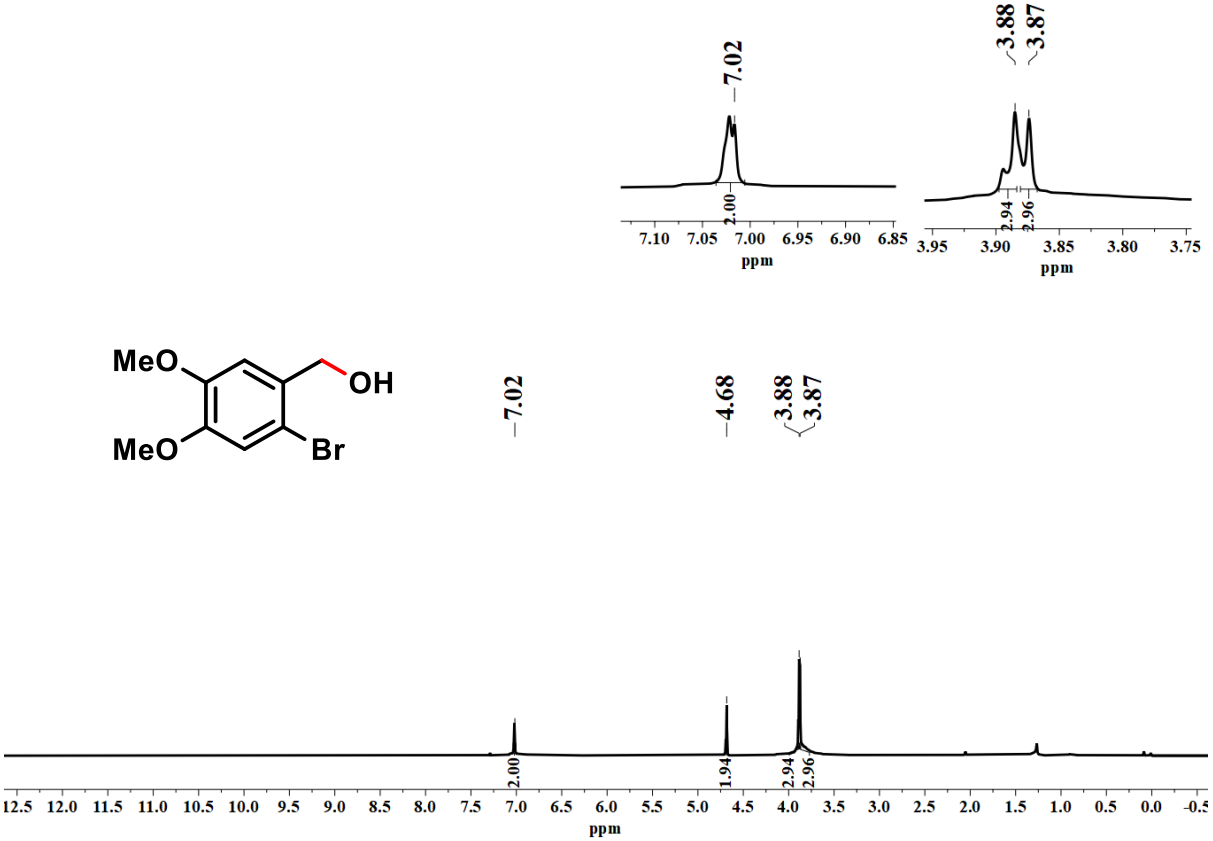

Figure S45. ^{1}H NMR spectrum of **Bd** in $CDCl_3$ (500 MHz).

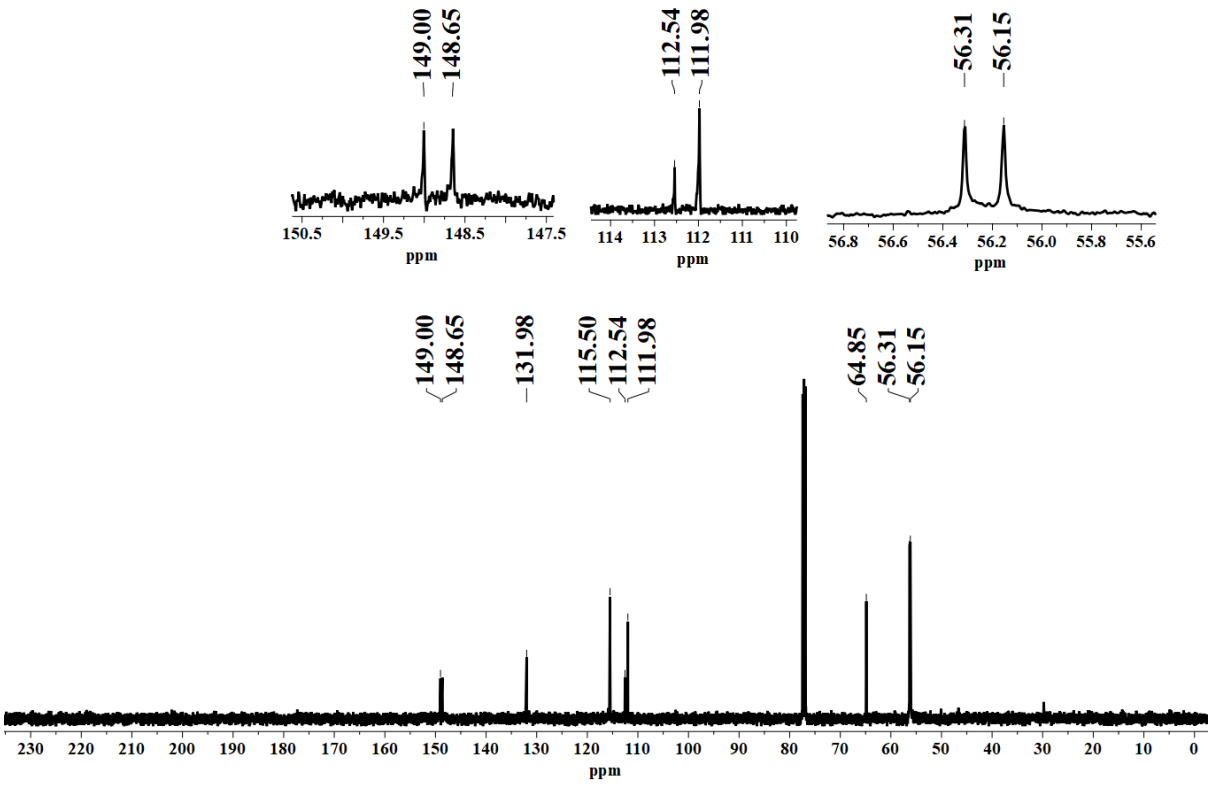

Figure S46. $^{13}C\{^{1}H\}$ NMR spectrum of **Bd** in $CDCl_3$ (126 MHz).

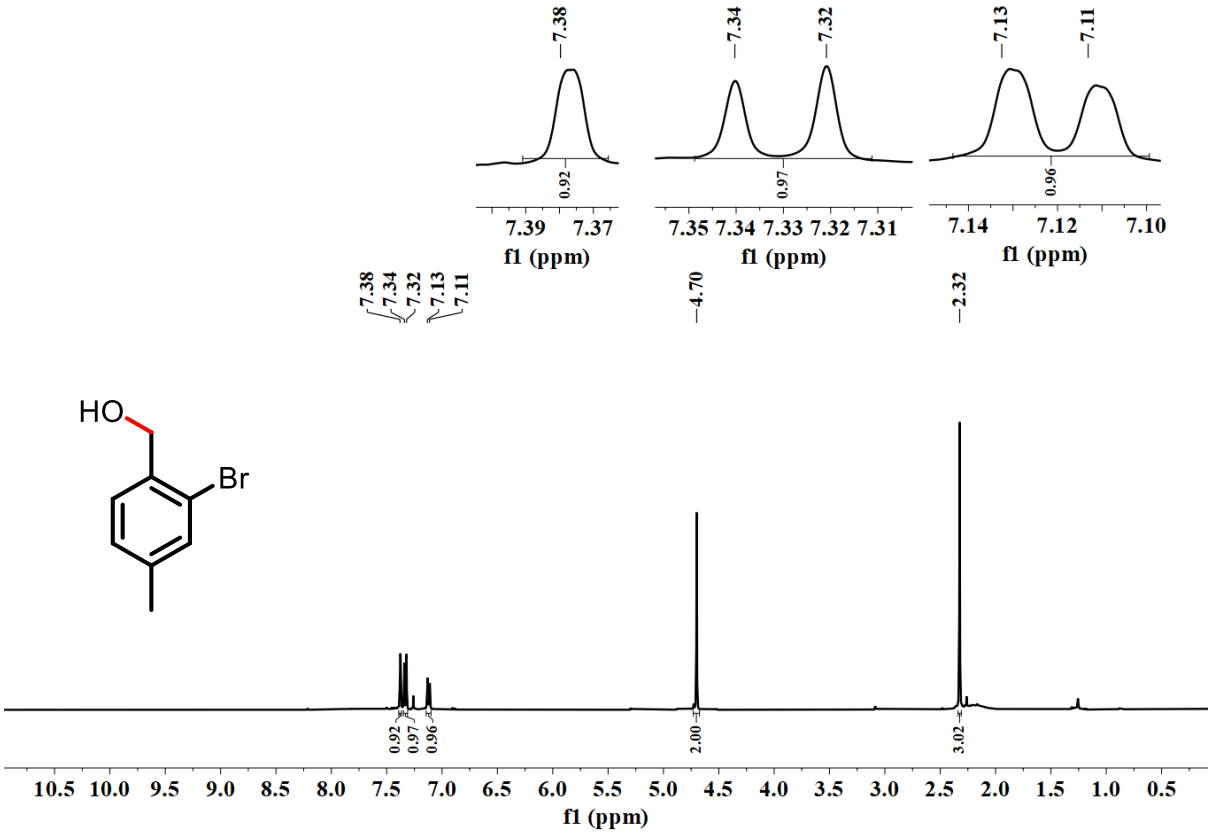

Figure S47. ^{1}H NMR spectrum of **Be** in $CDCl_3$ (400 MHz).

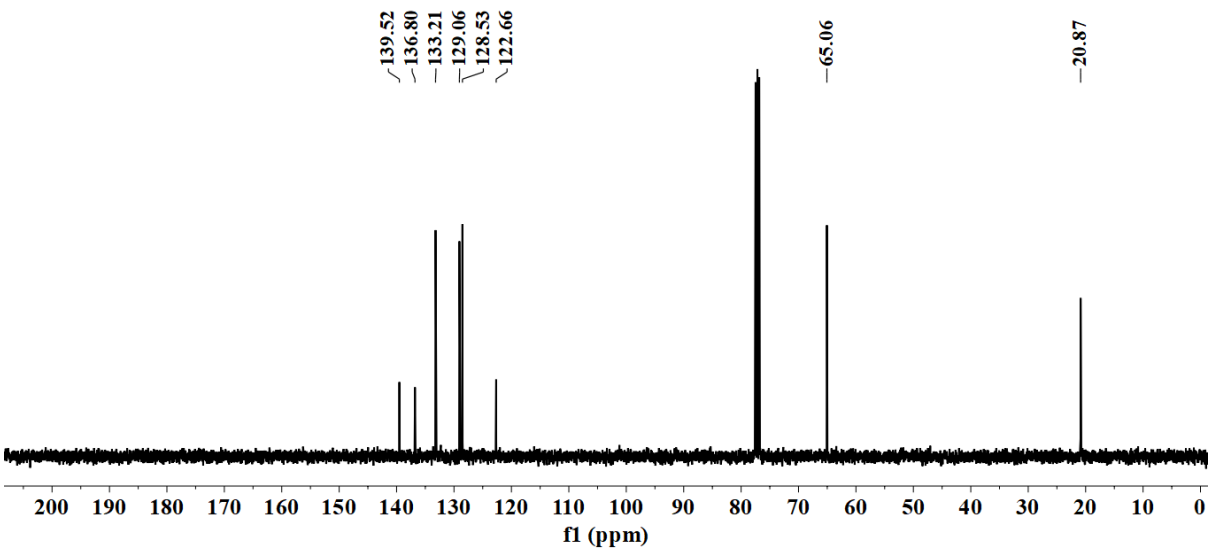

Figure S48. $^{13}C\{^{1}H\}$ NMR spectrum of **Be** in $CDCl_3$ (101 MHz).

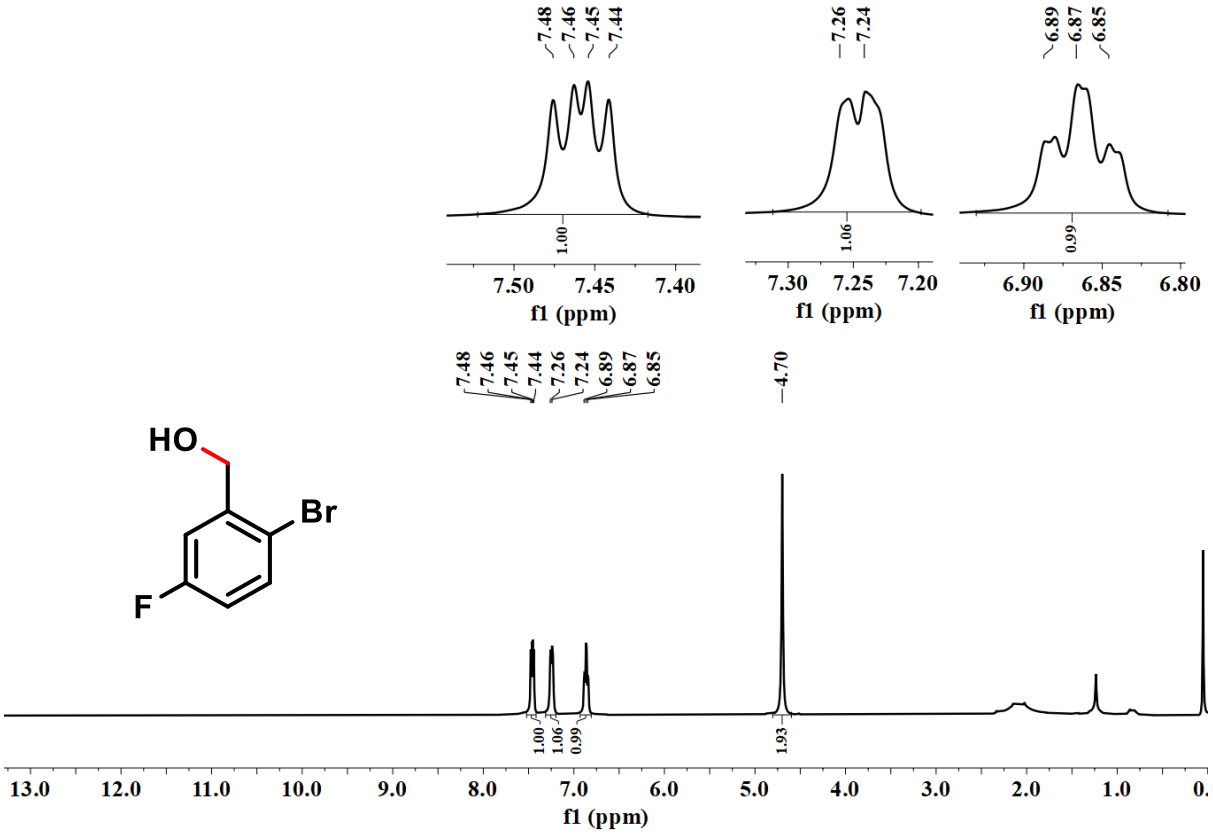

Figure S49. ^{1}H NMR spectrum of **Bf** in $CDCl_3$ (400 MHz).

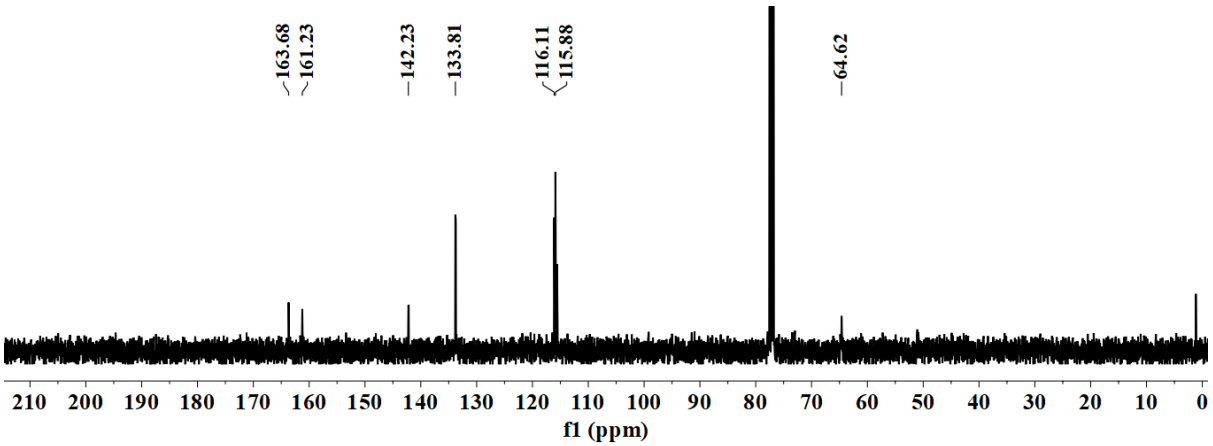

Figure S50. $^{13}C\{^{1}H\}$ NMR spectrum of **Bf** in $CDCl_3$ (101 MHz).

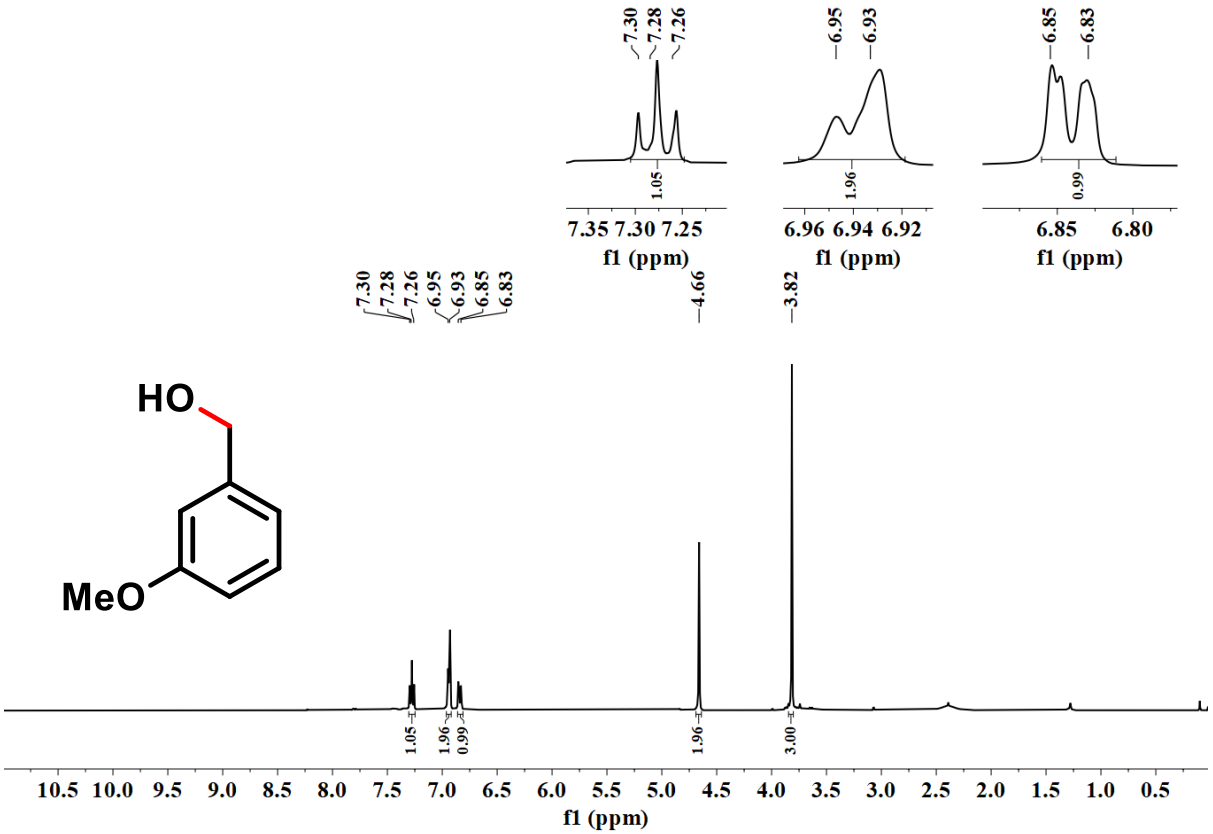

Figure S51. ^{1}H NMR spectrum of **Bg** in $CDCl_3$ (400 MHz).

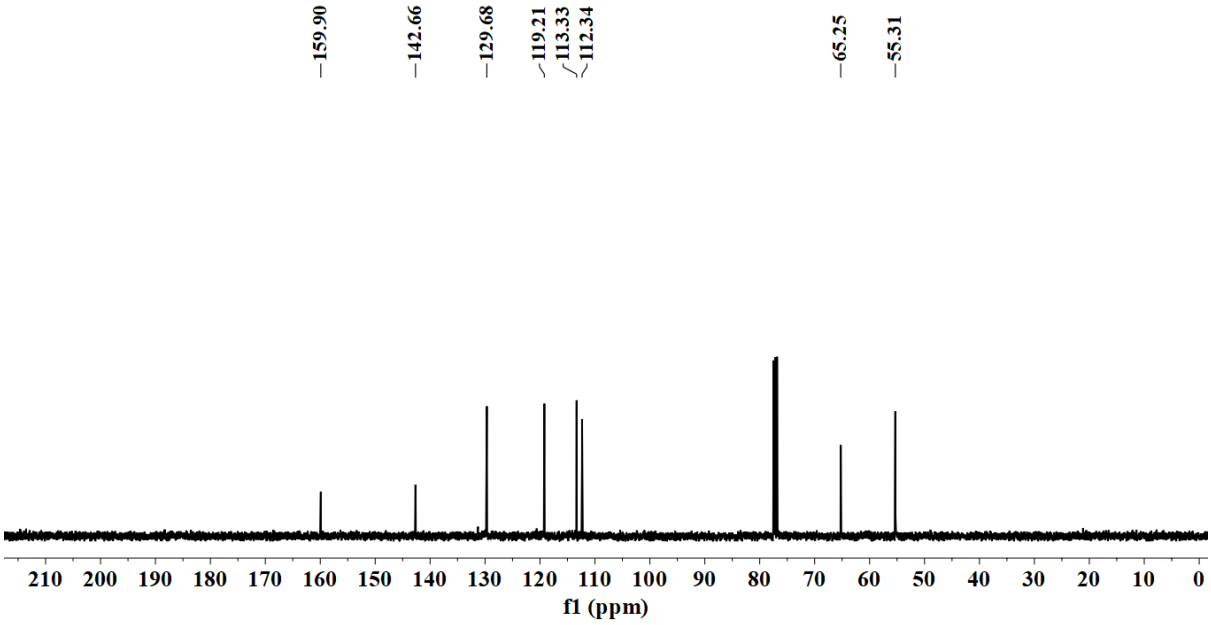

Figure S52. $^{13}C\{^{1}H\}$ NMR spectrum of **Bg** in $CDCl_3$ (101 MHz).

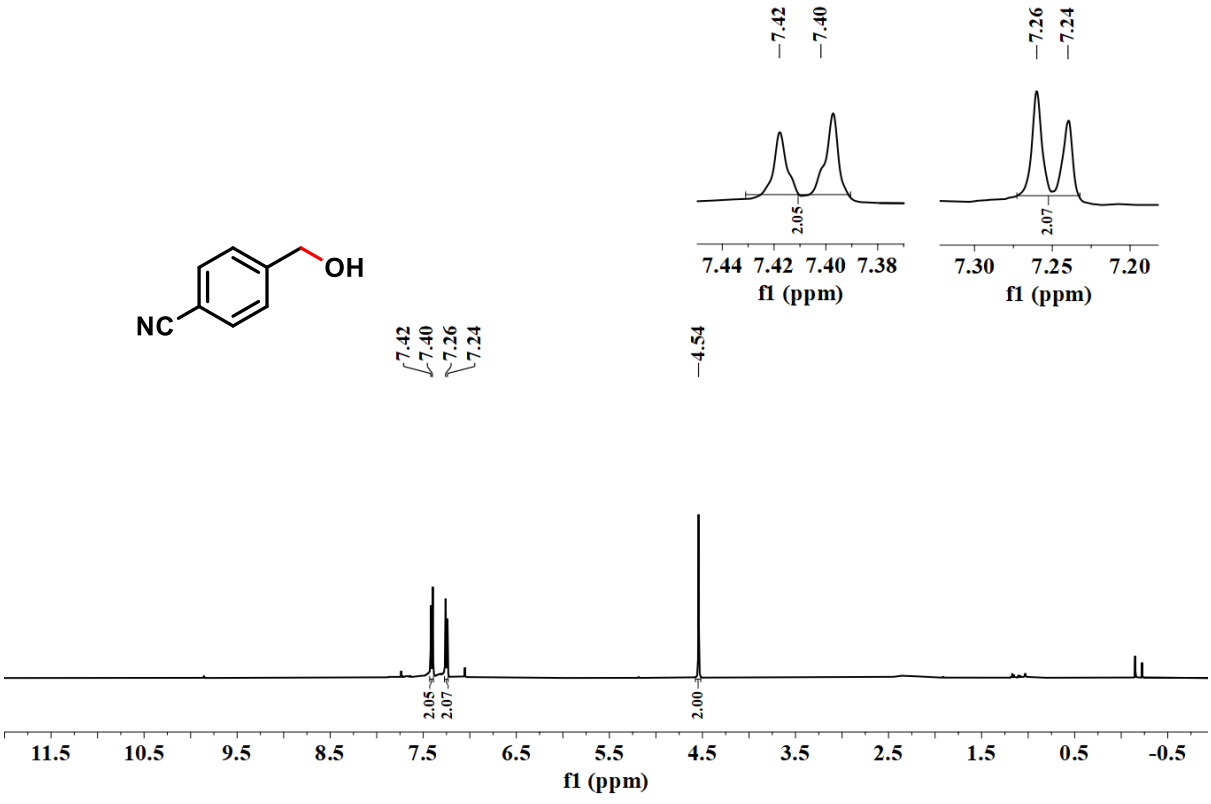

Figure S53. ^{1}H NMR spectrum of **Bh** in $CDCl_3$ (400 MHz).

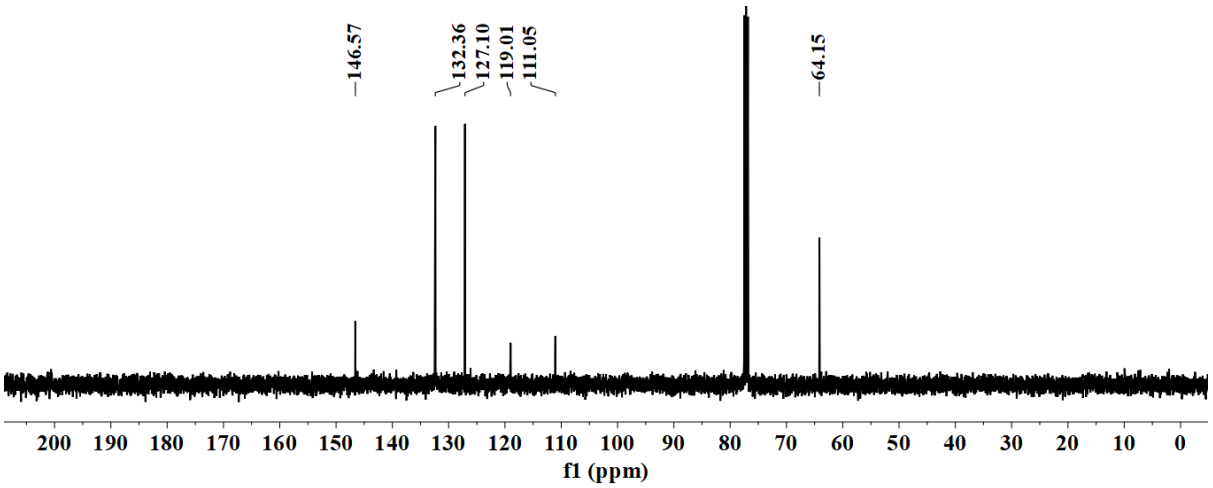

Figure S54. $^{13}C\{^{1}H\}$ NMR spectrum of **Bh** in $CDCl_3$ (101 MHz).

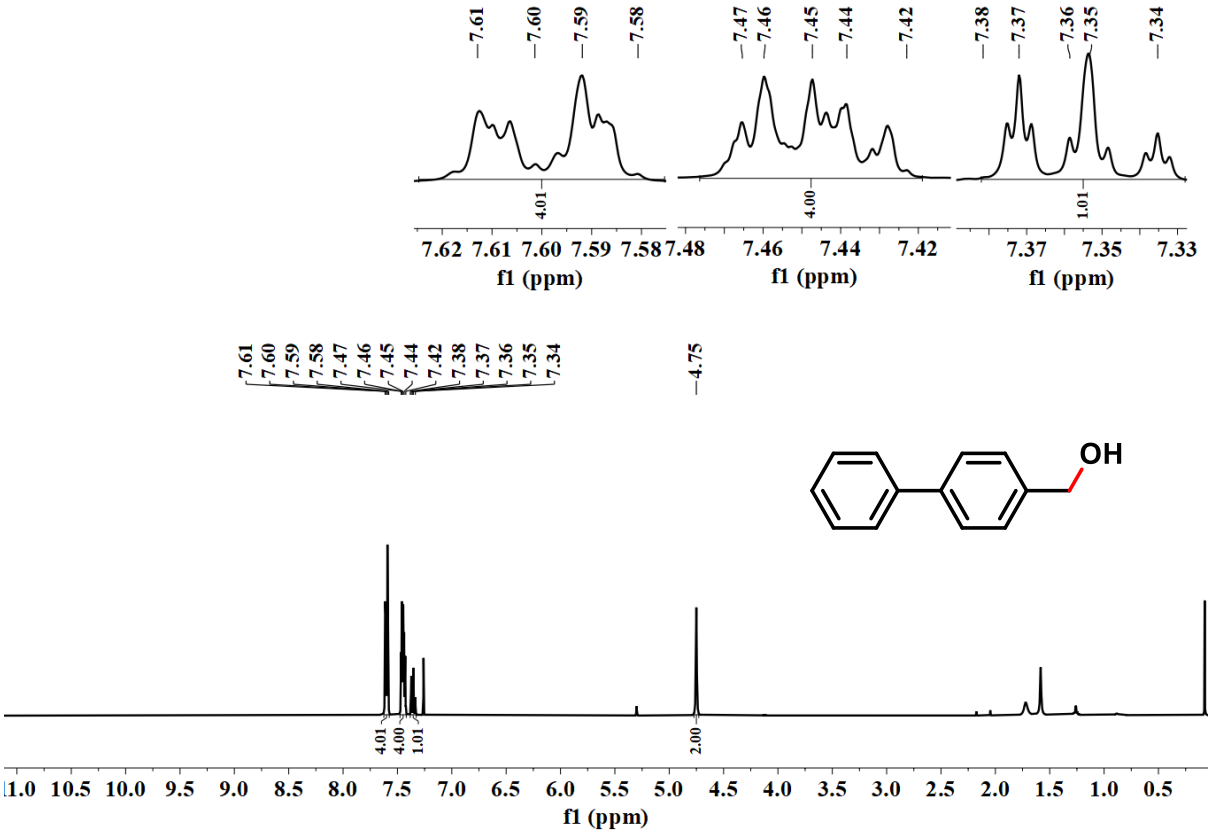

Figure S55. ^{1}H NMR spectrum of **Bi** in $CDCl_3$ (400 MHz).

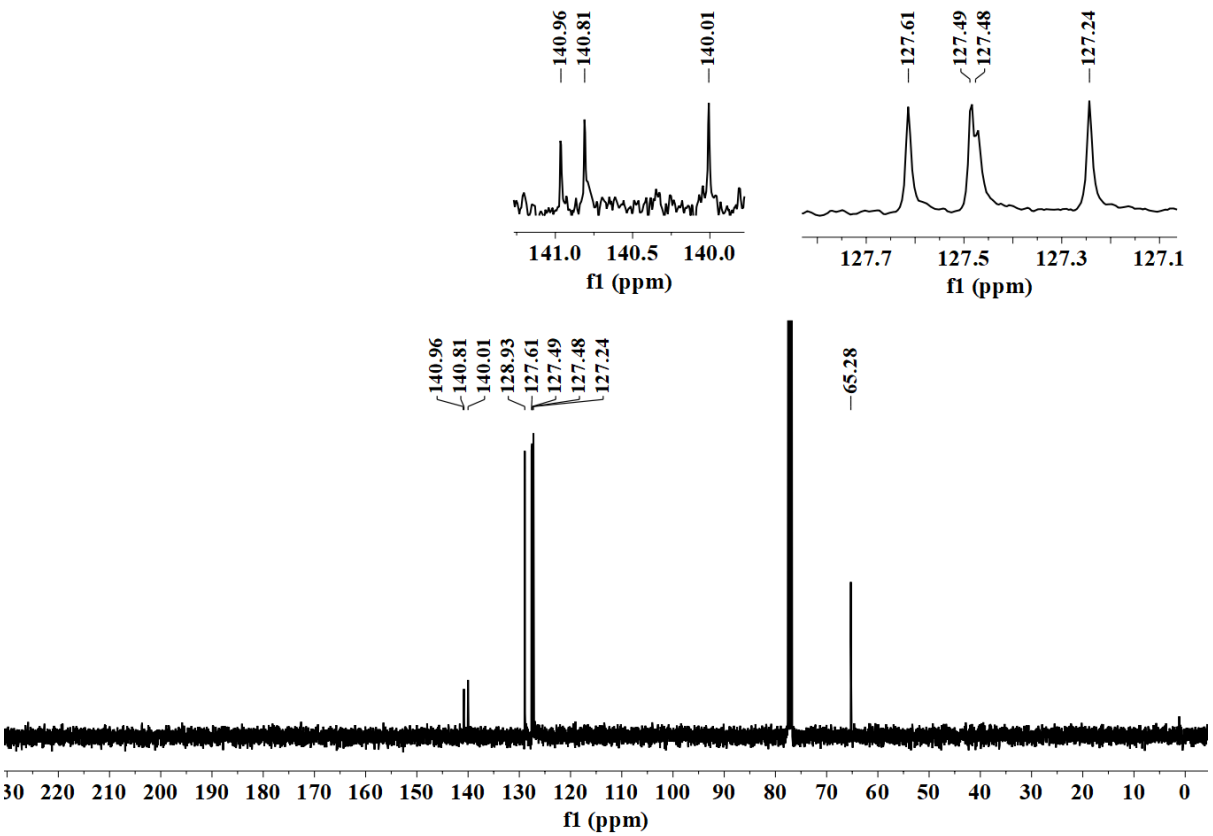

Figure S56. $^{13}C\{^{1}H\}$ NMR spectrum of **Bi** in $CDCl_3$ (101 MHz).

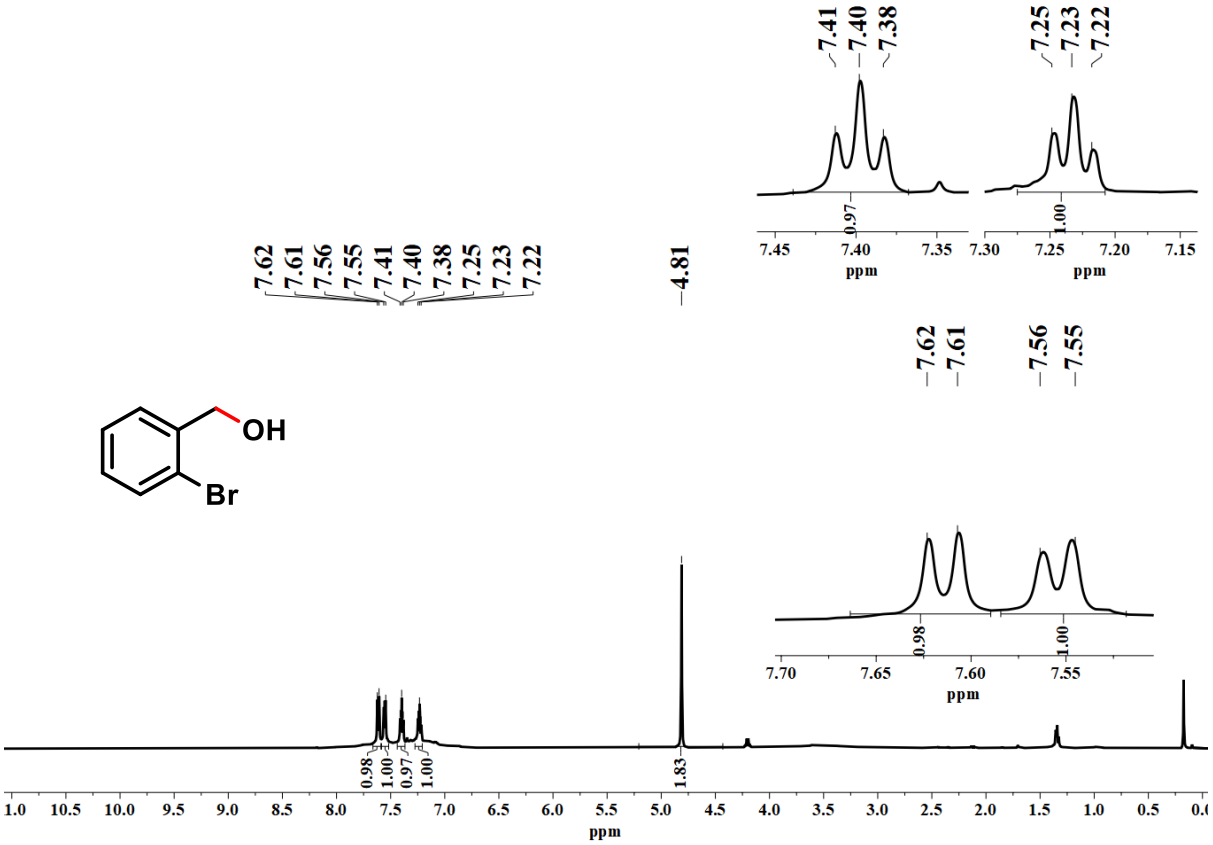

Figure S57. ^{1}H NMR spectrum of **Bj** in $CDCl_3$ (500 MHz).

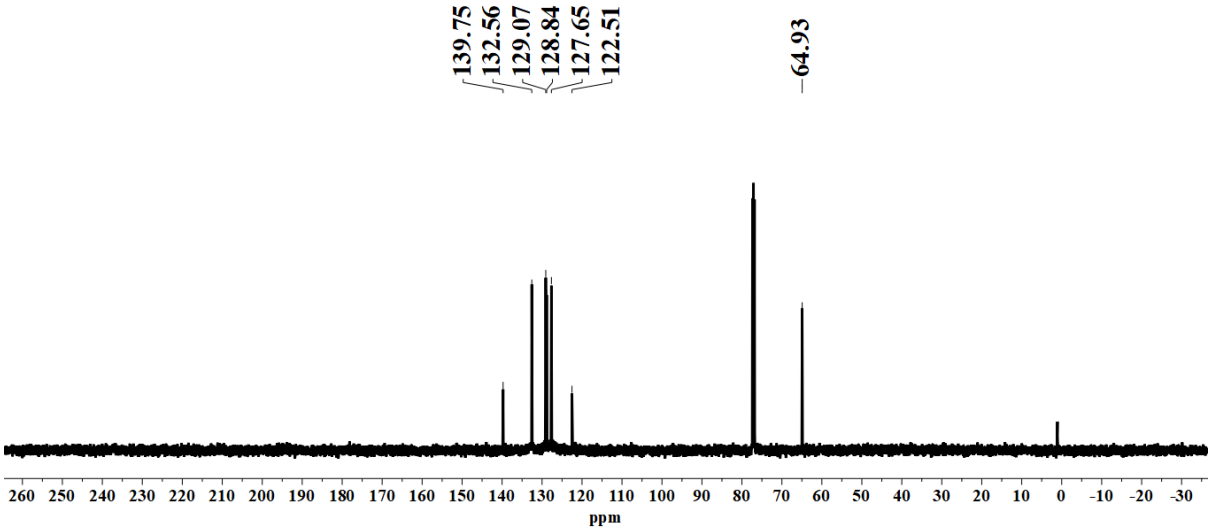

Figure S58. $^{13}C\{^{1}H\}$ NMR spectrum of **Bj** in $CDCl_3$ (126 MHz).

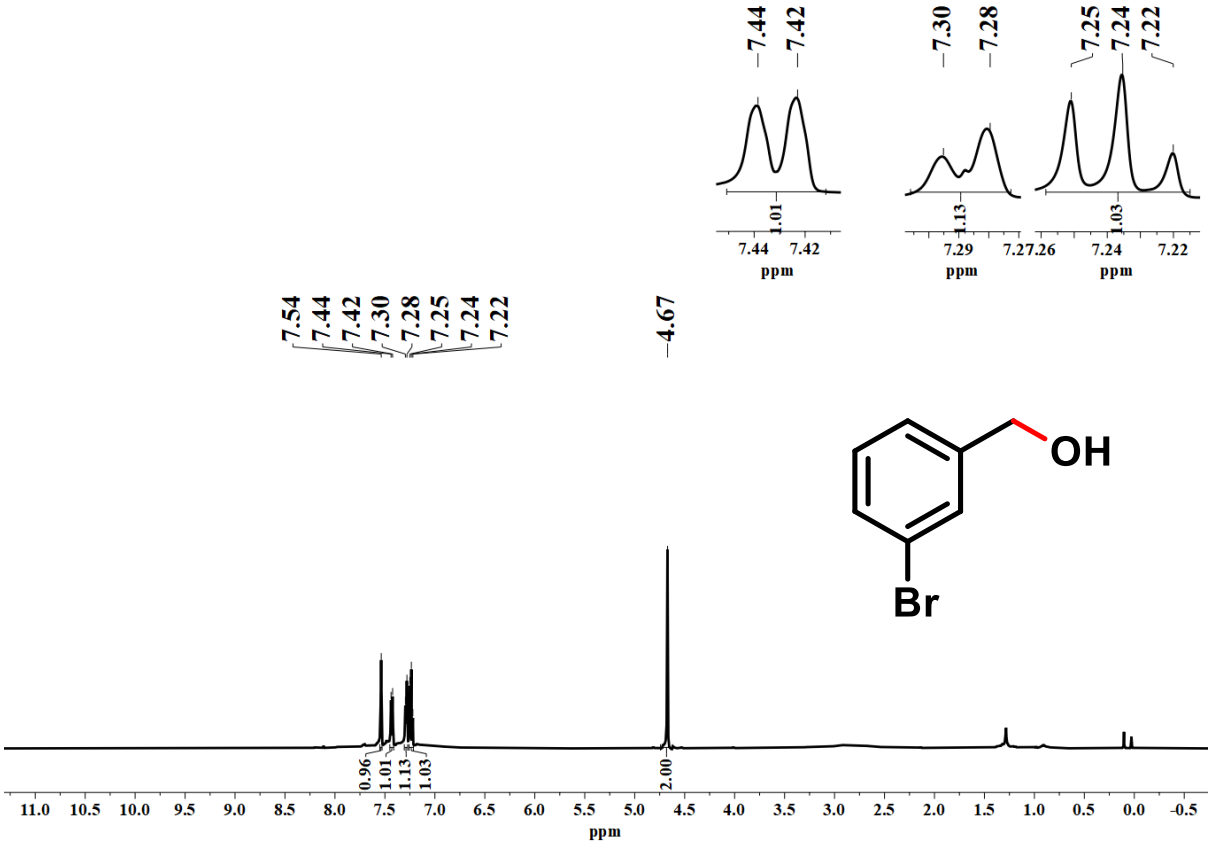

Figure S59. ^{1}H NMR spectrum of **Bk** in $CDCl_3$ (500 MHz).

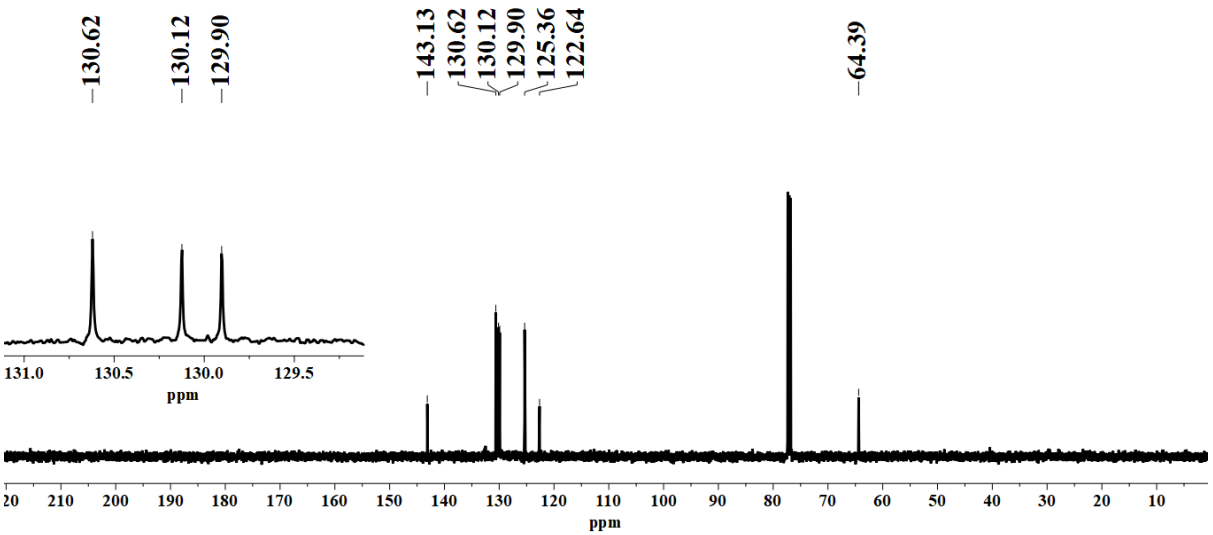

Figure S60. $^{13}C\{^{1}H\}$ NMR spectrum of **Bk** in $CDCl_3$ (126 MHz).

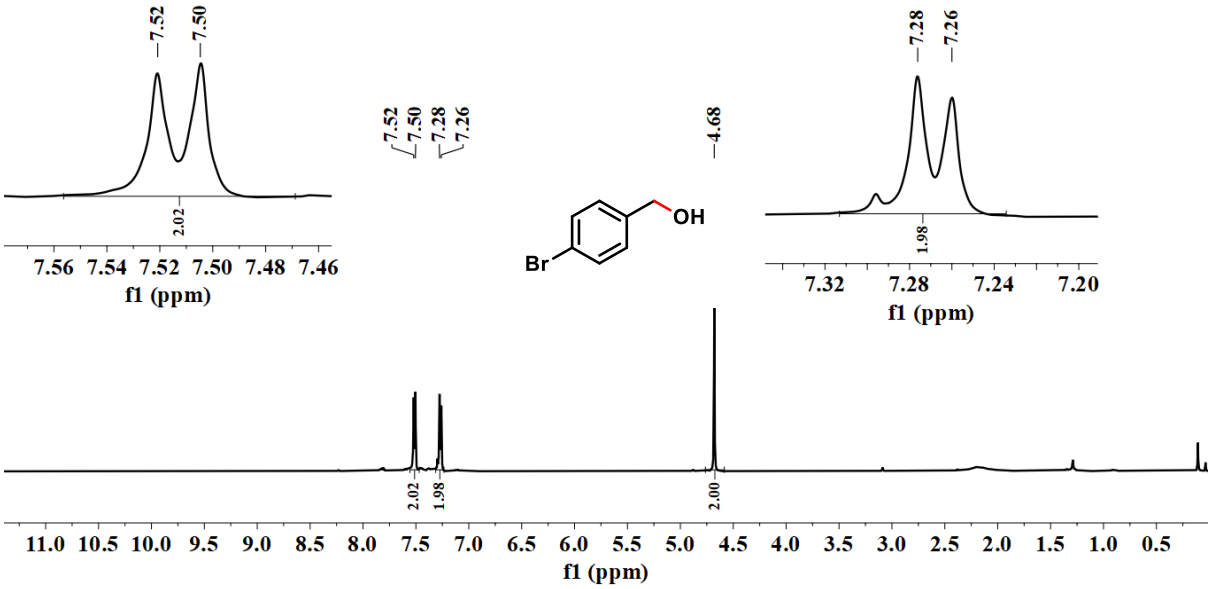

Figure S61. ^{1}H NMR spectrum of **Bl** in $CDCl_3$ (500 MHz).

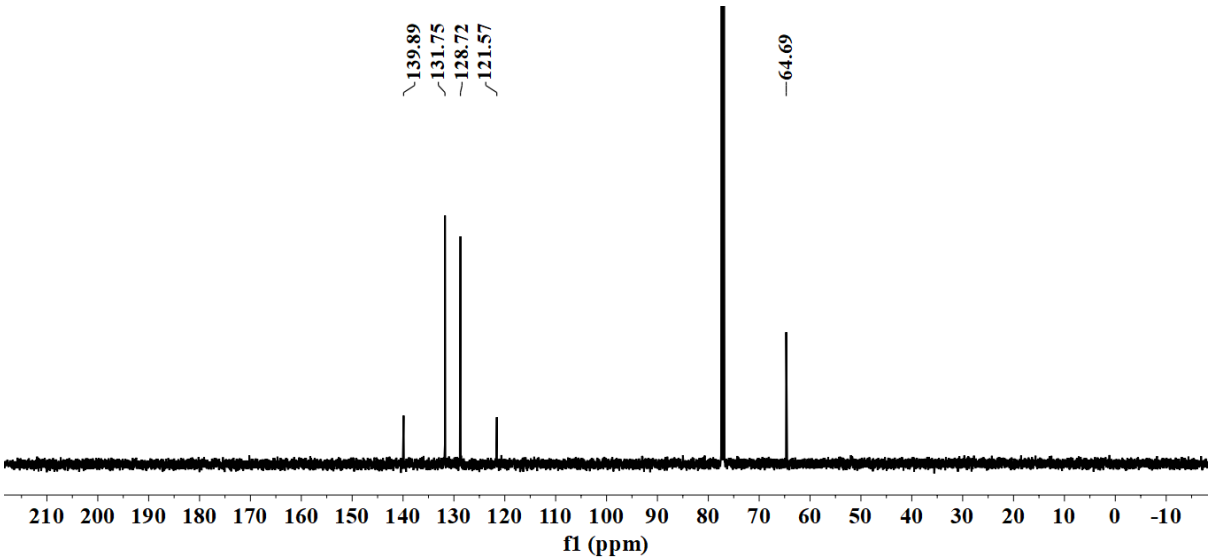

Figure S62. $^{13}C\{^{1}H\}$ NMR spectrum of **Bl** in $CDCl_3$ (126 MHz).

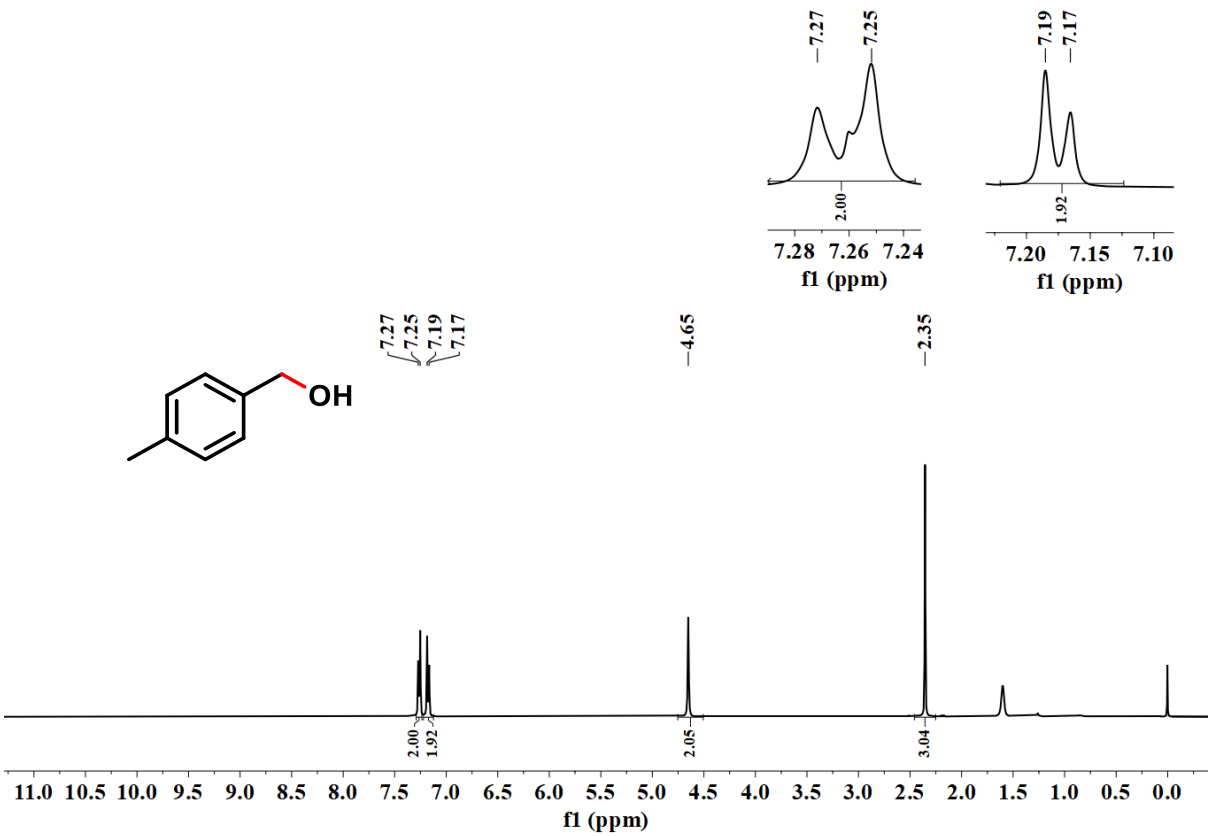

Figure S63. ^{1}H NMR spectrum of **Bm** in $CDCl_3$ (400 MHz).

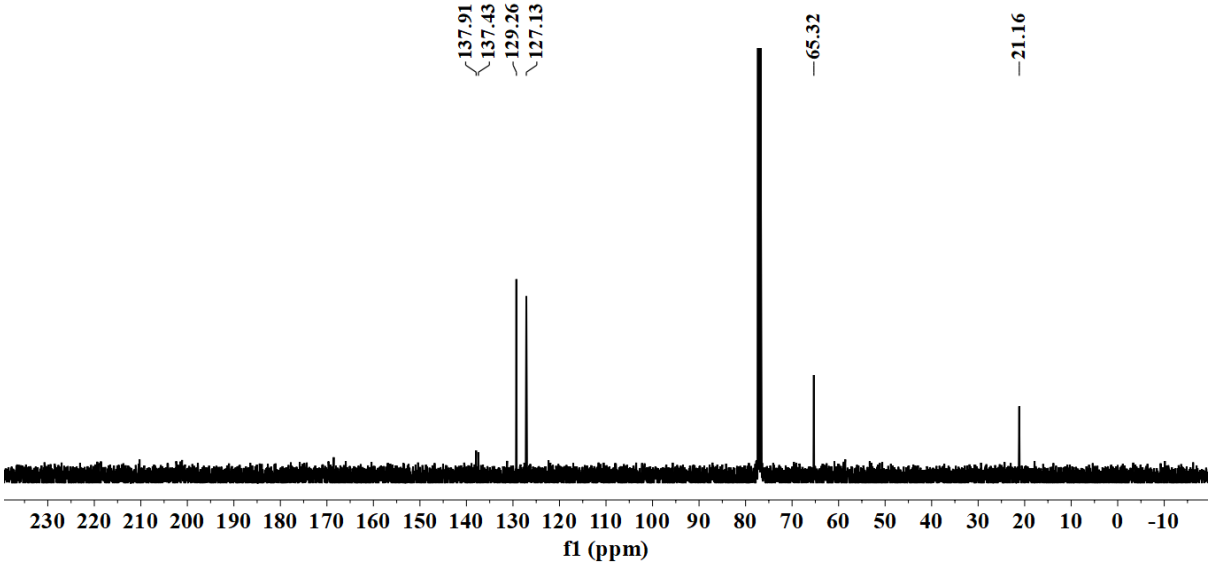

Figure S64. $^{13}C\{^{1}H\}$ NMR spectrum of **Bm** in $CDCl_3$ (101 MHz).

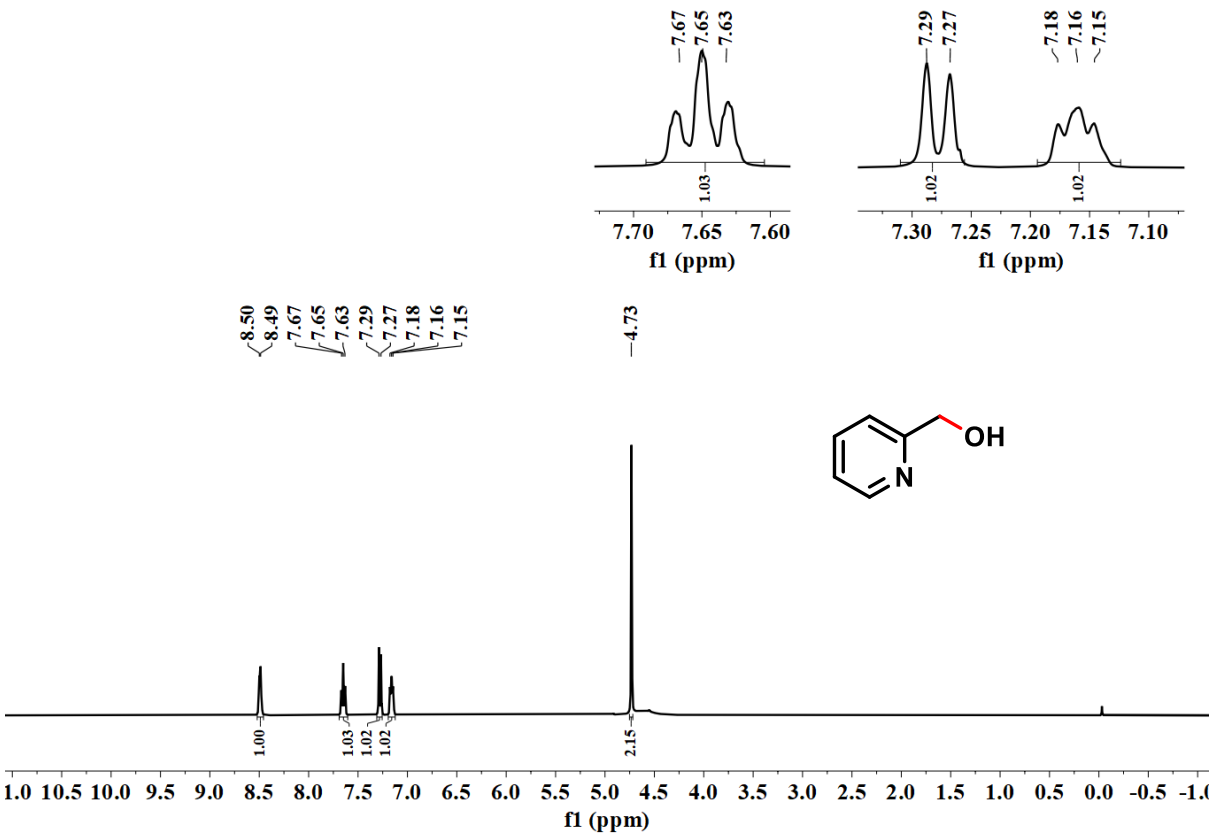

Figure S65. ^{1}H NMR spectrum of **Bn** in $CDCl_3$ (500 MHz).

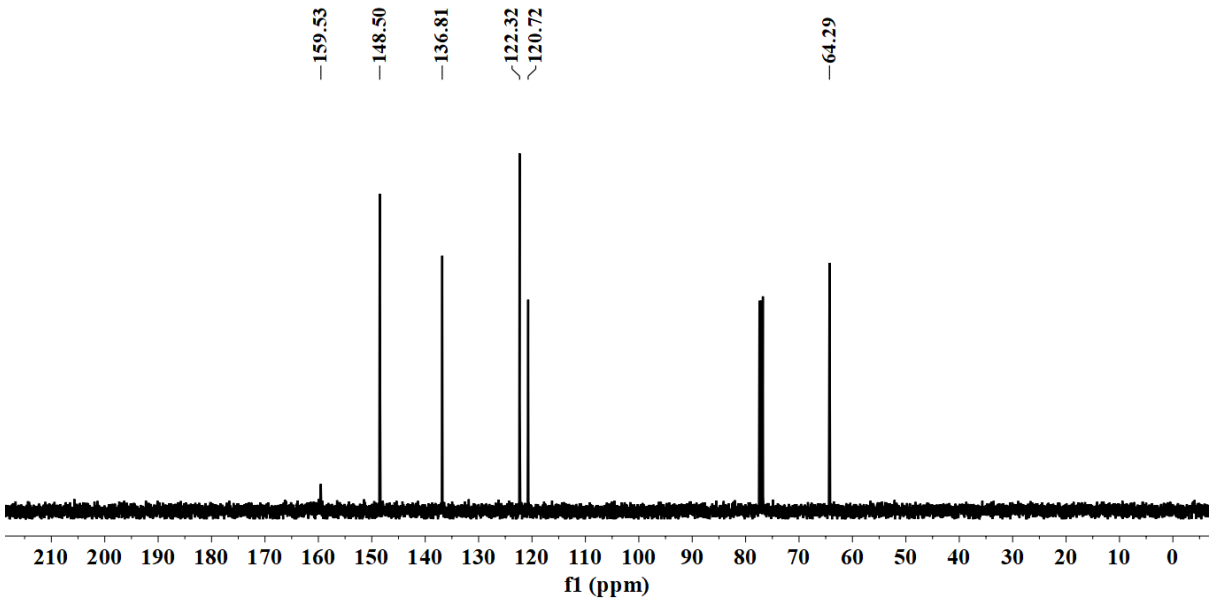

Figure S66. $^{13}C\{^{1}H\}$ NMR spectrum of **Bn** in $CDCl_3$ (126 MHz).

NMR spectra of catalytic products of indanone derivatives reduction

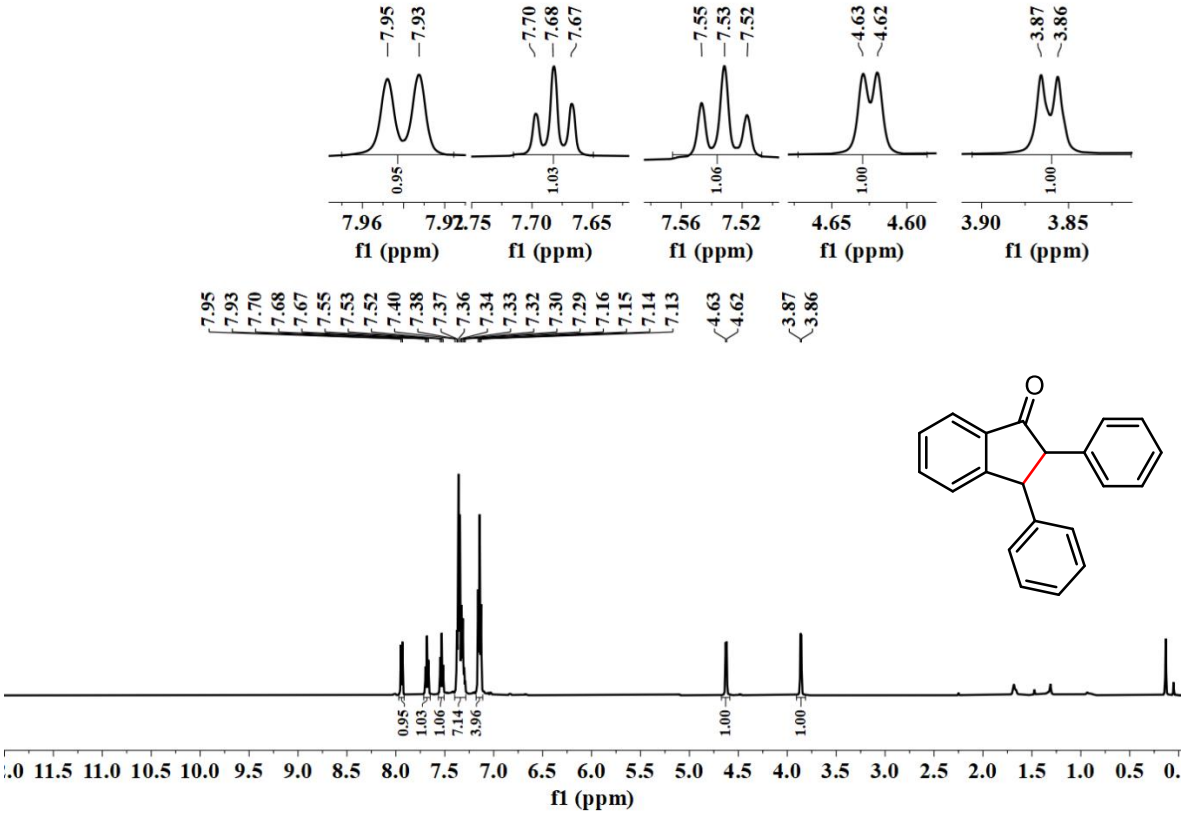

Figure S67. ^{1}H NMR spectrum of **Ca** in $CDCl_3$ (500 MHz).

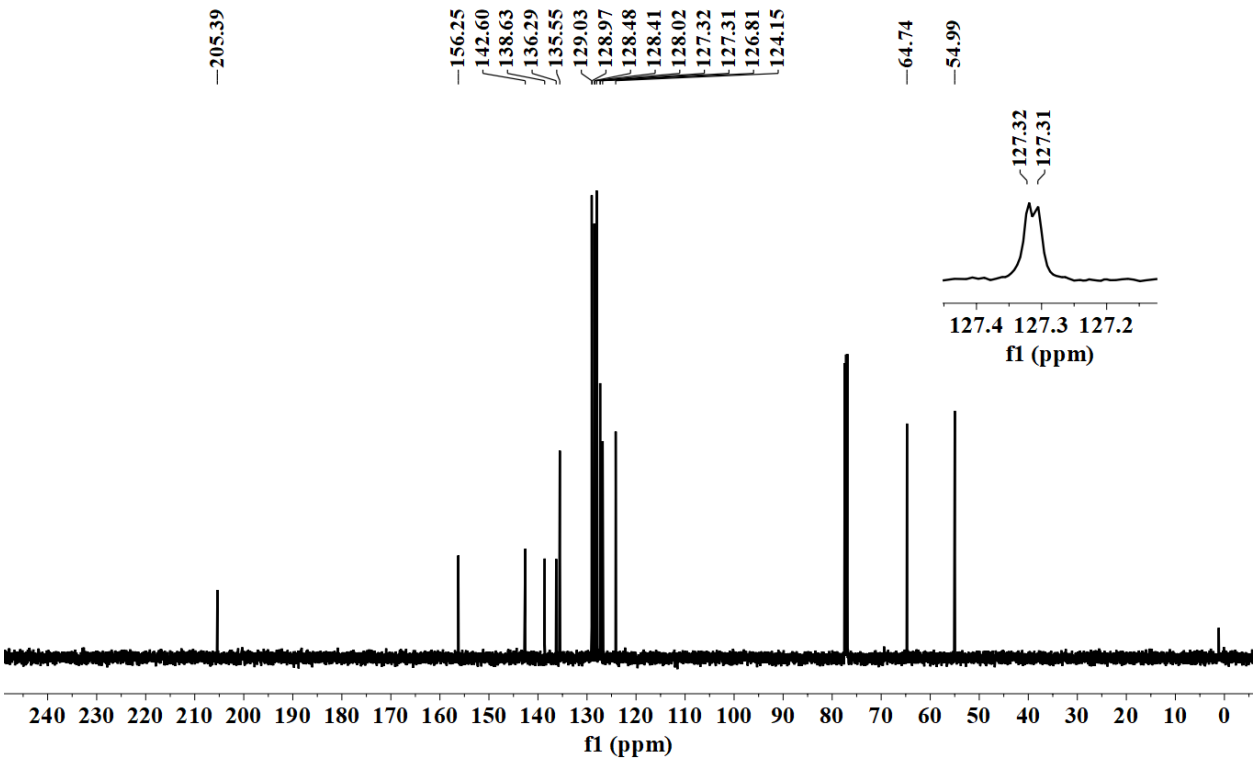

Figure S68. $^{13}C\{^{1}H\}$ NMR spectrum of **Ca** in $CDCl_3$ (126 MHz).

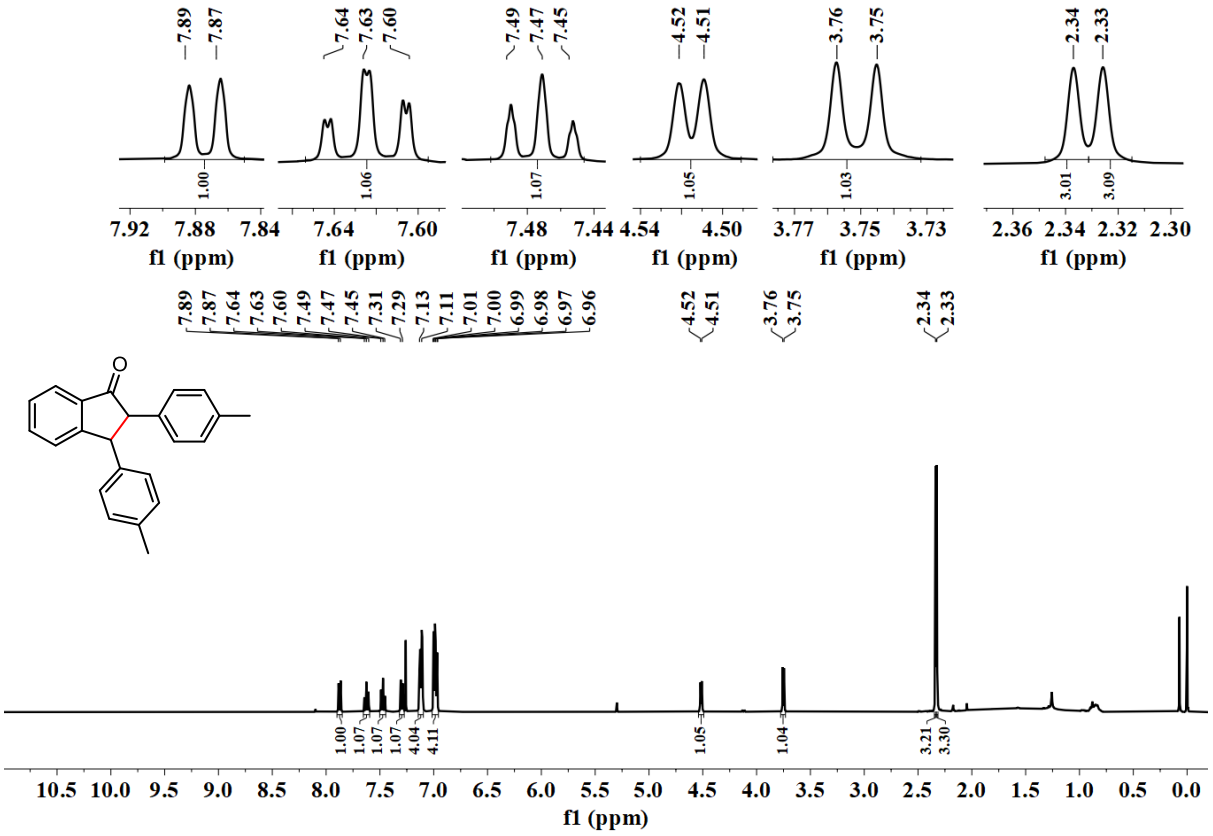

Figure S69. ^{1}H NMR spectrum of **Cb** in $CDCl_3$ (400 MHz).

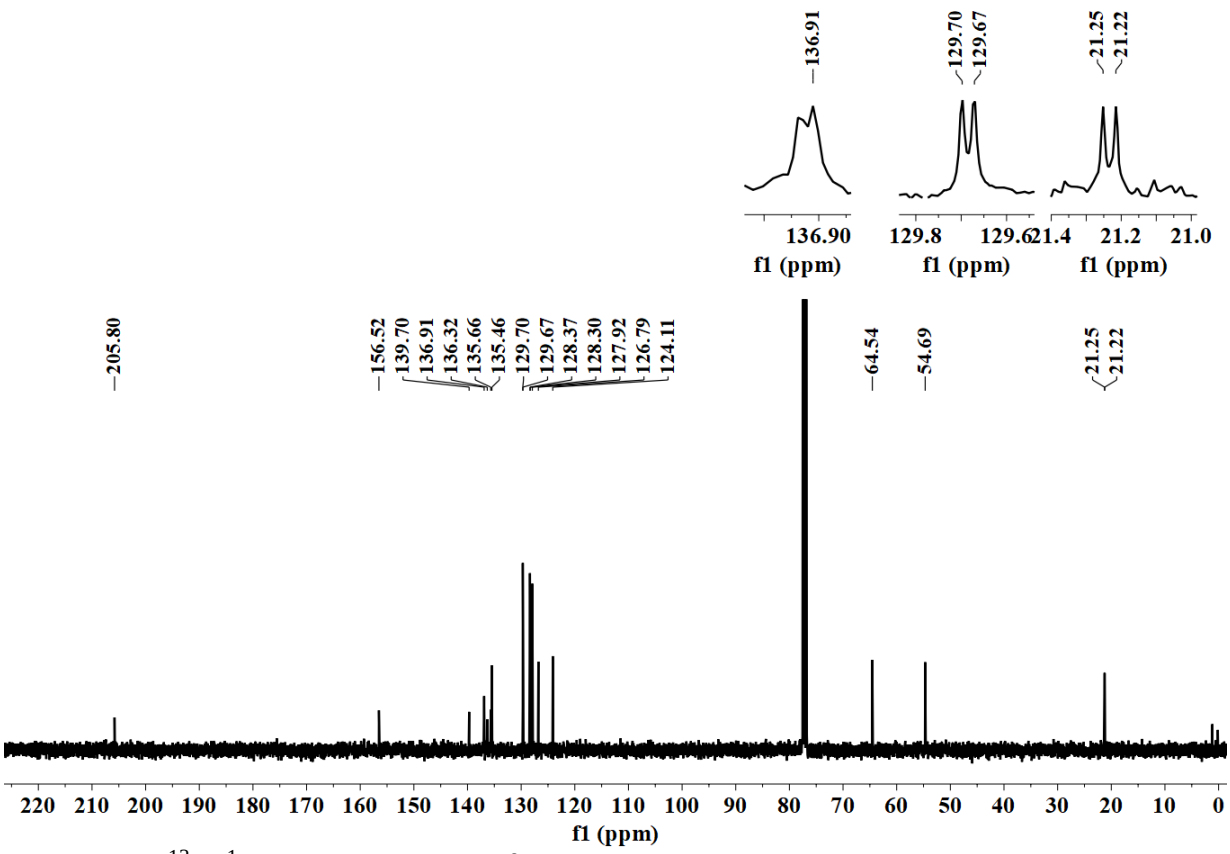

Figure S70. $^{13}C\{^{1}H\}$ NMR spectrum of **Cb** in $CDCl_3$ (101 MHz).

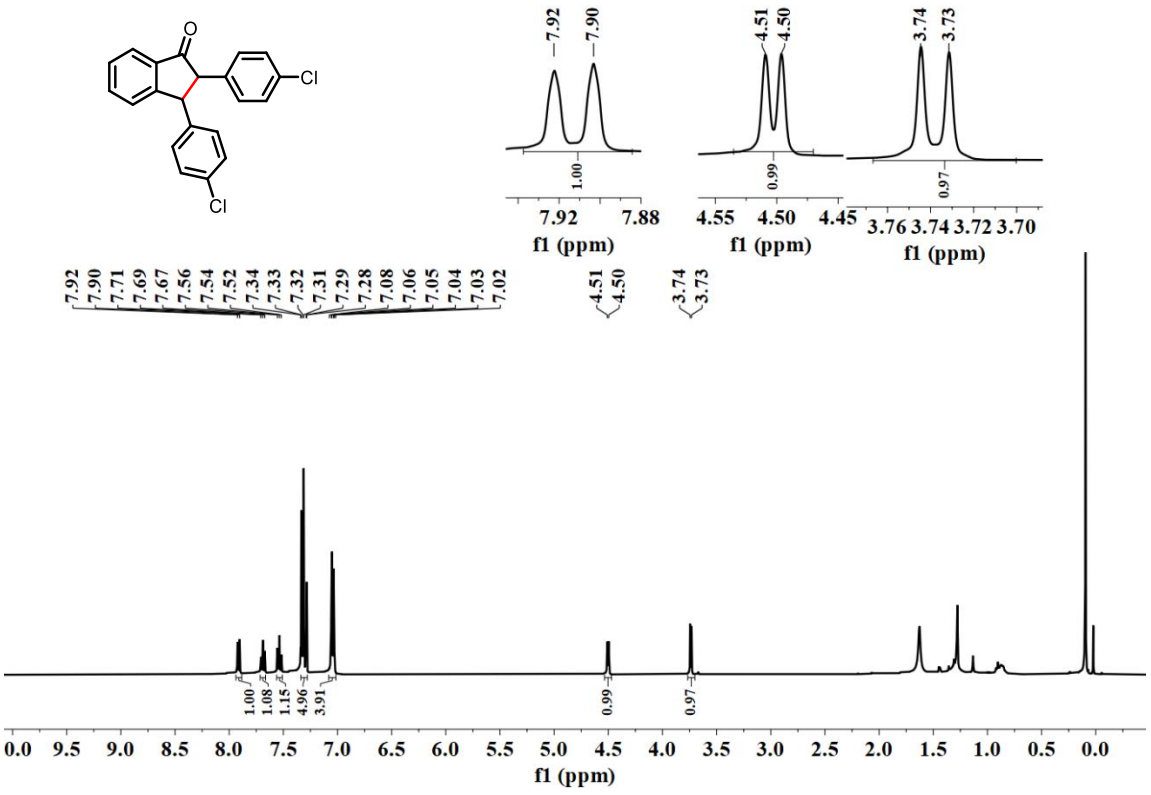

Figure S71. ^{1}H NMR spectrum of **Cc** in $CDCl_3$ (400 MHz).

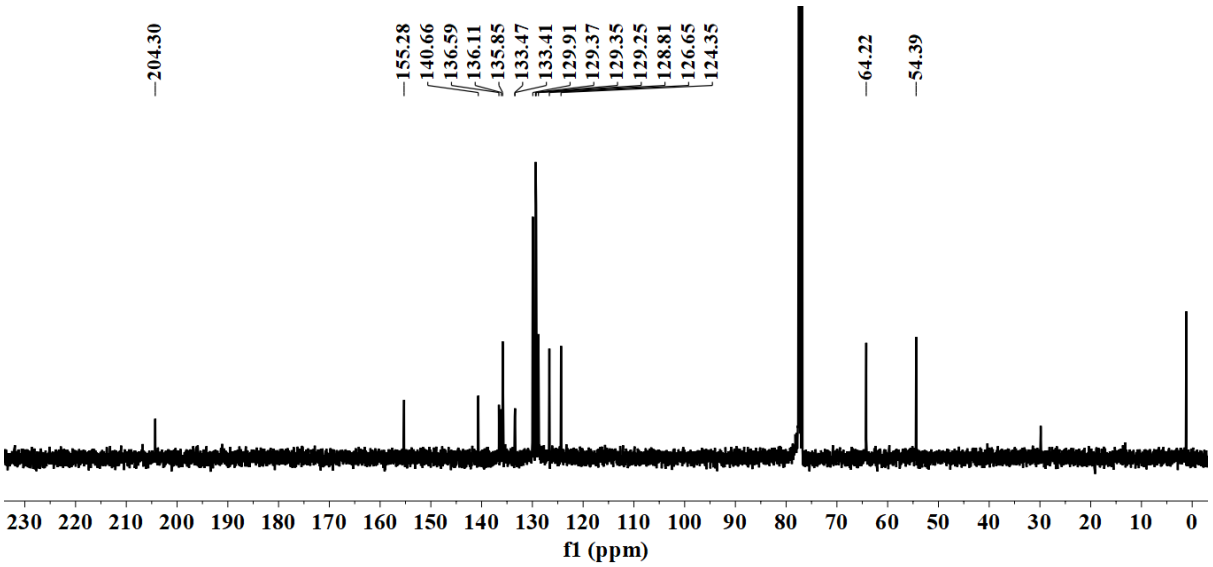

Figure S72. $^{13}C\{^{1}H\}$ NMR spectrum of **Cc** in $CDCl_3$ (101 MHz).

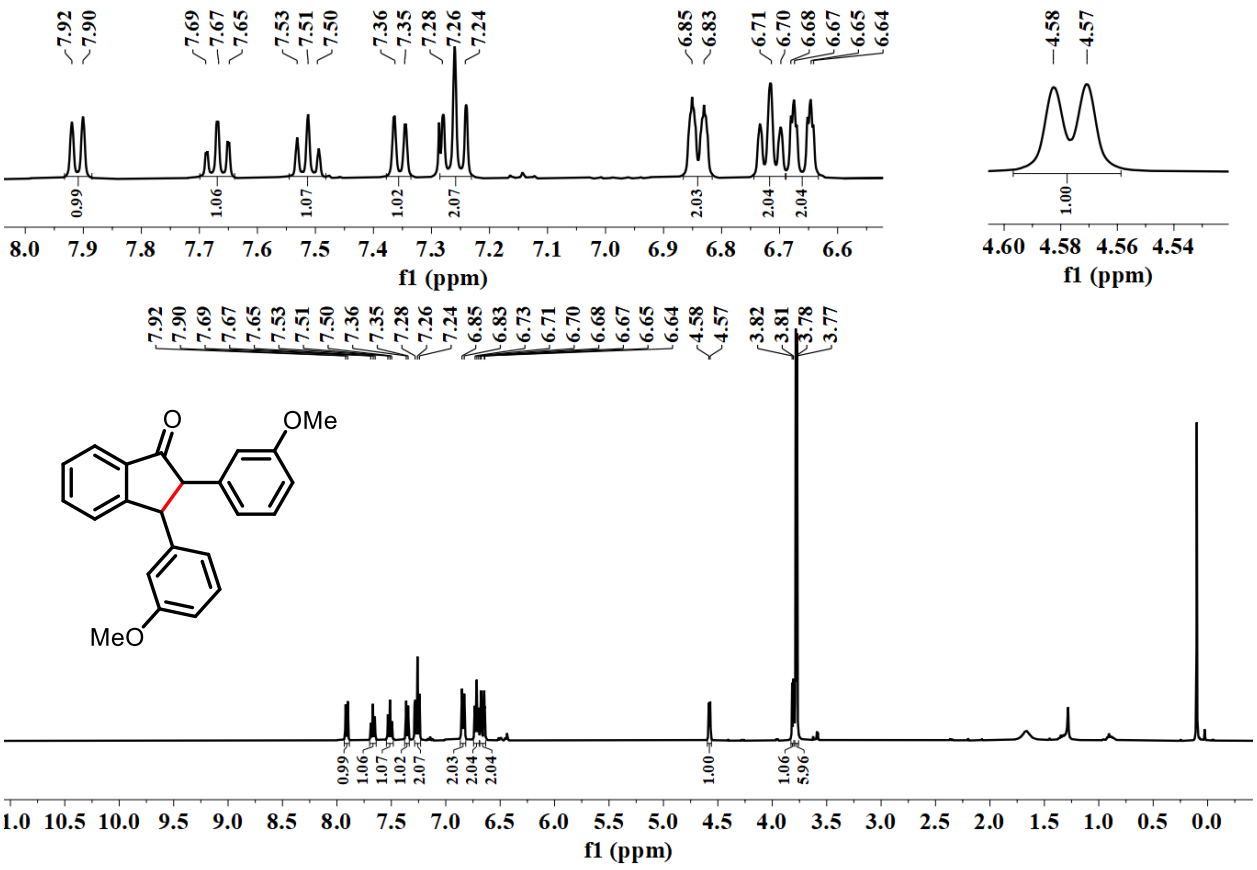

Figure S73. ^{1}H NMR spectrum of **Cd** in $CDCl_3$ (400 MHz).

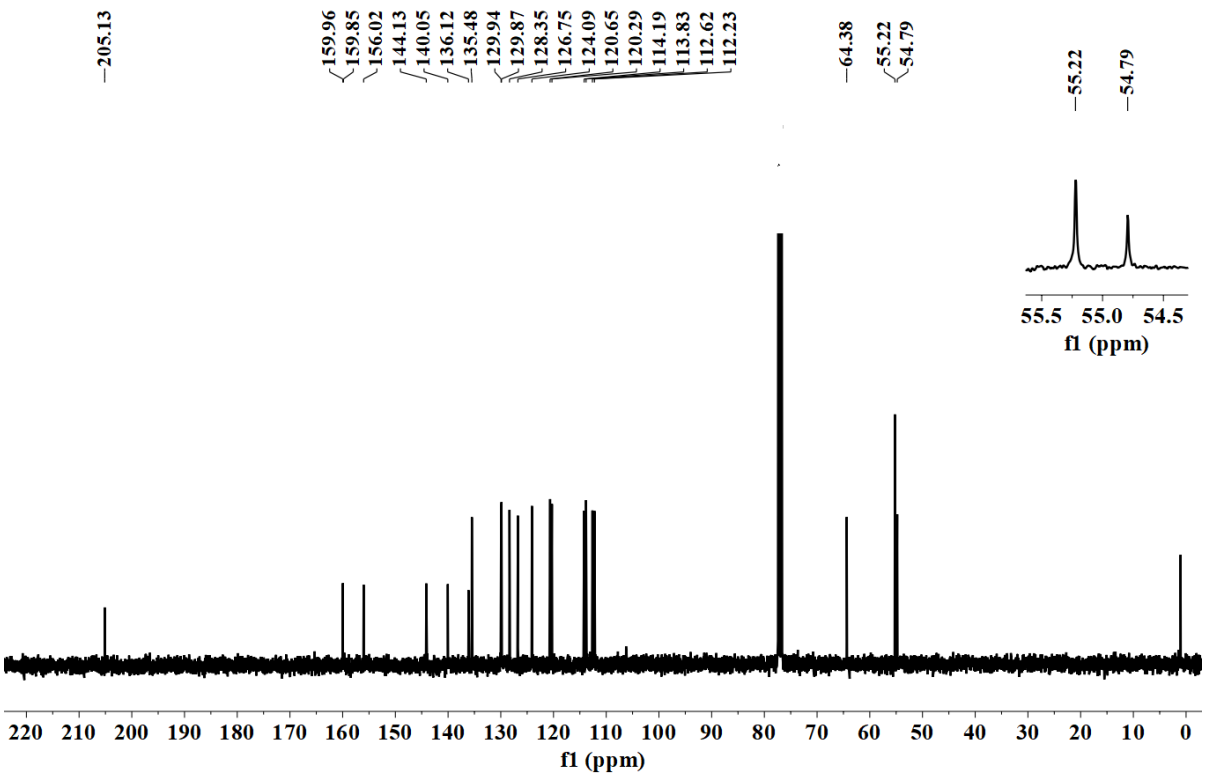

Figure S74. $^{13}C\{^{1}H\}$ NMR spectrum of **Cd** in $CDCl_3$ (101 MHz).

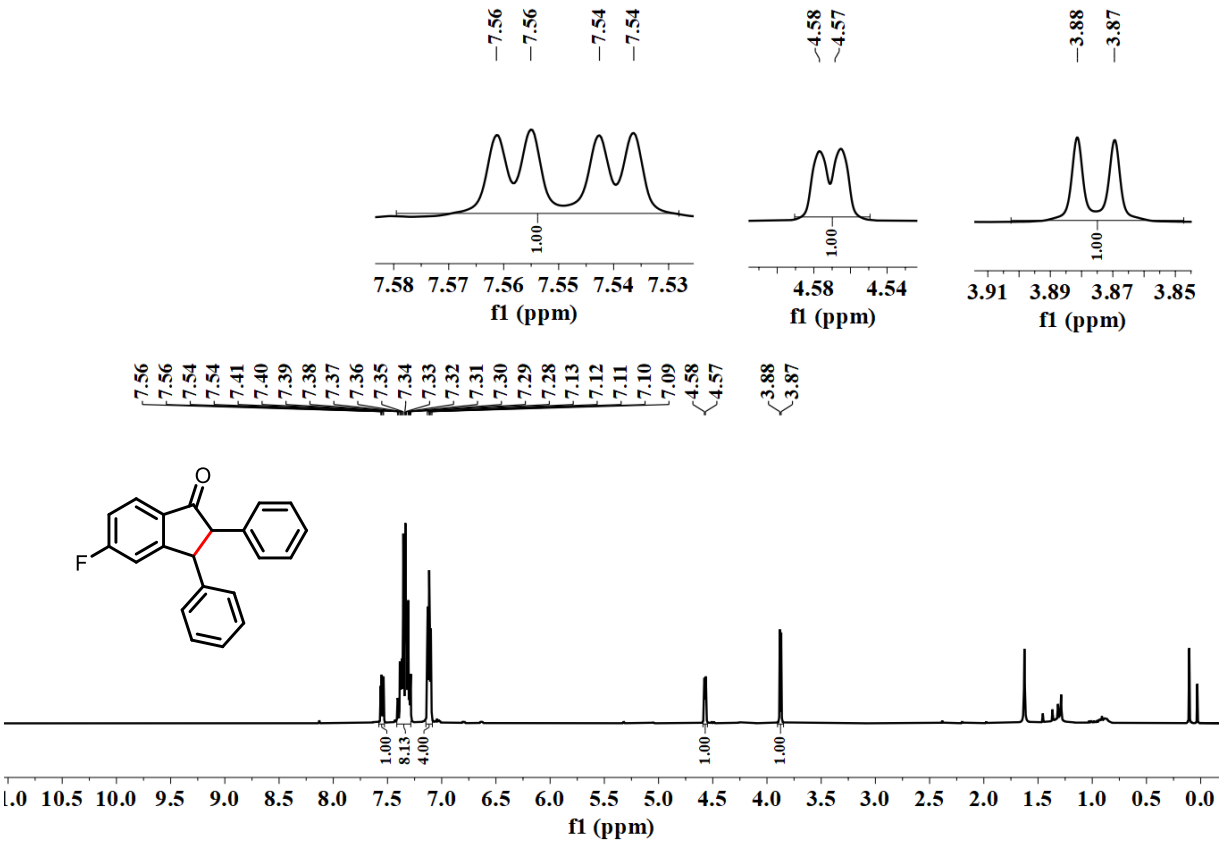

Figure S75. ^{1}H NMR spectrum of **Ce** in $CDCl_3$ (400 MHz).

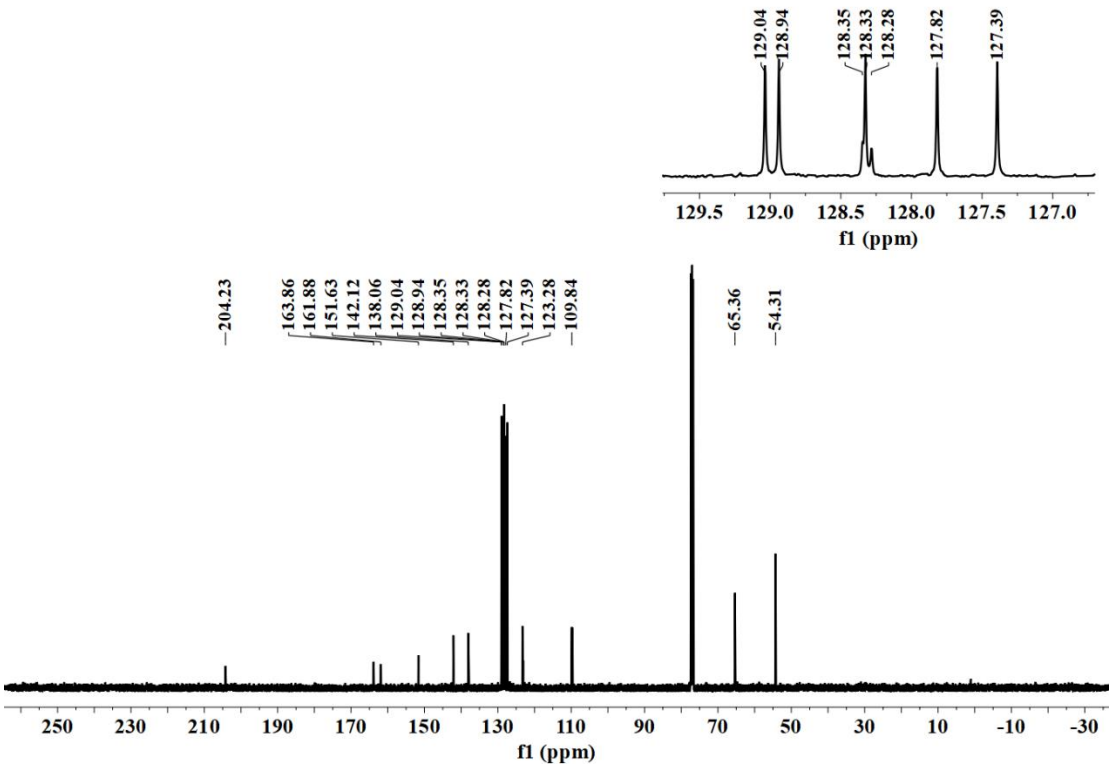

Figure S76. $^{13}C\{^{1}H\}$ NMR spectrum of **Ce** in $CDCl_3$ (101 MHz).

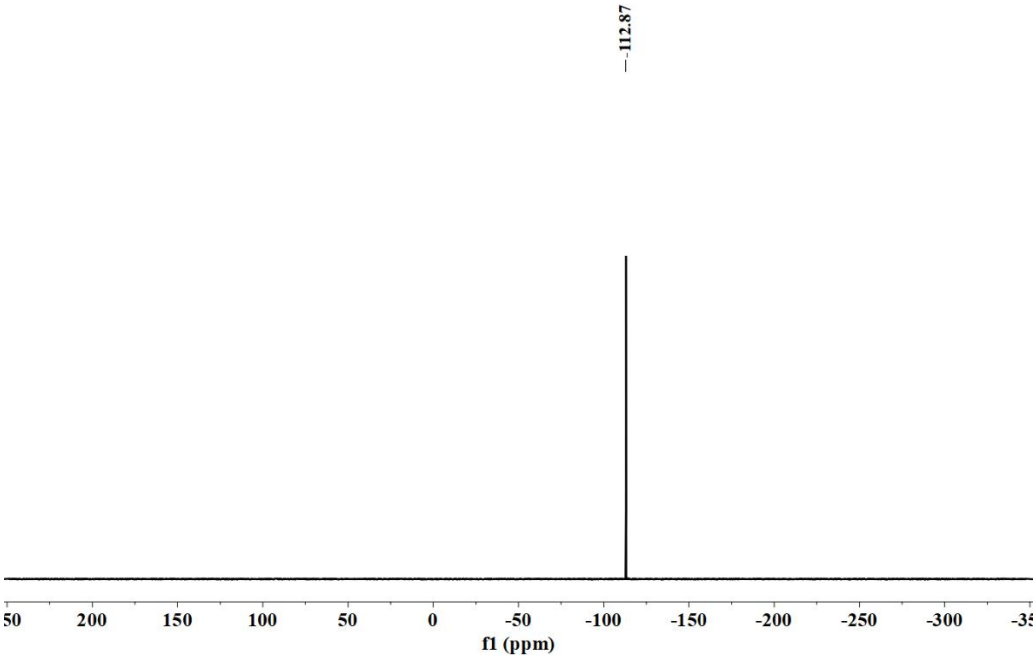

Figure S77. $^{19}F\{^{1}H\}$ NMR spectrum of **Cc** in $CDCl_3$ (376 MHz).

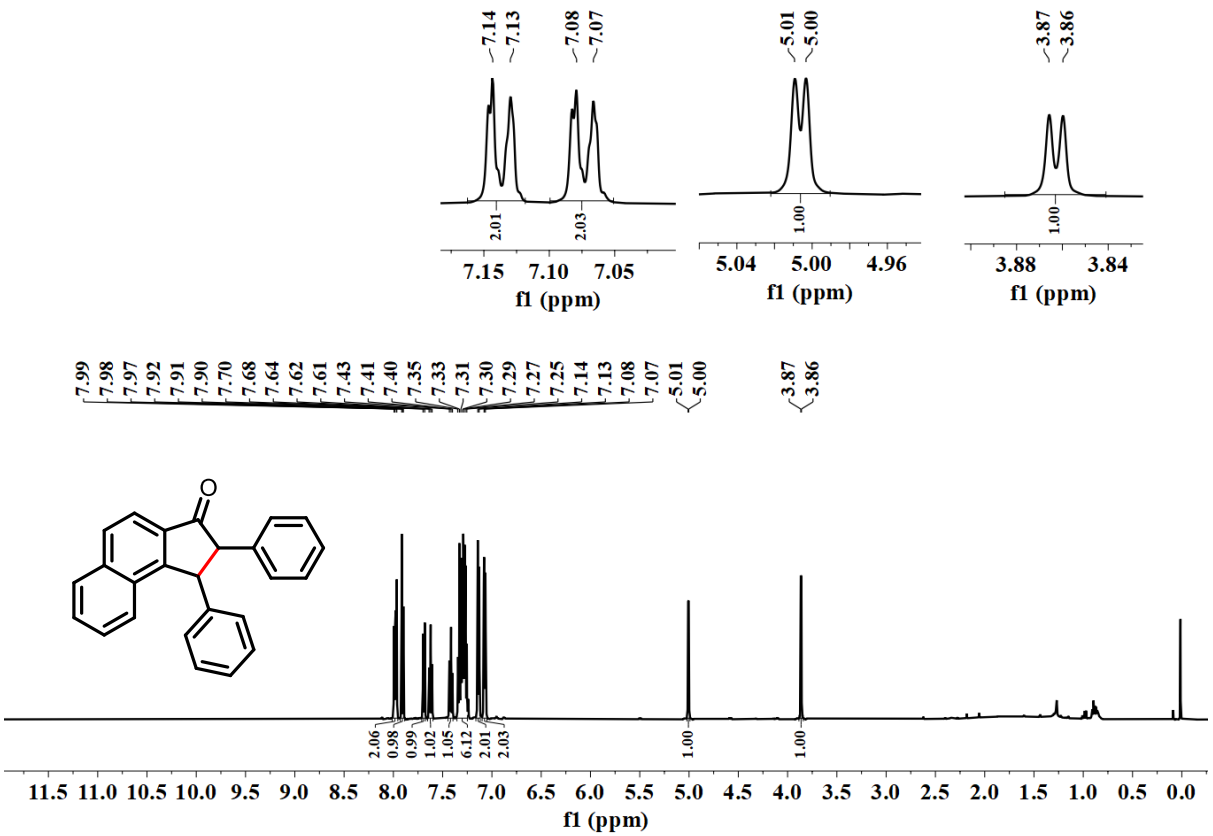

Figure S78. ^{1}H NMR spectrum of **Cf** in $CDCl_3$ (500 MHz).

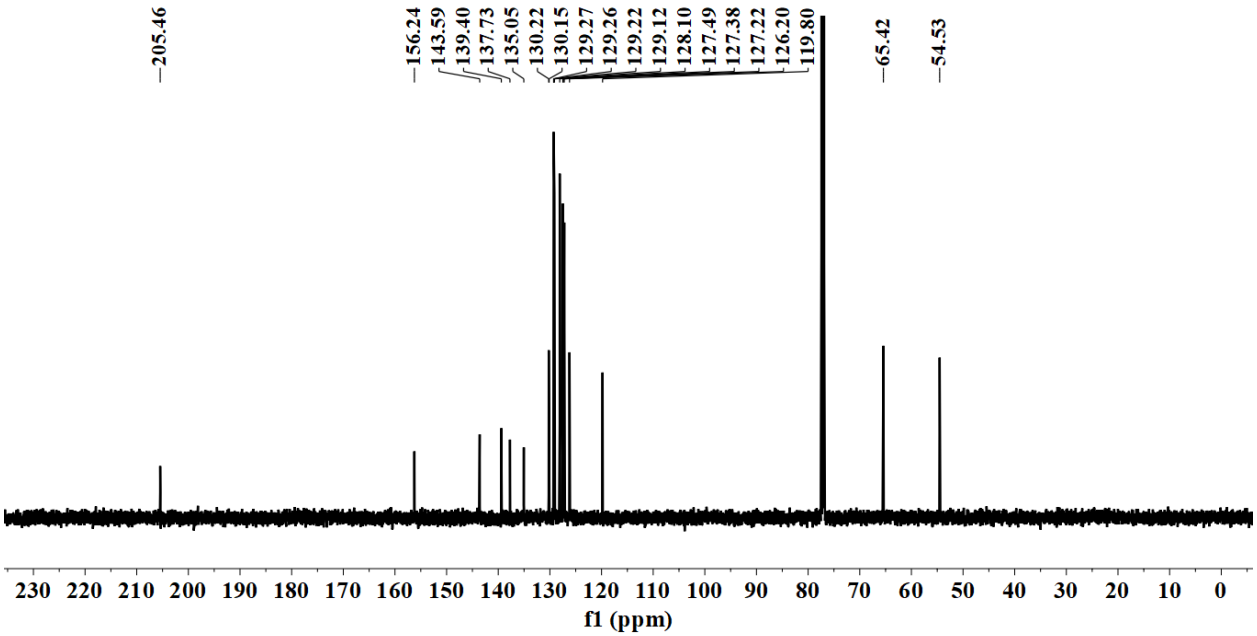

Figure S79. $^{13}C\{^{1}H\}$ NMR spectrum of **Cf** in $CDCl_3$ (126 MHz).

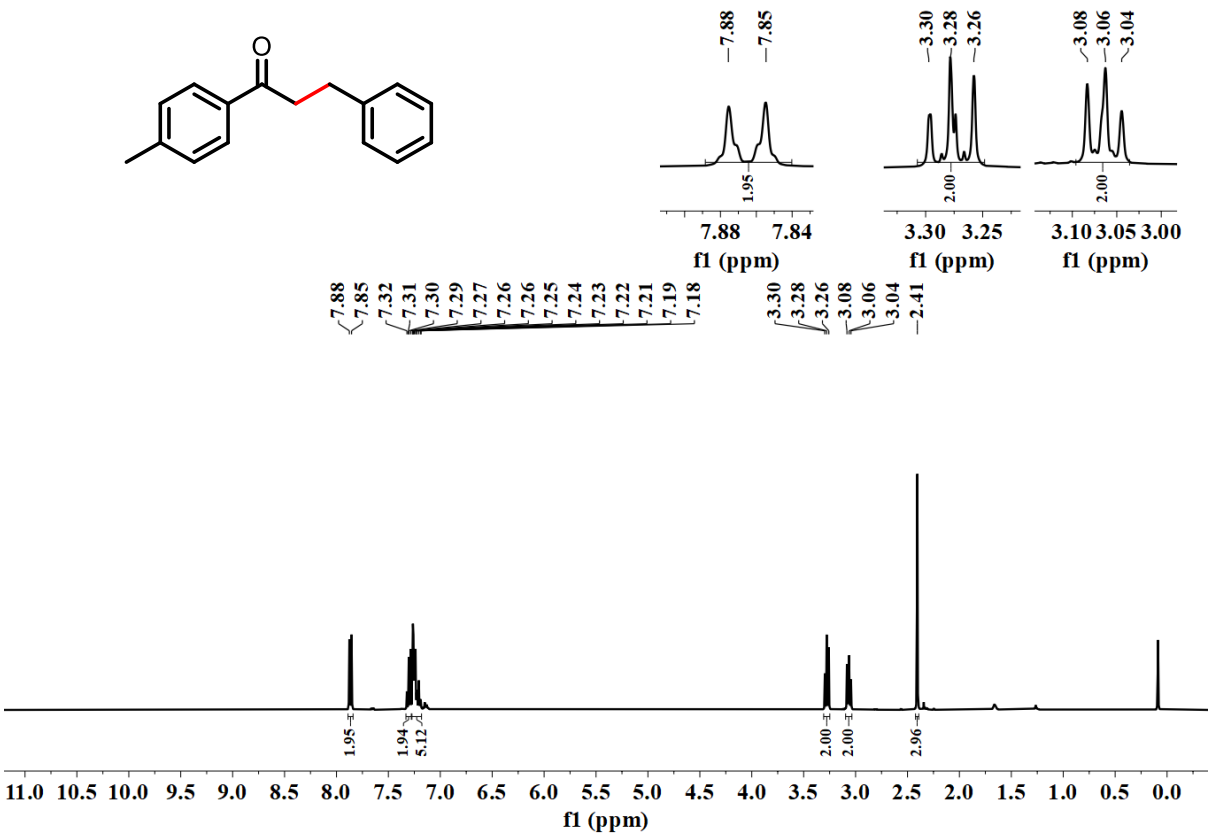

Figure S80. ^{1}H NMR spectrum of **Cg** in $CDCl_3$ (400 MHz).

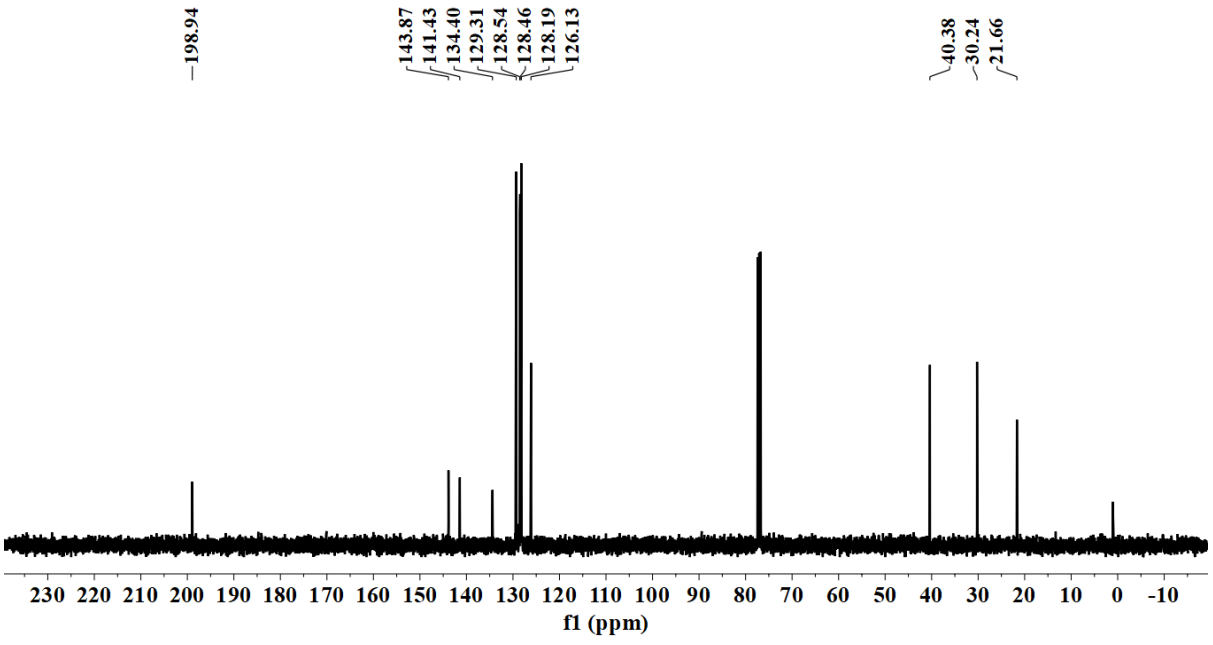

Figure S81. $^{13}C\{^{1}H\}$ NMR spectrum of **Cg** in $CDCl_3$ (101 MHz).

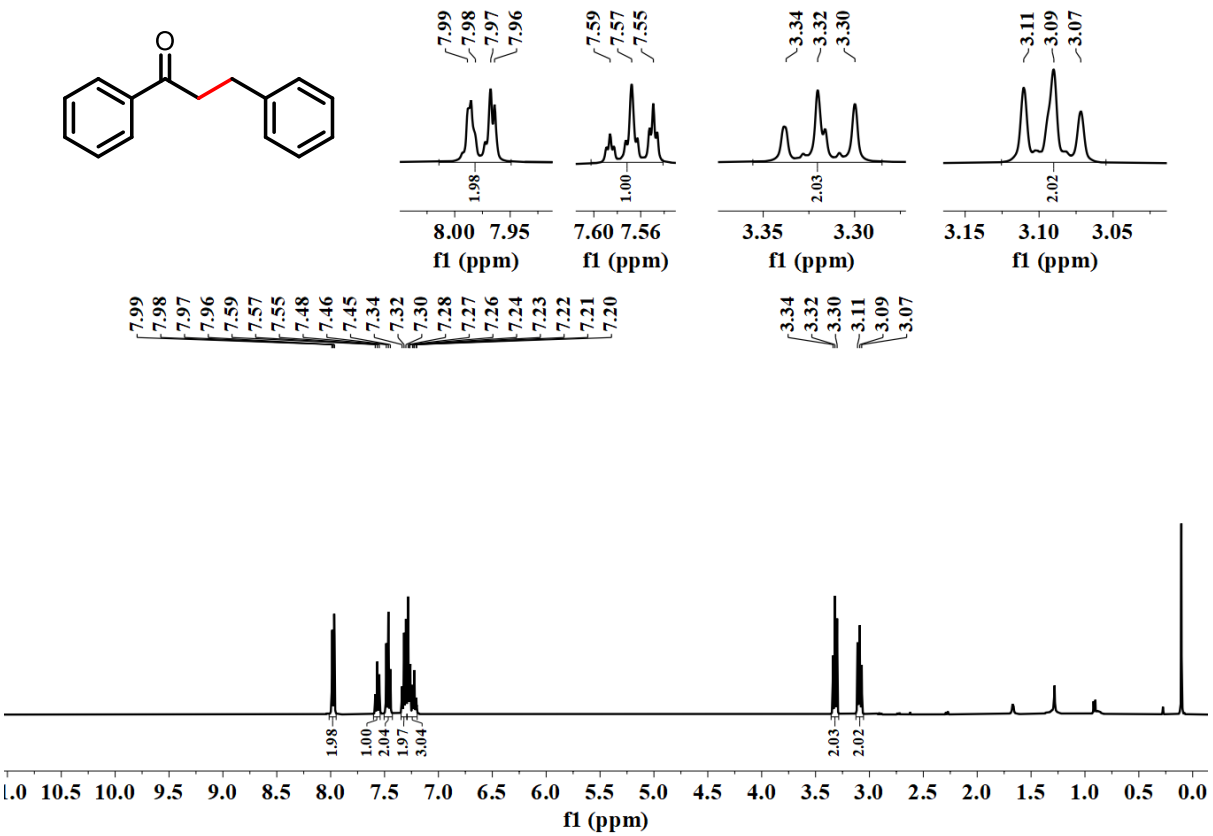

Figure S82. ^{1}H NMR spectrum of **Ch** in $CDCl_3$ (400 MHz).

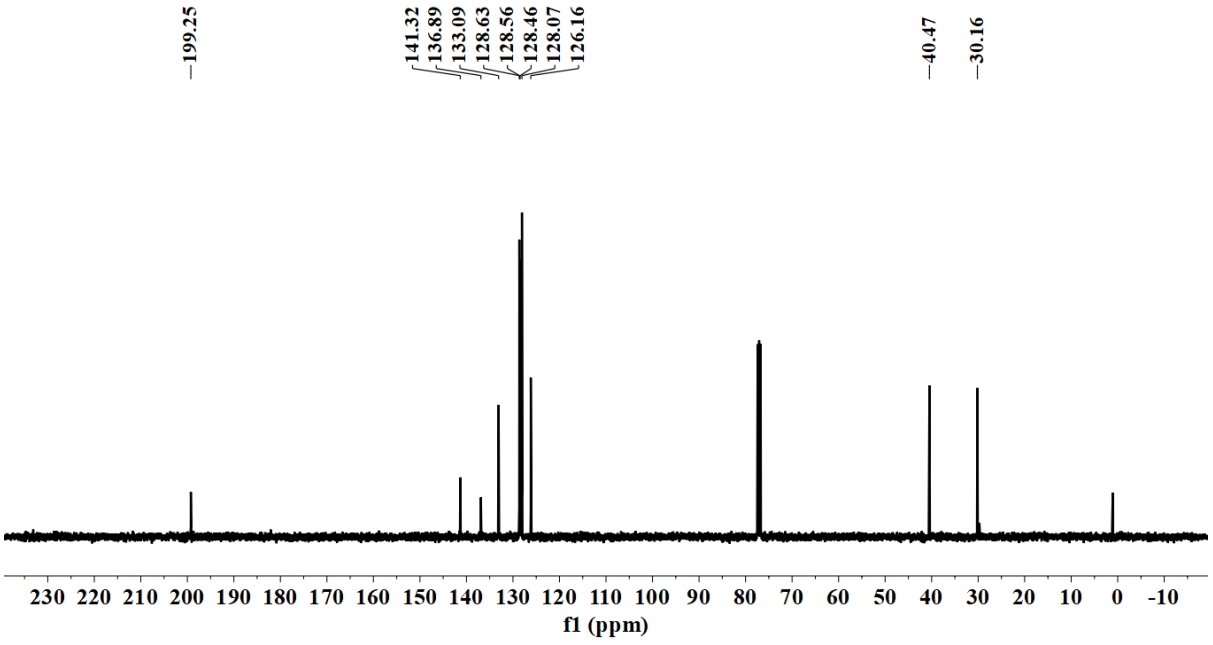

Figure S83. $^{13}C\{^{1}H\}$ NMR spectrum of **Ch** in $CDCl_3$ (101 MHz).

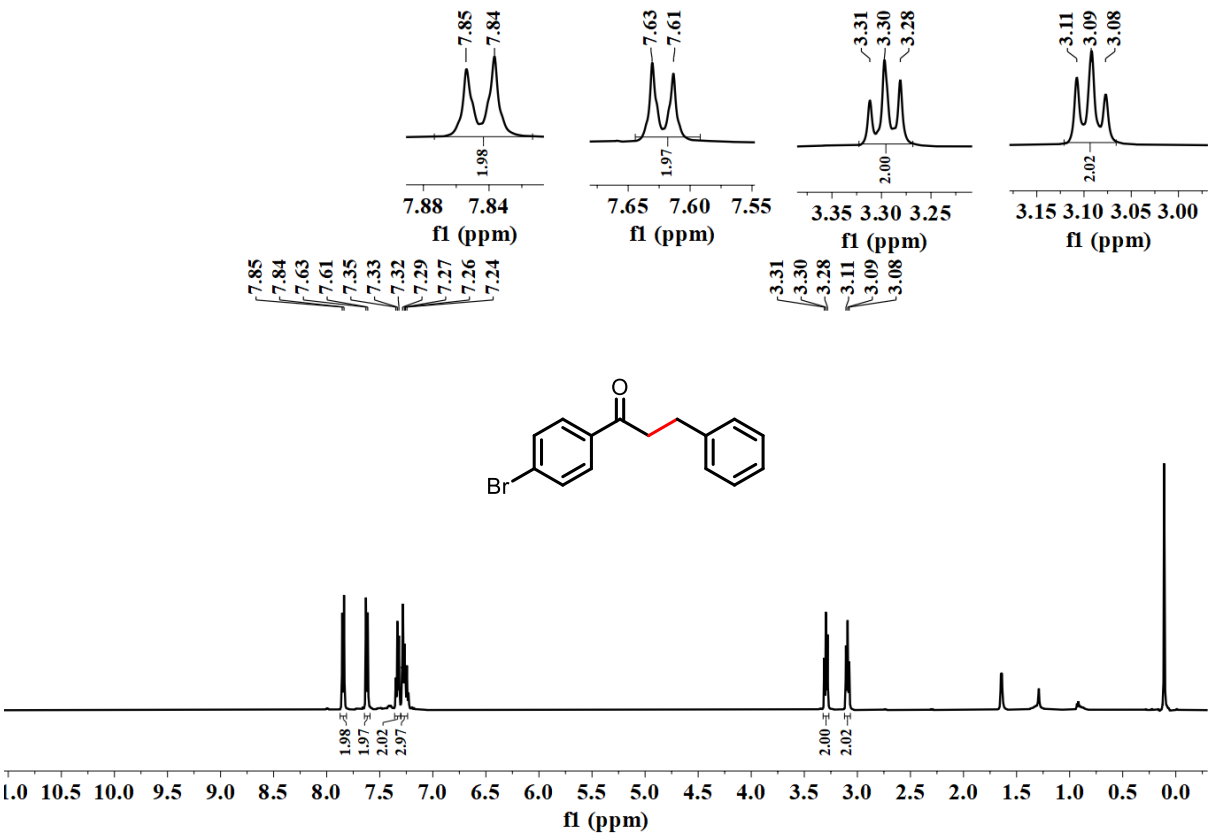

Figure S84. ^{1}H NMR spectrum of **Ci** in $CDCl_3$ (500 MHz).

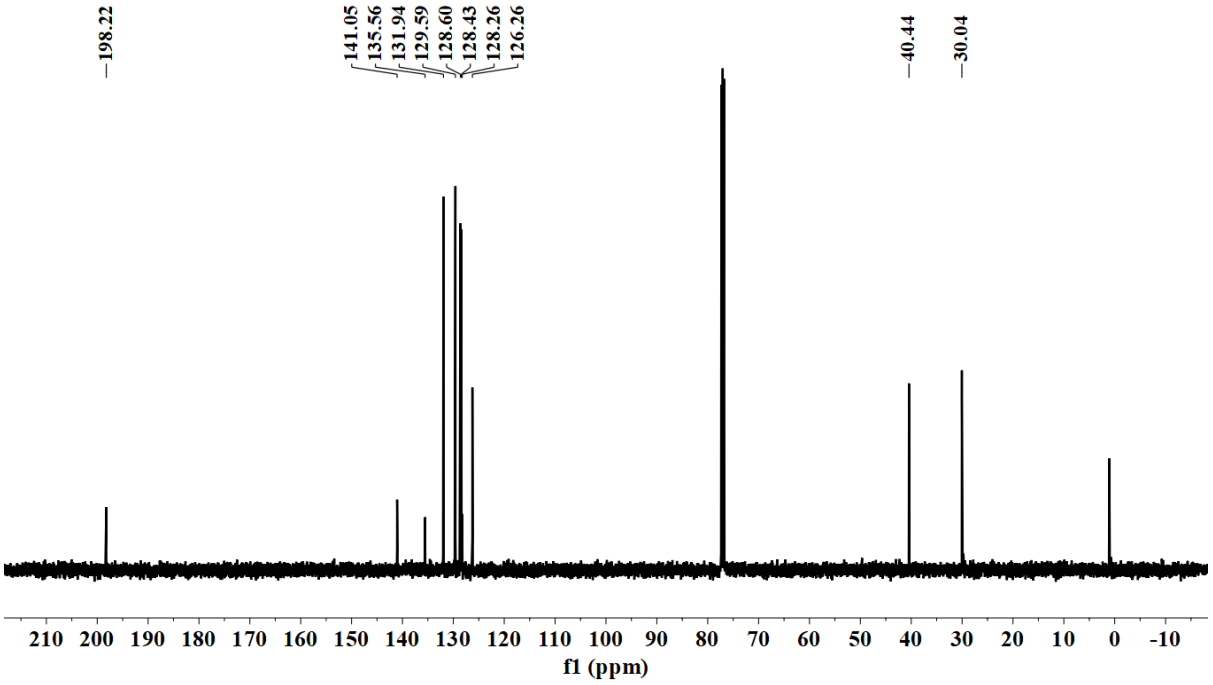

Figure S85. ^{13}C{^{1}H} NMR spectrum of **Ci** in $CDCl_3$ (126 MHz).

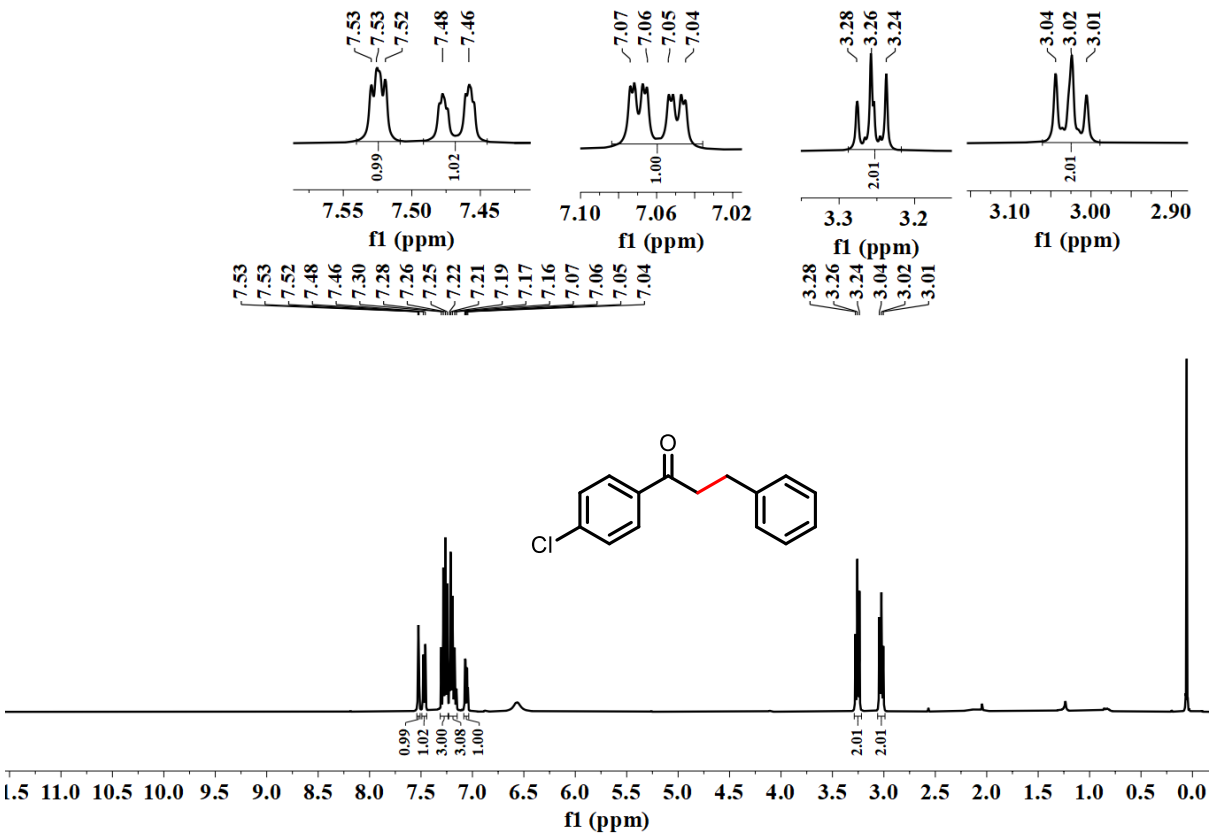

Figure S86. ^{1}H NMR spectrum of **Cj** in $CDCl_3$ (400 MHz).

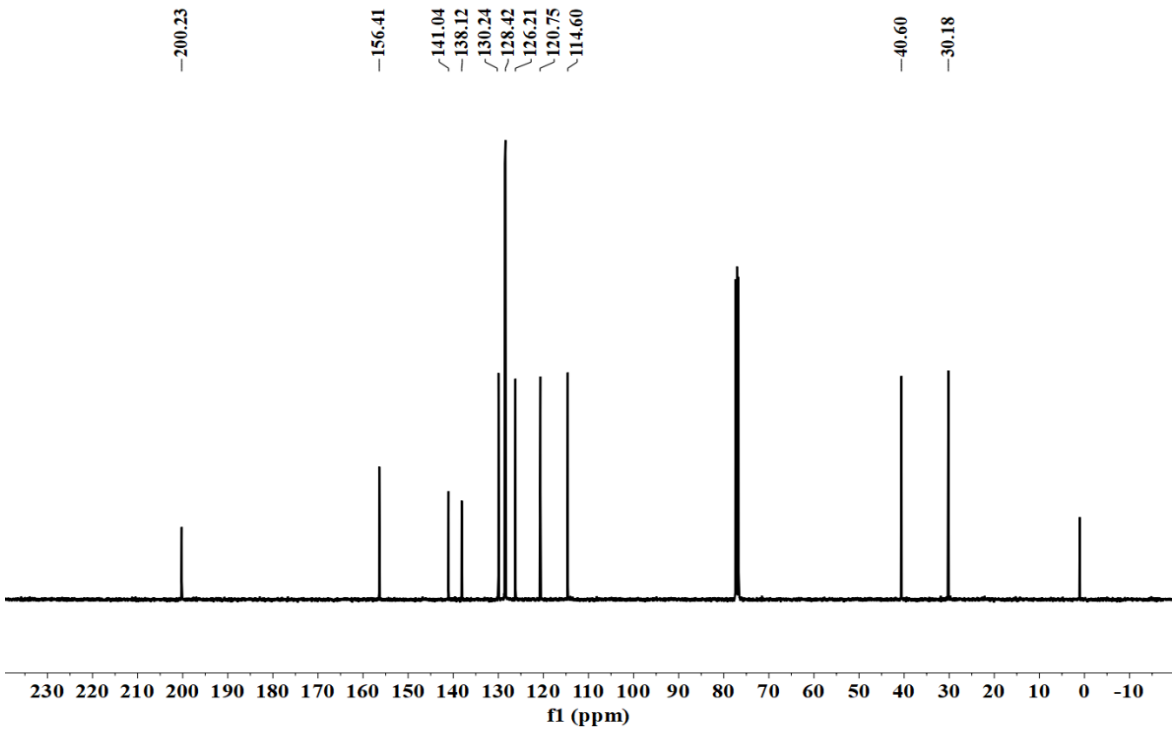

Figure S87. $^{13}C\{^{1}H\}$ NMR spectrum of **Cj** in $CDCl_3$ (101 MHz).

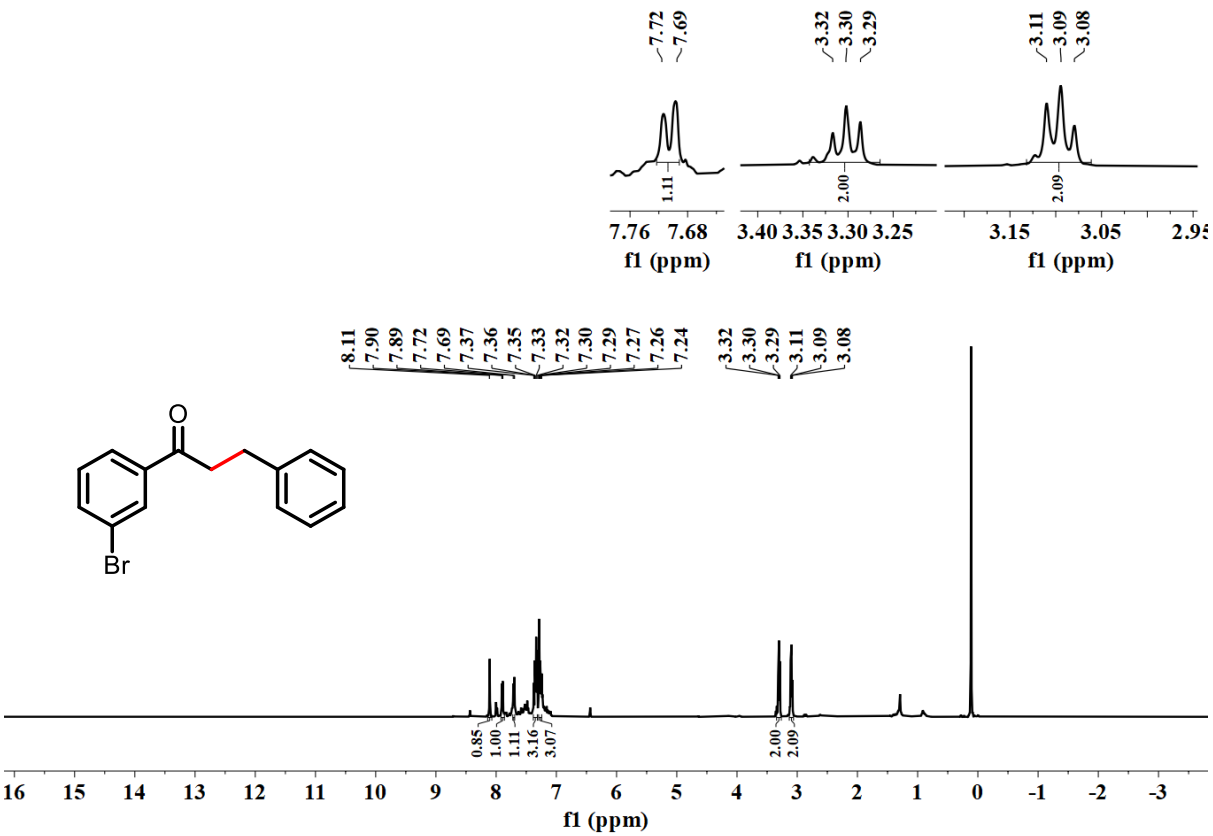

Figure S88. ^{1}H NMR spectrum of **Ck** in $CDCl_3$ (500 MHz).

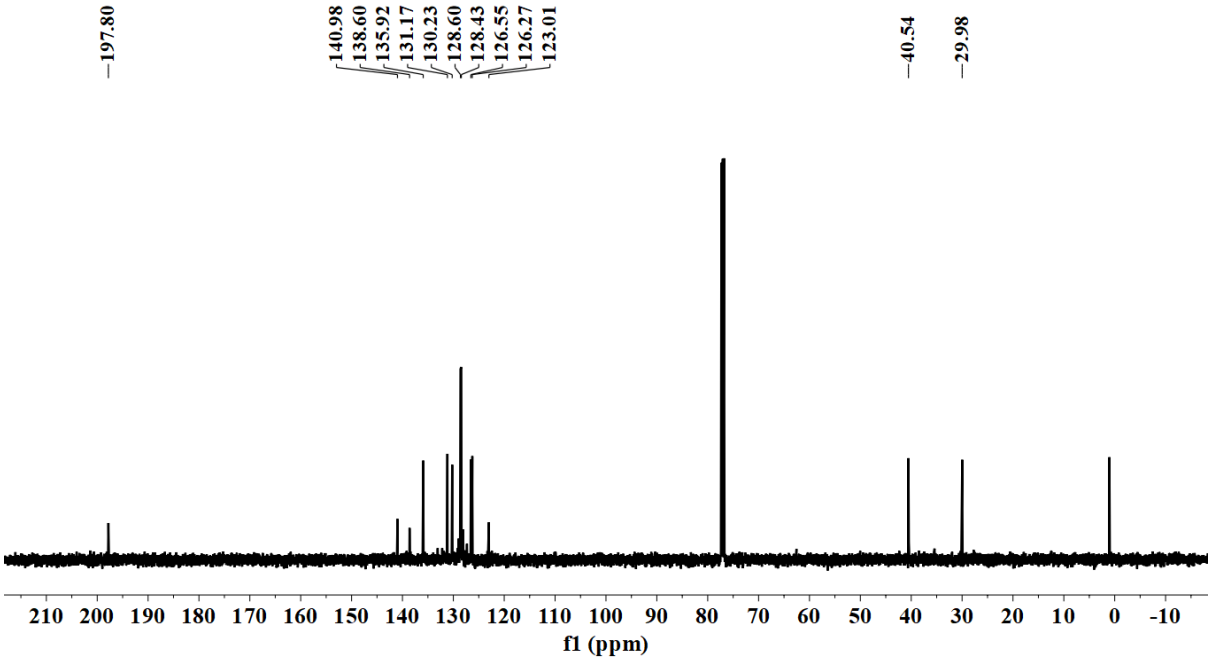

Figure S89. $^{13}C\{^{1}H\}$ NMR spectrum of **Ck** in $CDCl_3$ (126 MHz).

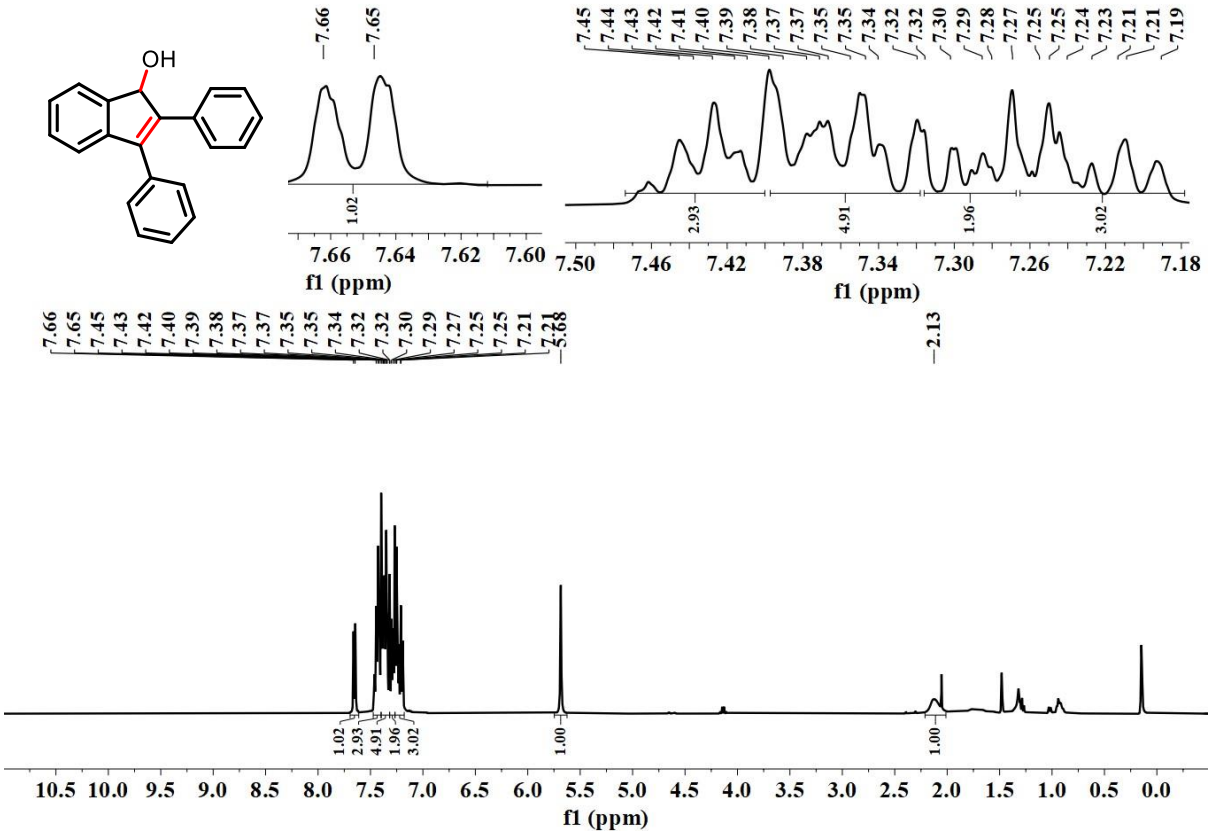

Figure S90. ^{1}H NMR spectrum of **Da** in $CDCl_3$ (400 MHz).

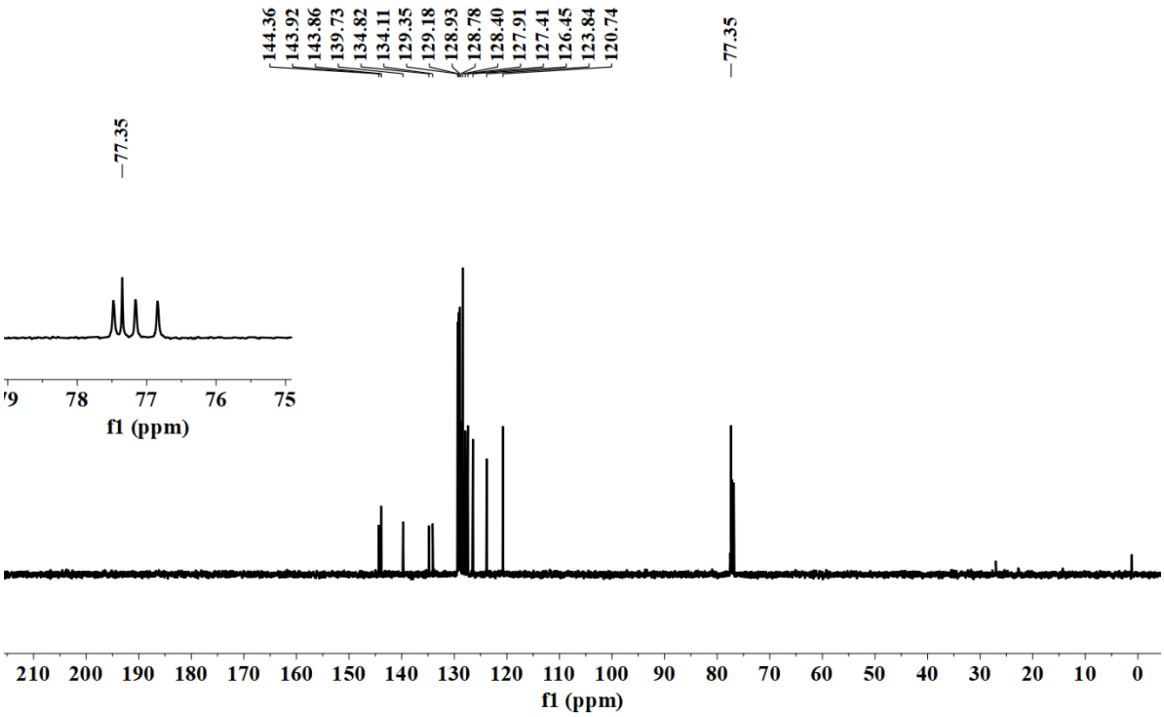

Figure S91. $^{13}C\{^{1}H\}$ NMR spectrum of **Da** in $CDCl_3$ (101 MHz).

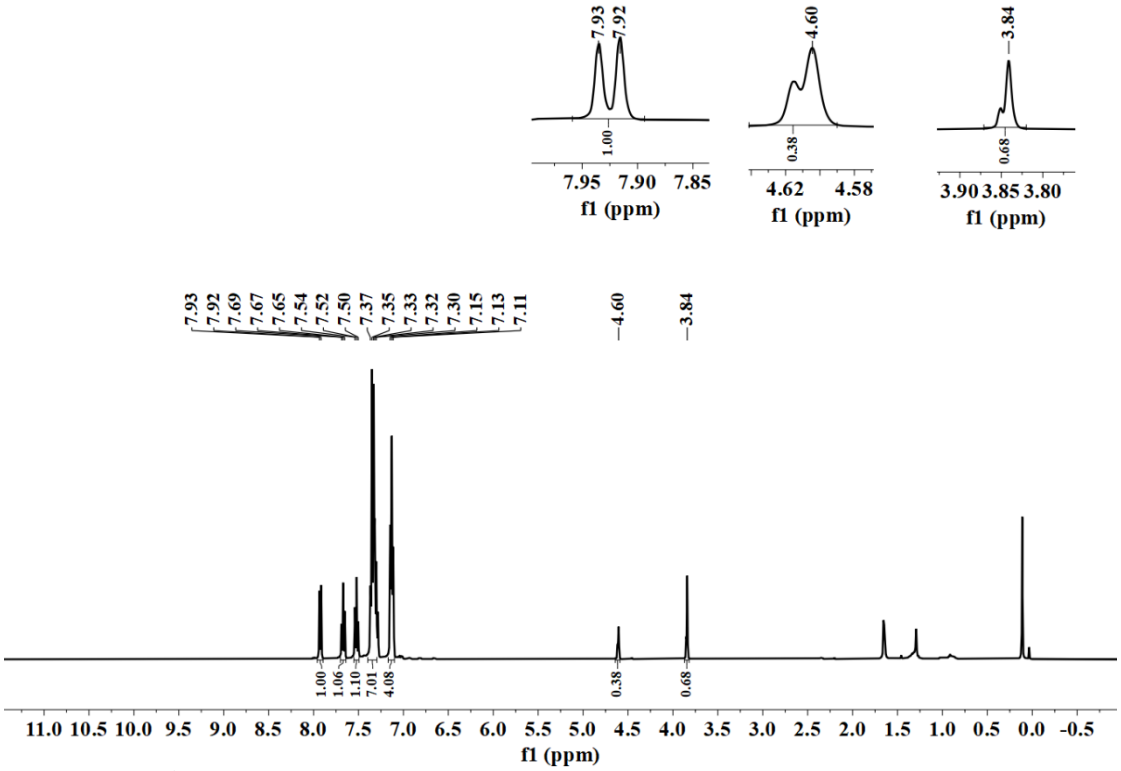

Figure S92. ^{1}H NMR spectrum of **I1** in $CDCl_3$ (400 MHz) (D_2O incorporation).

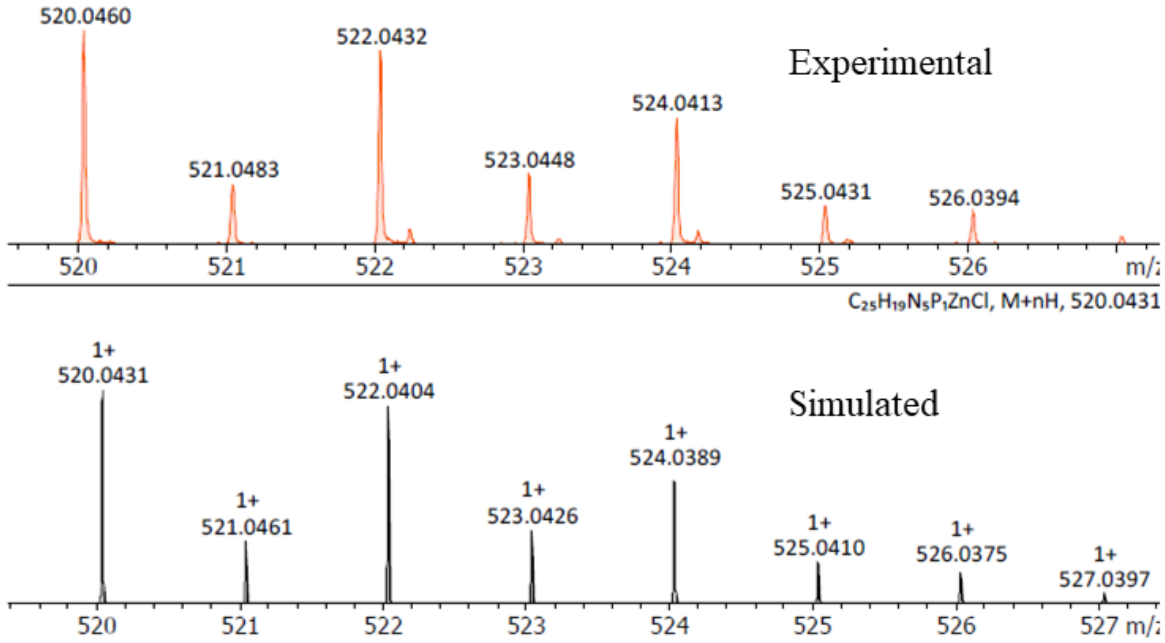

Figure S93. HRMS spectrum of **ZnClL5**.

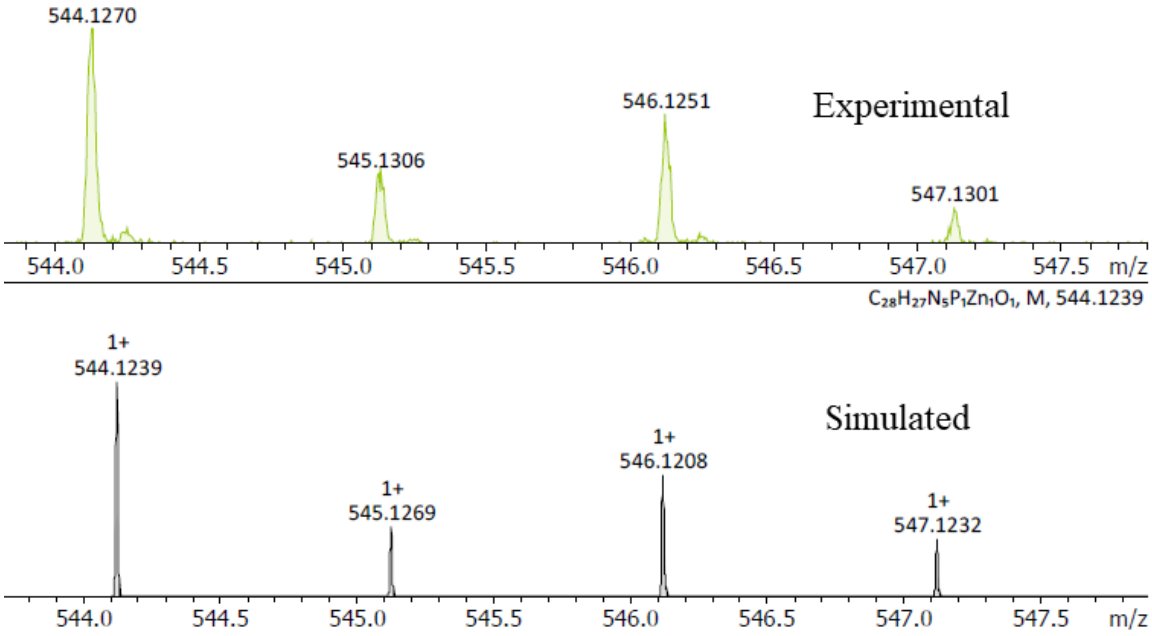

Figure S94. HRMS spectrum of **Z-^{i}OPr**.

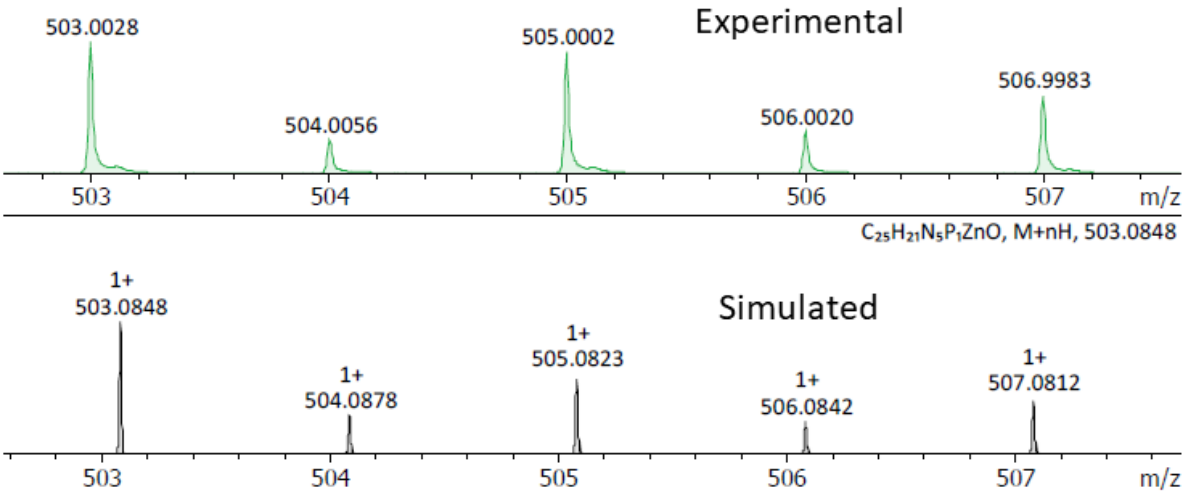

Figure S95. HRMS spectrum of **Z-H+H_2O**.

Computational details

In this investigation, we utilized Gaussian 09 Revision D.01 (Gaussian, Inc., Wallingford, CT, 2009) for all DFT calculations. The Grimme's dispersion-corrected B3LYP functional (B3LYP-D3) was employed for geometry optimization.[6] Geometry optimization and computation of imaginary frequencies were performed for all entities, encompassing reactants, intermediates, and transition states of L3 and L5-ligated ligands. The LanL2DZ basis set for zinc metal and the 6-31G* basis set for C, H, N, O, and P, Cl were used in the calculations.[6b, 7] Solvation energy was incorporated into the gas phase energy using a more advanced level of theory (B3LYP-D3/def2-TZVP).[8] Solvation energy determination employed the polarizable continuum model (PCM) with toluene as the solvent, accounting for electrostatic, dispersion-repulsion, and cavitation terms.[9] Frequency calculations were conducted to identify minima on the potential-energy surface (PES) and determine free energy correction energy. The choice of 2-propanol as the solvent matched the experimental conditions. Visualization of optimized geometries was done using Chemcraft 1.6 and Gaussview 6.0.[10] Gaussian 09 software was used for NBO (Natural Bond Orbital) and WBI (Wiberg Bond Index) analyses using DFT methods.[11] NBO analysis provided detailed insights into bonding orbitals and natural charge distribution (see Table S5-S6), while WBI analysis offered bond index values indicating bond nature.

Here we are considering the simple equation suggested via energy span approximation given as.[12]

$TOF \approx e^{-\delta E}$ ……eq(1)

{TDTS-TDI} if TDTS is coming after the TDI ……..1a

{TDTS-TDI+ΔG_r} if TDTS is coming before TDI …….1b

Mechanistic Insights from DFT Calculations

DFT calculations were carried out using the G09 suite of software (Gaussian, Inc., Wallingford, CT, 2009) employing B3LYP-D3/LanL2DZ(Zn);6-31G*(rest)//B3LYP-D3/def2-TZVP(PCM) level of theory (see computational details).[6b, 7a, 7c, 8] To understand the role of the ligand in catalysis, we have thoroughly studied the full mechanistic cycle of [**$ZnCl_2L3$**] and [**ZnClL5**] catalysts, with the former being the least efficient and the latter the most efficient (39 vs 85 % conversion; see Table S1) (Figure S96-S101). The mechanism, adapted from experimental findings and earlier literature precedents, is depicted in Scheme S1. In the proposed scheme, the initial step entails the cleavage of the Zn–Cl bond, and concurrently, chloride abstracts hydrogen from the O–H bond of the isopropanol species during the formation of transition state **TS1** (Scheme S1). The elimination of hydrochloric acid (HCl) leads to the formation of **Int1** species. The **Int1** species diverge into two possible pathways with the C–H bond activation of the ketone facilitated by Zn (**TS2**) or by the ligand (**TS2'**). In the subsequent step, the formation of Zn-H is assumed (**Int2**), which has been suggested as a key intermediate in this catalytic transformation in earlier studies.[13] In the next step, acetophenone is expected to react with **Int2** via **TS3** where in Zn…O bond formation and Zn…H bond cleavage are expected to occur simultaneously leading to the formation of alkoxy bound Zn intermediate (**Int3**). In the final step, isopropanol once again facilitates protonation, leading to the formation of the final product and the regeneration of the **Int1** species, thereby restarting the catalytic cycle. (Scheme S1).

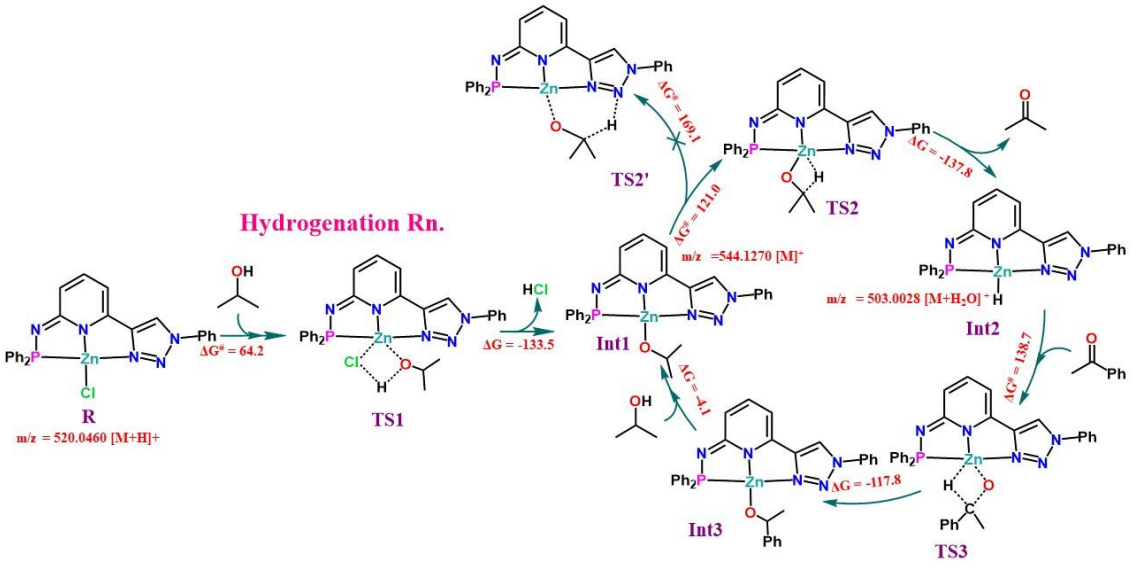

Scheme S1. Schematic mechanism adapted for the transfer hydrogenation of carbonyl compounds by [**ZnClL5**].

The optimised geometry of the [**$ZnCl_2$L3**] and [**ZnClL5**] catalysts, along with other intermediates, is shown in Figures S97 and S100. Strikingly, the geometry around Zn^{II} in [**$ZnCl_2$L3**] is distorted tetrahedral, whereas in [**ZnClL5**] it is distorted T-shaped geometry, due to the pincer-type PNN coordination of the ligand. Further NBO analysis were performed to ascertain the nature of the donor-acceptor interaction to ascertain the strength of the individual Zn–N/P coordinate bond. This analysis suggests that among both the catalysts, the Zn–P bond being the strongest (239.5 kJ/mol in NBO second-order PT theory donor-acceptor interactions), (Table S2), and the Zn–N interactions in L3 catalyst, on the other hand, are relatively weaker (46.8 kJ/mol). In the next step, Zn–Cl bond cleavage is assumed (see Table S2-S3). In the next step, the cleavage of the Zn–Cl(1) bond and formation of the Zn–O(1) bond is assumed to take place simultaneously via **TS1**. It has been noted that the energy required for the formation of the transition state in **L5–TS1** is 4.9 kJ/mol higher than that in **L3–TS1** (Figure S102 and S103). With both ligands at TS1, the Zn–Cl bond is fully broken, and the Zn–O(1) bond is nearly formed, indicating a product-like transition state. Further, the cleaved chloride ion was found to lie closer to the H atom of the alcohol, indicating the formation of HCl. **L5–TS1** has an unusual seesaw geometry, while distorted tetrahedral geometry is maintained at **L3-TS1**. The variance in energy is attributable to the steric effects introduced by the L5 ligand when compared to the **L3** ligand (Figures S98 and S101). After the elimination of hydrochloric acid, the subsequent step involves the formation of intermediate **Int1**. In the case of **L5–Int1**, the energy difference obtained is -69.3 kJ/mol, whereas for **L3–Int1** species, it is -72.1 kJ/mol. The exothermic formation of this intermediate suggests the facile formation of this species. The optimized geometry of these intermediates reveals Zn–O bond distances of 1.875 Å and 1.884 Å for **L3–Int1** and **L5–Int1**, respectively, in the **Zn–O^{i}Pr** species (Figure S97 and S100). The exothermic formation of this intermediate and subsequent step having a significant kinetic barrier (vide infra) suggests that this species is likely to have a significant lifetime time, and this is affirmed by the experimental HRMS studies where these intermediates are unambiguously detected. In the next step, the β-hydrogen elimination via **TS2** or **TS2'** is assumed. In the first case, this simultaneous breaking of the O(1)–H(2) bond and the formation of the Zn–H(2) bond incurs an energy barrier of 137 kJ/mol for the **L3–TS2** transition state and 121 kJ/mol for the **L5–TS2** transition state, respectively. The larger energy barrier in **L3–TS2** may stem from the absence of the phosphine donor group, whereas in **L5–TS2**, this

deficiency is compensated. This suggests that the donor ability of the phosphine group influences the barrier height of the transition state. In the case of the second possible pathway via **TS2'**, computed energies reveal that the transfer of hydrogen H(2) to the N(4) atom of the **L5** ligand has a steep energy barrier compared to **TS2** (121.0 vs 169.1 kJ/mol) and hence this pathway can be eliminated safely. This suggests that the role of ligands lies in influencing the acidity of the metal centre rather than acting as a hydrogen atom reservoir.

The computed transition state geometry for **L3–TS2** and **L5–TS2** transition states indicate the elongation of the C(1)–H(2) bond to 1.704 Å and 1.799 Å, respectively. Simultaneously, the formation of the Zn–H(2) bond is found to be 1.749 Å and 1.759 Å for **L3–TS2** and **L5–TS2**, respectively (Figure S98 and S101). The breaking and forming of bonds can also be observed through computed Wiberg bond index (WBI) and Natural bond orbital (NBO) analysis (WBI→(**L3–TS2**, O(1)–H(2):0.33/Zn–H(2):0.41) & (**L5–TS2**, O(1)–H(2):0.36/Zn–H(2):0.37), see (Figure S104 and Table S3-S6). The formation of Int2 is found to be exothermic by -93.7 kJ/mol and -86.1 kJ/mol for **L3–Int2** and **L5–Int2**, respectively, with the former leading to relatively stable Zn-H intermediate compared to the latter, which is attributed to the P→Zn donation vis-à-vis Cl→Zn donation (Figure S97 and S101, Table S2). Such a strong exothermic formation, combined with a reasonably large barrier for the next step (see below), suggests that this intermediate could be identified in experiments. As expected, the HRMS experiments performed unambiguously suggest the formation of this intermediate, offering confidence both in the established mechanism and also in the methodology employed. In the subsequent step, Zn–H is expected to activate the C=O of the acetophenone via **TS3** with an estimated barrier of 174.6 kJ/mol and 138.7 kJ/mol for **L3–TS3** and **L5–TS3**, respectively. A careful look at the frontier orbitals reveals that the phosphorous ligand donation to the $d_{x^2-y^2}$ orbital of Zn^{II} facilitates the transfer of hydride from Zn to the oxygen atom of the ketone moiety in the case of **L5-TS3**. While in the case of **L3-TS3**, the ligand contribution is found to be minimal at the HOMO with a weak π-donation from the -Cl ligand facilitating the hydride transfer. This, in fact, leads to a huge energy barrier, and this step becomes the rate-limiting step for the catalytic reaction by the L3 ligand. The barrier height for the transition state and the computed HOMO-LUMO gap were also found to have one-to-one correspondence with a lower gap yielding lower barrier heights. As **L3-TS3** is the rate-limiting step and **L5-TS3** is not, we also carefully look at the NBO second-order perturbation theory analysis to quantify the donation from the ligand to the metal ion at the transition state geometry (see Figure S104-S106). This analysis indicates a strong P(3*s*)→ Zn(4*s*) donation at the transition state with the

donor-acceptor strength of 48.4 kcal/mol, while the strongest donation at this transition state in the case of L3 is found to be N($2p_y$)→Zn($4p_x$) amounting to 11.7 kcal/mol. This clearly suggests that the incorporation of the P-donor atom is important in stabilising the transition state, reducing the kinetic energy penalty. Furthermore, a robust C-H•••π interaction has been observed, playing a crucial role in stabilizing the L5-TS3 transition state and effectively lowering the barrier (see Figure S107).

During this transition state, the Zn–H(2) bond elongates to 1.768 Å in both the cases (**L3**/**L5–TS3**). Simultaneously, the formation of the C(2)–H(2) bond takes place at bond distances of 1.791 Å and 1.680 Å, respectively, leading to the formation of intermediate **Int3**. This has been further validated by NBO and WBI analysis (WBI→(**L3–TS3**, O(2)–H(2):0.34/Zn–H(2):0.39) & (**L5–TS3**, O(2)–H(2):0.37/Zn–H(2):0.34)). The formation of this intermediate is found to be exothermic for both the ligands (-66.0 kJ/mol and -65.0 kJ/mol for **L3–Int3** and **L5–Int3**, respectively; Figure S97 and S100). In the final step, the hydrolysis of the Zn-O(R) bond with isopropanol results in the formation of 1-phenyl methanol and the regeneration of **Int1**. This catalyst regeneration, occurring under nearly thermoneutral conditions, completes the process along with the formation of the final product.The catalysts with **L3** and **L5** ligands exhibit different rate-determining steps. To assess their catalytic efficiency, the energy span approximation is employed as suggested earlier for such complex catalytic cycles.[12] In the case of the **L3** ligated catalyst, **L3–TS3** is considered as the turnover frequency determining transition state (TDTS), and **L3–Int2** is regarded as the turnover frequency determining Intermediate state (TDI). The energy difference (TDTS-TDI) for the **L3**-catalyst is determined to be 174.6 kJ/mol. Since the maximum TDTS occurs before TDI in the case of the **L5**-catalyst, the **L5–TS1** state is considered the TDTS state, and the **L5–Int2** state is considered the TDI state. Hence, here the resulting overall kinetic barrier is (TDTS-TDI+ΔG_r) as 151.8 kJ/mol (see Figure S102 and S103). This energy difference directly correlates with TOF. Therefore, it implies a lower TOF for **L3** compared to **L5**. This suggests that the **L5**-ligated catalyst exhibits higher catalytic efficiency, aligning well with experimental results. In summary, DFT calculations employed to investigate the electronic structure and reactivity of the direct hydrogenation reaction with Zn(II) catalyst with various designer ligands unveil the importance of ligand contribution. A comparative analysis of **L3** and **L5** ligands provided insights into metal-ligand cooperation (MLC), where the presence of phosphine donor in the L5 ligand framework makes a significant donation to the Zn(II) atom at the transition states leading to the lower kinetic barrier. Although the PNN pincer ligand put in greater steric strain during the

catalytic cycle compared to the pyridinic ligand, this steric strain is more than compensated by the stronger donation in the transition states and also the corresponding intermediates. Particularly, our calculations reveal that two ligands have two different rate-limiting steps with the pincer ligand, the rds being the Zn–Cl bond cleavage followed by Zn-O(R) bond formation, while in the case of the pyridinic ligand, the rds being the cleavage of Zn-H bond followed by Zn-O(R) bond formation. A strong P → Zn donation at the Zn-H bond cleavage step ensures that the Zn(II) ion in the L5 environment is less acidic than in the L3 environment leading to this changeover. Further TDTS-TDI analysis reveals important insight into the overall energetics of the catalytic cycle, strengthening this approach to understanding such a complex catalytic cycle. The observation of a substantial exothermic formation energy, followed by a more pronounced kinetic barrier in the subsequent step during the formation of Zinc-alkoxy species, implies a relatively extended half-life for this particular species. This inference gains further validation through experimental results obtained via High-Resolution Mass Spectrometry (HRMS). The confidence in the chosen mechanism and methodology is bolstered by the consistency between the theoretical predictions and the experimental outcomes.

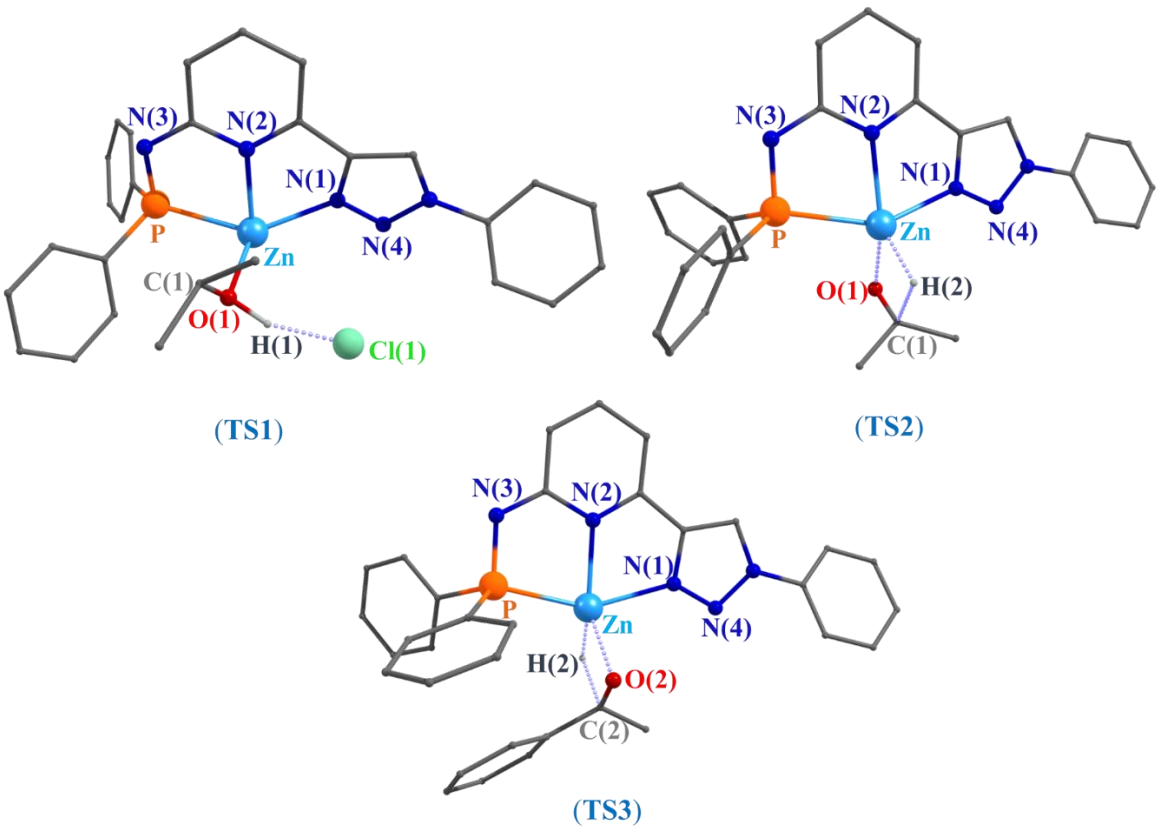

Figure S96. Atom numbers and positions demonstration via transition state structures. Colour code: Zinc (sky blue), Chloride (light green), phosphorus (orange), oxygen (red), nitrogen (blue), carbon (grey), hydrogen (white).

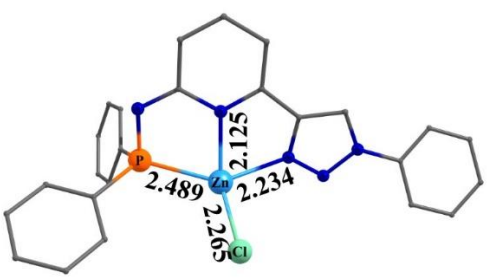

∠ N(2)–Zn–Cl(1) = 134.9°, ∠ P–Zn–N(1) = 140.9°

(R)

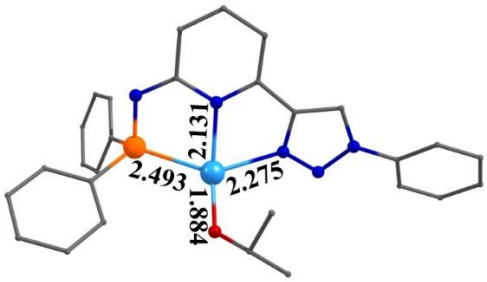

∠ N(2)–Zn–O(1) = 138.9°, ∠ P–Zn–N(1) = 141.1°
Zn–O(1)-C(1) = 127.8°

(Int1)

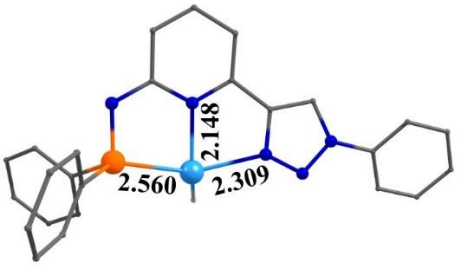

C(2)–H(2) = 1.633 Å
∠ N(2)–Zn–H(2) = 141.3°, ∠ H(2)–Zn–P = 118.8°

(Int2)

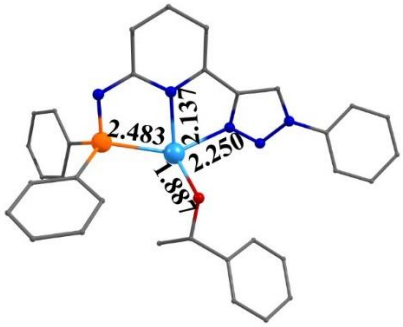

∠ N(2)–Zn–O(2) = 130.4°, ∠ P–Zn–N(1) = 145.0°
Zn–O(2)-C(2) = 130.6°

(Int3)

Figure S97. Computed bond lengths (Å) and bond angles (°) for reactant and intermediate species, optimized using B3LYP-D3/Lanl2DZ, 6-31G* level of theory.

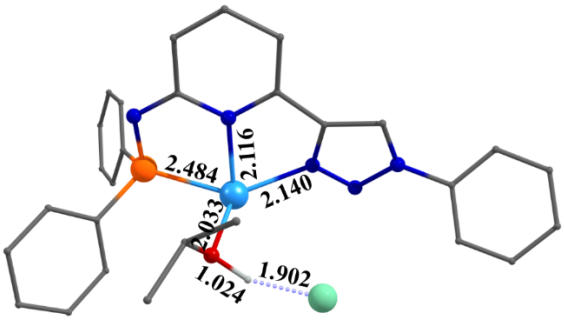

∠ N(2)–Zn–O(1) = 107.2°, ∠ P–Zn–N(1) = 141.5°
∠ Zn–O(1)-C(1) = 119.9°, ∠ O(1)-H(1)-Cl(1) = 154.7°

(TS1)

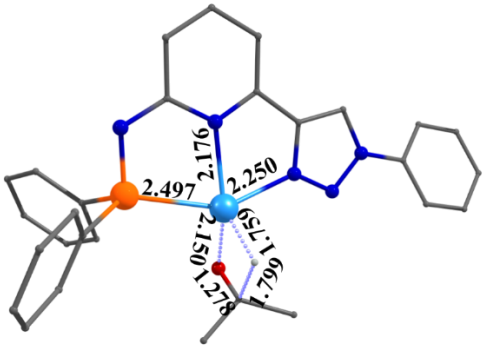

∠ N(2)–Zn–O(2) = 144.4°, ∠ P–Zn–N(1) = 147.2°
∠ Zn–O(1)-C(1) = 87.9°, ∠ Zn–H(2)–C(1) = 87.5°
∠ H(2)–C(1)–O(1) = 106.4°, ∠ O(1)–Zn–H(2) = 78.1°

(TS2)

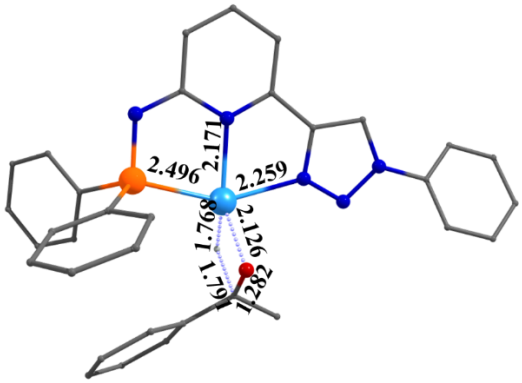

∠ N(2)–Zn–O(2) = 130.7°, ∠ P–Zn–N(1) = 150.8°
∠ Zn–O(2)-C(2) = 88.6°, ∠ Zn–H(2)-C(2) = 87.2°
∠ H(2)–C(2)-O(2) = 105.8°, ∠ O(2)–Zn-H(2) = 78.2°

(TS3)

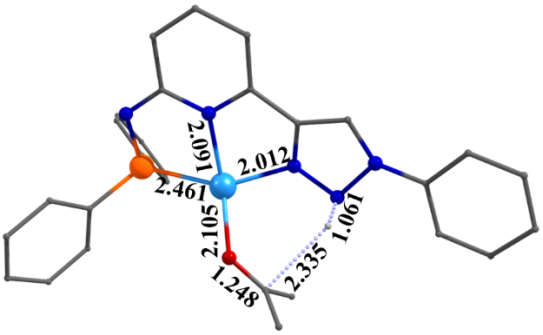

∠ N(2)–Zn–O(1) = 127.7°, ∠ P–Zn–N(1) = 151.1°
∠ Zn–O(1)-C(1) = 131.5°, ∠ C(1)–H(2)–N(4) = 125.0°

(TS2')

Figure S98. Computed bond lengths (Å) and bond angles (°) for transition state species, optimized using B3LYP-D3/Lanl2DZ, 6-31G* level of theory.

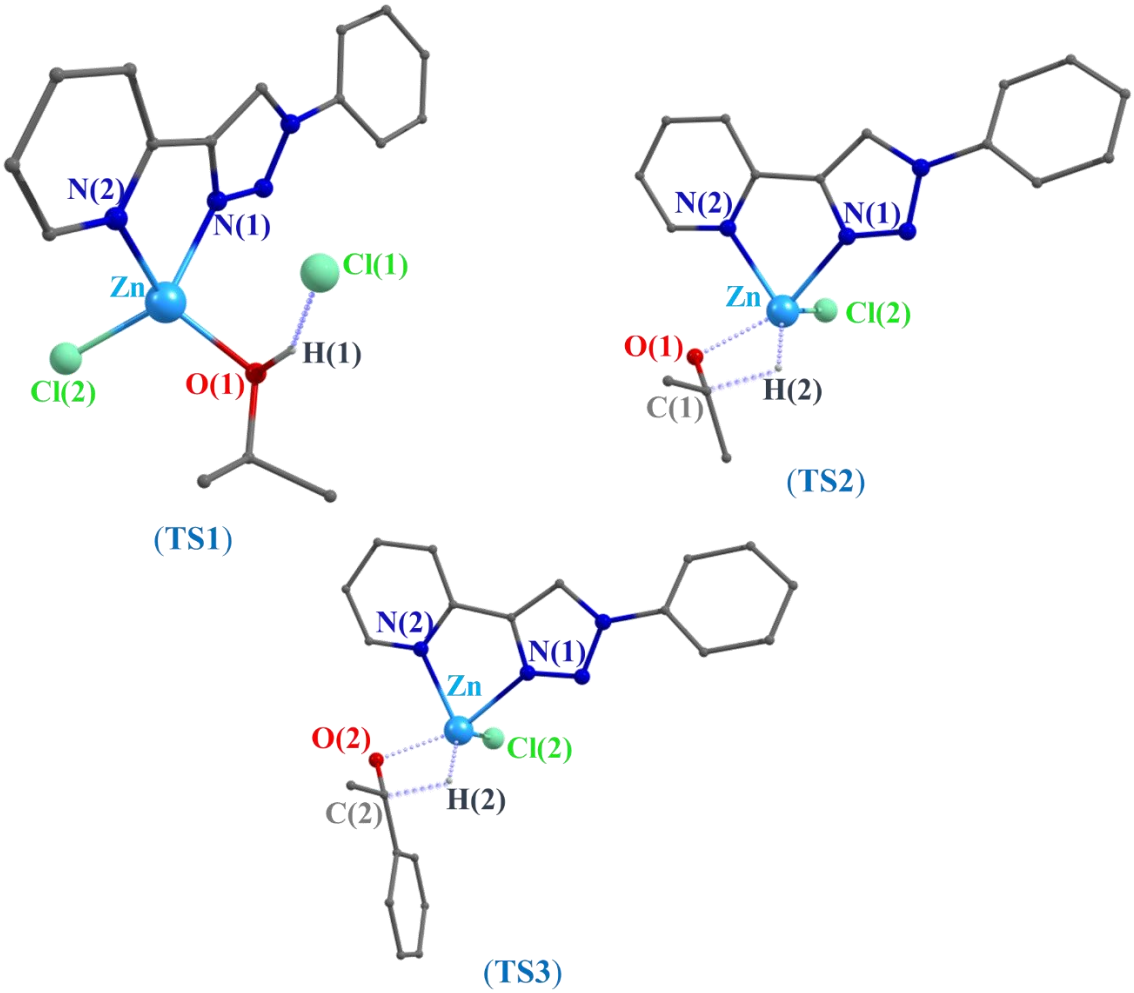

Figure S99. Atom numbers and positions demonstration via transition state structures. Colour code: Zinc (sky blue), Chloride (light green), oxygen (red), nitrogen (blue), carbon (grey), hydrogen (white).

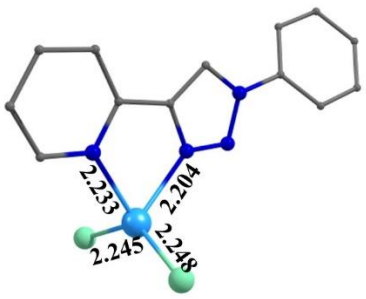

∠ N(1)–Zn–N(2) = 75.3°, ∠ Cl(1)–Zn–Cl(2) = 135.0°
∠ N(2)–Zn–Cl(2) = 104.5°, ∠ N(1)–Zn–Cl(l) = 107.9°

(R)

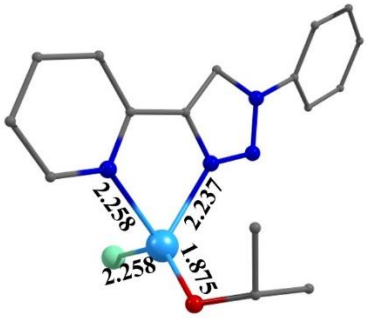

∠ N(2)–Zn–Cl(2)= 102.5°, ∠ N(1)–Zn–N(2) = 74.3°
∠ Cl(1)–Zn–O(1) = 133.3, ∠ Zn–O(1)-C(1) = 123.4°

(Int1)

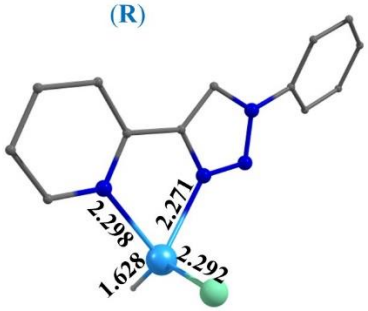

∠ N(1)–Zn–N(2) = 73.2°, ∠ H(2)–Zn–N(2) = 114.2°
∠ N(1)–Zn–Cl(2) = 99.2°, ∠ H(2)–Zn–Cl(2) = 137.9°

(Int2)

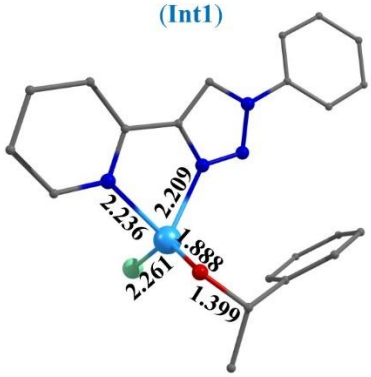

∠ N(1)–Zn–N(2) = 75.1°, ∠ N(2)–Zn–Cl(2) = 106.3°,
∠ Zn–O(2)–C(2) = 122.7°, ∠ Cl(2)–Zn–O(2) = 135.4°

(Int3)

Figure S100. Computed bond lengths (Å) and bond angles (°) for reactant and intermediate species, optimized using B3LYP-D3/Lanl2DZ, 6-31G* level of theory.

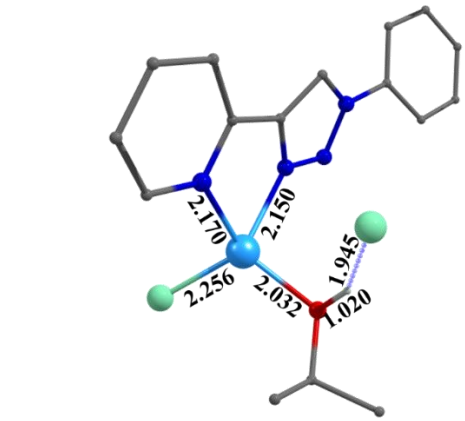

∠ N(1)–Zn–N(2) = 77.3⁰, ∠ Cl(1)–H(1)–O(1) = 154.1⁰
∠ N(2)–Zn–Cl(2) = 102.8, ∠ O(1)–Zn–Cl(2) = 111.0⁰

(TS1)

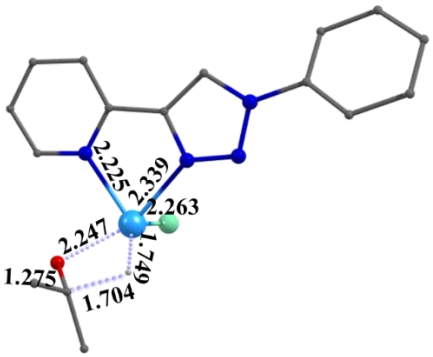

∠ N(2)–Zn–Cl(2)= 110.6⁰, ∠ Cl(2)–Zn–O(1) = 108.9⁰
∠ O(1)–C(1)–H(2) = 108.1⁰, ∠ Zn–O(1)–C(1) = 85.6⁰
∠ Zn–H(2)-C(1) = 92.7, ∠ Cl(2)–Zn–H(2) = 133.1⁰

(TS2)

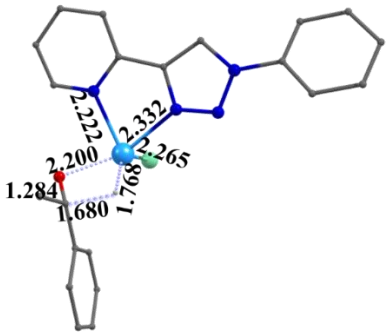

∠ N(2)–Zn–Cl(2)= 112.8⁰, ∠ Cl(2)–Zn–O(2) = 107.1⁰
∠ O(2)–C(2)–H(2) = 107.0⁰, ∠ O(2)–Zn–H(2) = 73.3⁰
∠ Zn–H(2)–C(2) = 92.4⁰, ∠ Cl(2)–Zn–H(2) = 131.4⁰

(TS3)

Figure S101. Computed bond lengths (Å) and bond angles (°) for transition state species, optimized using B3LYP-D3/Lanl2DZ, 6-31G* level of theory.

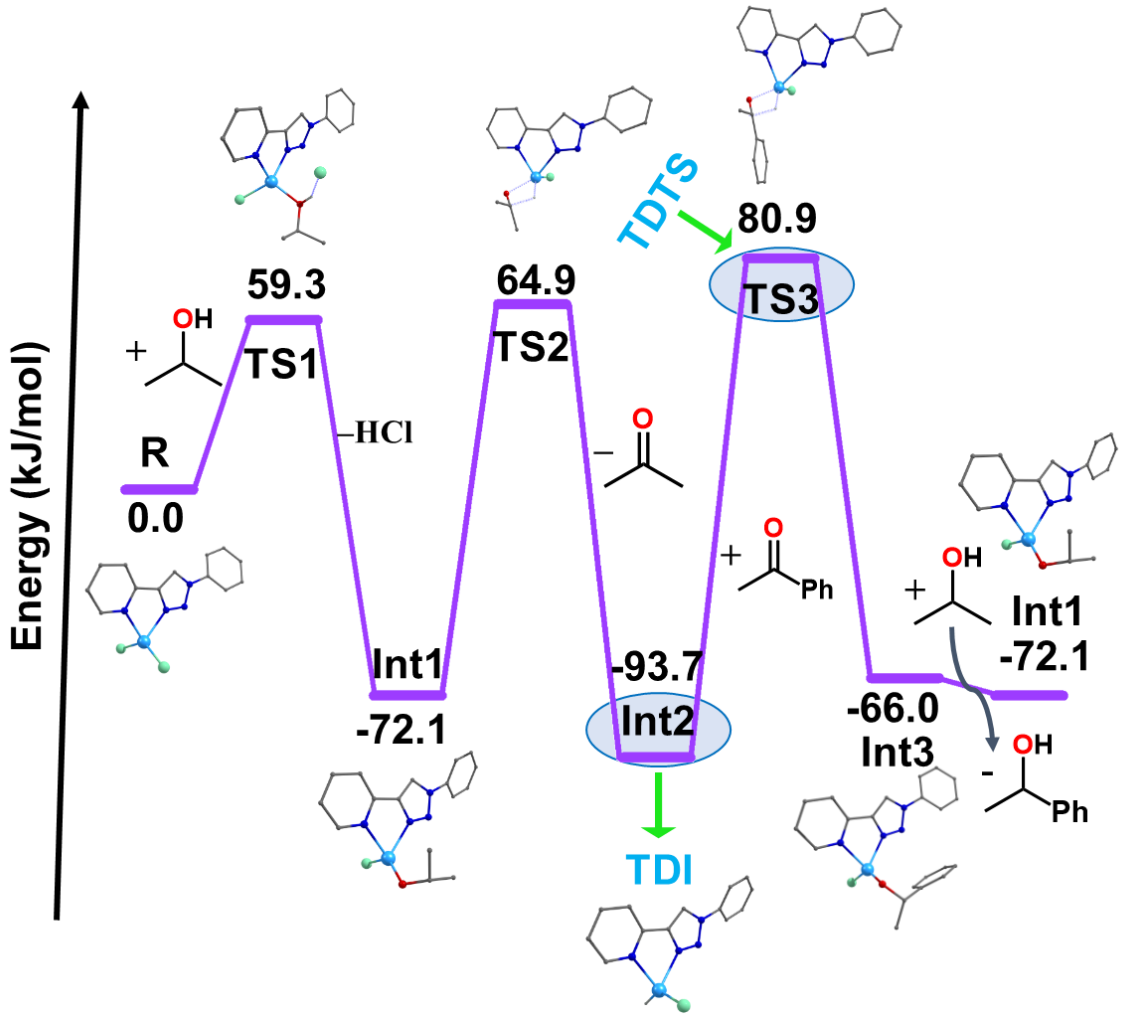

Figure S102. Computed energy profile diagram for the hydrogenation of carbonyl compounds by [**$ZnCl_2$L3**].

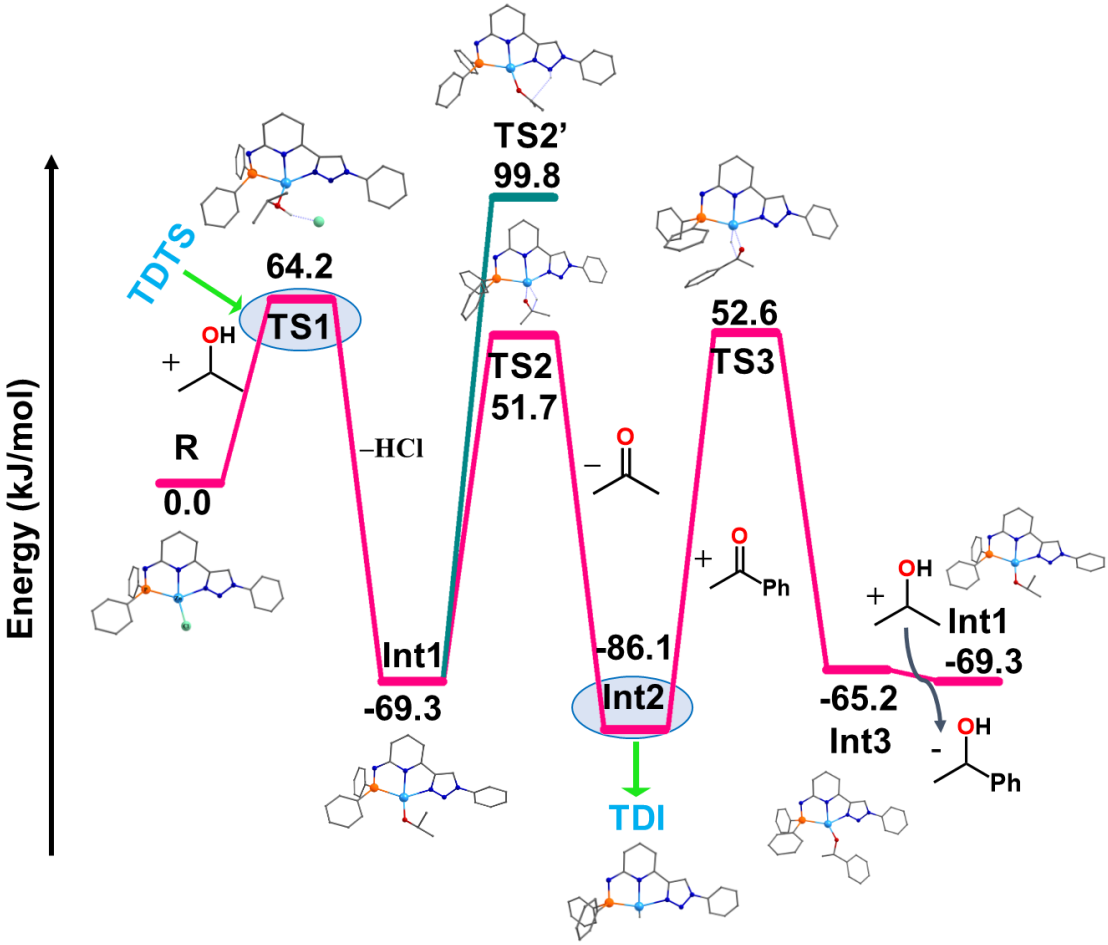

Figure S103. Computed energy profile diagram for the hydrogenation of carbonyl compounds by [**ZnClL5**].

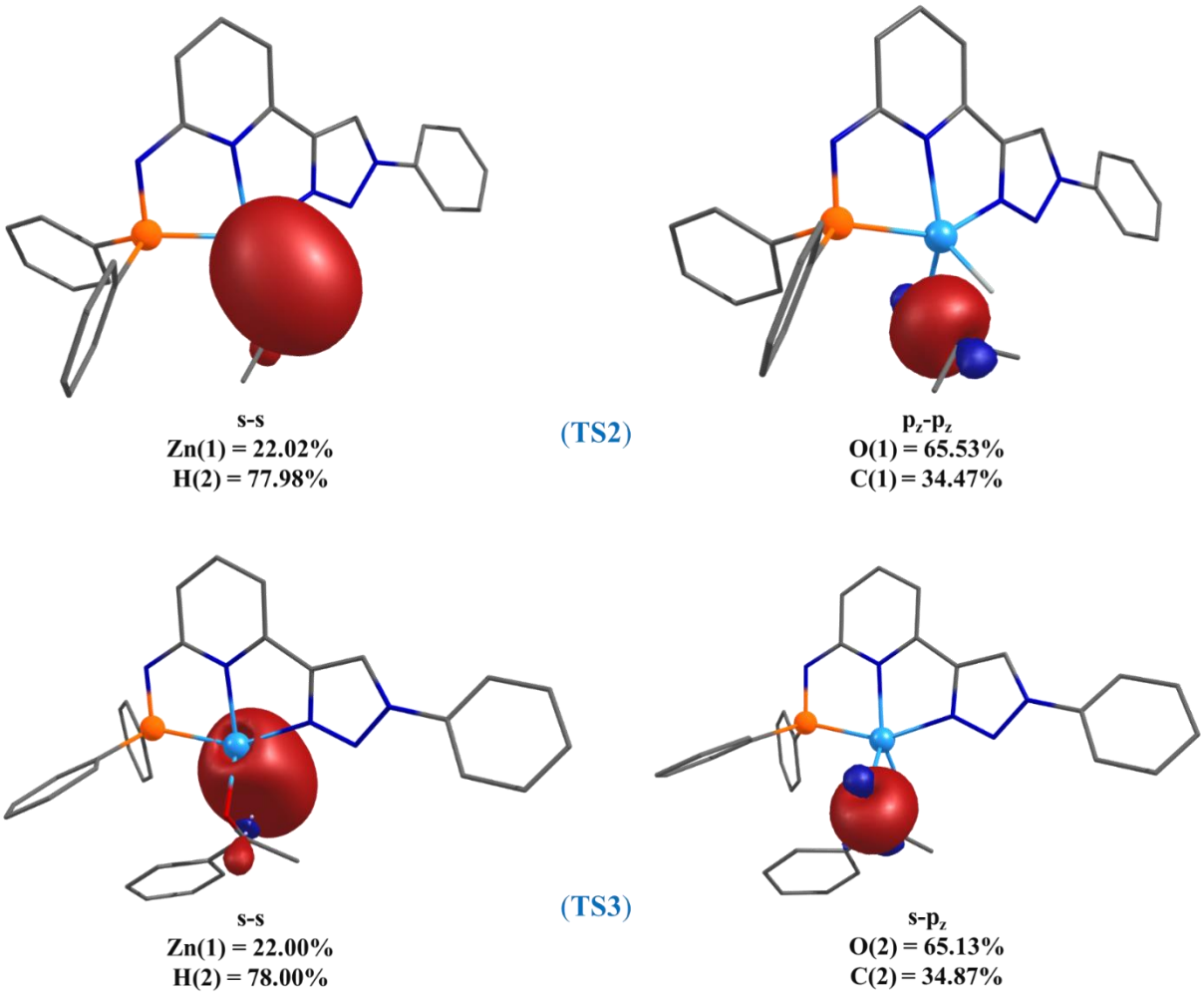

Figure S104. Computed natural bonding orbital (NBO) plots of the transition states (**TS2,** and **TS3**) for **L5**, calculated at B3LYP-D3/Lanl2dz, 6-31g* level of theory.

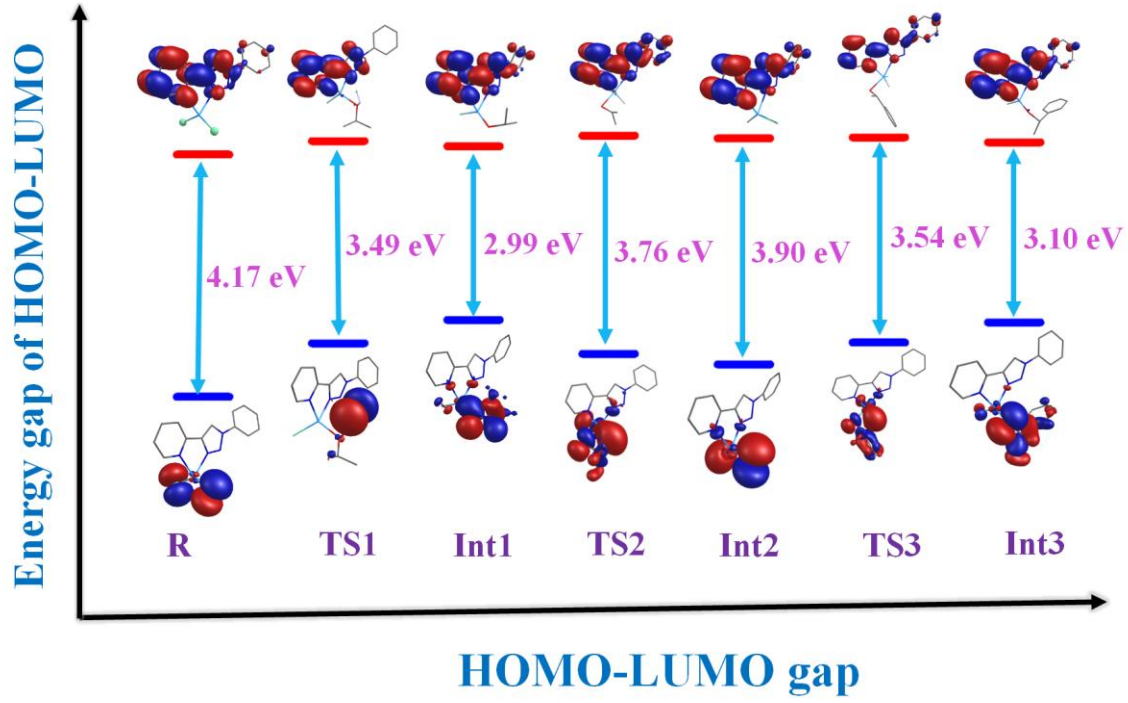

Figure S105. HOMO-LUMO gap of reactant (R), transition states (TS1-TS3), and intermediates species (Int1-Int3) for **L3**.

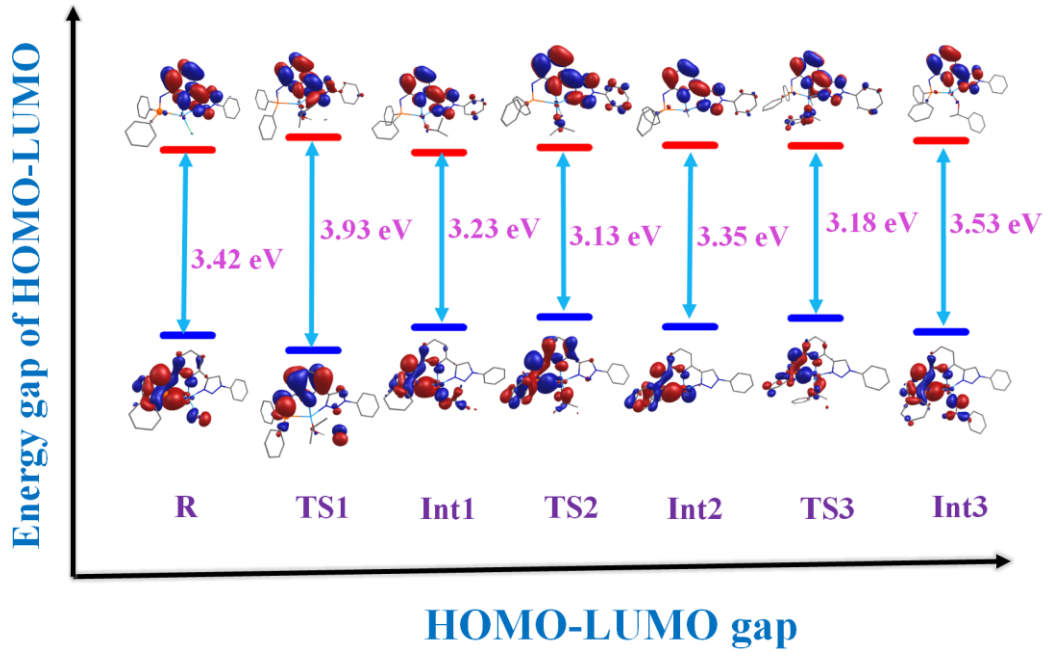

Figure S106. HOMO-LUMO gap of complex (**L5-R**), transition states (**L5-TS1** – **L5-TS3**)), and intermediates species (**Int1-L5** – **L5-Int3**) of [**ZnClL5**] complex.

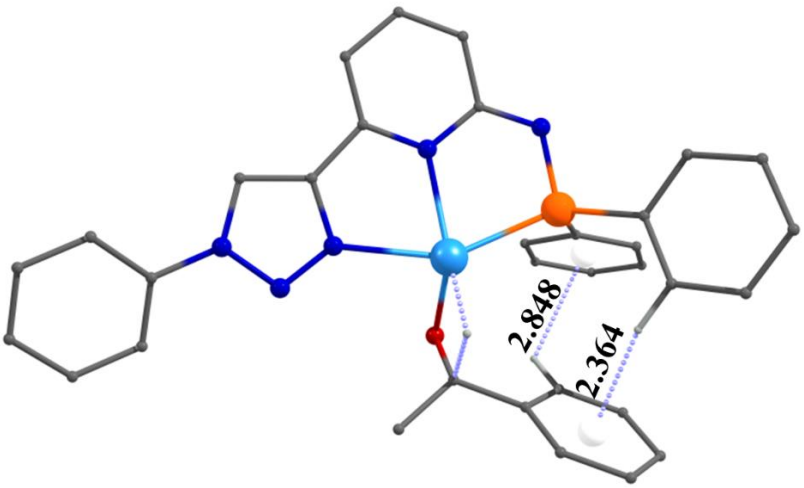

Figure S107. C-H•••π interaction observed in stabilizing the **L5-TS3** transition state, calculated at B3LYP-D3/Lanl2dz, 6-31g* level of theory.

Table S2. The second-order perturbation analysis of donor (i) and accepter (j) orbital with their stabilization energies (E_2) (in kcal/mol).

	Donar (i)	**Acceptor (j)**	**Stabilization Energy (E_2)**
L5–R	LP {P[p_x]}	LP* {Zn[s]}	239.5
	LP {N(2)}	LP* {Zn}	67.3
L3–R	LP {Cl(2)}	LP* {Zn}	169.7
	LP {N(2)[p_y]}	LP* {Zn[s]}	46.8
L5–TS1	LP {P[p_x]}	LP* {Zn[s]}	219.9
L3–TS1	LP {N(2)[p_x]}	LP* {Zn[s]}	67.7
L5–TS2	LP {P[s]}	LP* {Zn[s]}	283.0
L3–TS2	LP {N(2)[p_y]}	LP* {Zn[p_y]}	56.8
L5–TS3	LP {P[s]}	LP* {Zn[s]}	202.3
L3–TS3	LP {N(2)[p_y]}	LP* {Zn[p_x]}	48.9

Table S3. Computed Wiberg bond index (WBI) value of reactant, intermediates, and transition states, calculated with B3LYP-D3/Def2-TZVP level of theory for L5-ligated catalyst.

species	Zn–Cl	Zn–P	Zn–N(1)	Zn–N(2)	Zn–O(1)	Zn–O(2)	O1-C1	O2-C2	Zn–H1	Zn–H2	C1-H2	C2-H2	O1-H2	O2-H2	H1-Cl
R	0.60	0.51	0.22	0.24	-	-	-	-	-	-	-	-	-	-	-
TS1	0.13	0.48	0.23	0.18	0.18	-	0.89	-	0.01	-	0.91	-	0.55	-	0.18
Int1	-	0.47	0.19	0.21	0.39	-	0.99	-	-	-	0.90	-	-	-	-
TS2	-	0.47	0.22	0.24	0.20	-	1.40	-	-	0.41	0.33	-	-	-	-
Int2	-	0.44	0.19	0.25	-	-	-	-	-	0.77	-	-	-	-	-
TS3	-	0.46	0.21	0.24	-	0.21	-	1.37	-	0.39	-	0.34	-	-	-
Int3	-	0.47	0.19	0.22	-	0.37	-	1.00	-	-	-	0.89	-	-	-

Table S4. Computed Wiberg bond index (WBI) value of reactant, intermediates, and transition states, calculated with B3LYP-D3/Def2-TZVP level of theory for L3-ligated catalyst.

species	Zn–Cl(1)	Zn–Cl(2)	Zn–N(1)	Zn–N(2)	Zn–O(1)	Zn–O(2)	O(1)-C(1)	O(2)-C(2)	Zn–H(1)	Zn–H(2)	C(1)-H(2)	C(2)-H(2)	O(1)-H(1)	O(2)-H(1)	H(1)-Cl(1)
R	0.61	0.62	0.21	0.18	-	-	-	-	-	-	-	-	-	-	-
TS1	0.12	0.59	0.22	0.18	0.21	-	0.89	-	0.01	-	1.02	-	0.56	-	0.17
Int1	-	0.59	0.18	0.15	0.43	-	1.01	-	-	-	0.90	-	-	-	-
TS2	-	0.62	0.17	0.20	0.15	-	1.40	-	-	0.37	0.36	-	-	-	-
Int2	-	0.56	0.19	0.16	-	-	-	-	-	0.79	-	-	-	-	-
TS3	-	0.61	0.17	0.20	-	0.16	-	1.35	-	0.34	-	0.37	-	-	-
Int3	-	0.59	0.19	0.16	-	0.39		1.00	-	-	-	0.90	-	-	-

Table S5. Computed natural charges of reactant, intermediates, and transition states, calculated with B3LYP-D3/Def2-TZVP level of theory by natural bonding orbitals (NBO) calculations for L5-ligated catalyst.

species	Zn	Cl	N1	N2	P	O1	O2	C1	C2	H1	H2	N3	N4
R	0.97	-0.62	-0.29	-0.62	1.10	-	-	-	-	-	-	-0.91	-0.01
TS1	1.15	-0.77	-0.34	-0.64	1.09	-0.84	-	0.10	-	0.52	-	-0.93	0.03
Int1	1.13	-	-0.29	-0.63	1.07	-0.94	-	0.12	-	-	0.14	-0.90	-0.03
TS2	0.92	-	-0.26	-0.59	1.11	-0.74	-	0.52	-	-	-0.28	-0.92	-0.03
Int2	0.82	-	-0.27	-0.61	1.08	-	-	-	-	-	-0.40	-0.92	-0.03
TS3	0.93	-	-0.26	-0.60	1.11	-	-0.75	-	0.49	-	-0.27	-0.91	-0.03
Int3	1.13	-	-0.29	-0.62	1.07	-	-0.94	-	0.10	-	0.15	-0.91	-0.02

Table S6. Computed natural charges of reactant, intermediates, and transition states, calculated with B3LYP-D3/Def2-TZVP level of theory by natural bonding orbitals (NBO) calculations for L3-ligated catalyst.

species	Zn	Cl(1)	Cl(2)	N(1)	N(2)	O(1)	O(2)	C(1)	C(2)	H1	H2
R	1.03	-0.62	-0.63	-0.26	-0.45	-	-	-	-	-	-
TS1	1.19	-0.79	-0.65	-0.30	-0.49	-0.81	-	0.10	-	0.51	0.19
Int1	1.18	-	-0.65	-0.27	-0.46	-0.92	-	0.12	-	-	0.14
TS2	1.01	-	-0.62	-0.23	-0.47	-0.76	-	0.49	-	-	-0.28
Int2	0.86	-	-0.65	-0.24	-0.44	-	-	-	-	-	-0.41
TS3	1.02	-	-0.63	-0.23	-0.47	-	-0.78	-	0.46	-	-0.25
Int3	1.17	-	-0.65	-0.27	-0.47	-	-0.92	-	0.10	-	0.15

Table S7. B3LYP-D3/SDD, 6-31G* level optimized coordinates of the reactant species **L5**–**R**.

0, 1

Zn	-0.063690000	0.722840000	0.005482000
Cl	0.352679000	2.937643000	-0.221725000
P	-2.411482000	-0.102704000	-0.021311000
N	3.113638000	0.426136000	0.779203000
N	4.149648000	-0.115415000	0.117434000
N	2.034019000	-0.019539000	0.203027000
N	0.044518000	-0.963248000	-1.283247000
N	-2.325488000	-1.175564000	-1.311361000
C	5.490477000	0.188351000	0.495393000
C	5.774372000	1.433569000	1.062638000
H	4.973275000	2.148868000	1.210445000
C	8.107866000	0.789652000	1.203471000
H	9.131347000	1.026264000	1.479271000
C	-1.116686000	-1.515779000	-1.765652000
C	-5.061631000	0.684341000	-0.505380000
H	-5.311880000	-0.358749000	-0.333693000
C	-0.984347000	-2.517296000	-2.792874000
H	-1.895746000	-2.914590000	-3.225999000
C	-3.116772000	-1.068653000	1.365948000
C	-3.724871000	1.103742000	-0.401291000
C	-3.632537000	-0.411265000	2.494043000
H	-3.663617000	0.675530000	2.520697000
C	-3.099719000	-2.468529000	1.327356000
H	-2.718917000	-2.965679000	0.440023000
C	7.090343000	1.723975000	1.420764000
H	7.320766000	2.689113000	1.861985000
C	0.258518000	-2.964617000	-3.170353000
H	0.345777000	-3.734763000	-3.932855000
C	3.721949000	-0.916456000	-0.900278000

H	4.404384000	-1.408539000	-1.573523000
C	2.347115000	-0.851161000	-0.843027000
C	1.260012000	-1.456139000	-1.620272000
C	6.492628000	-0.761158000	0.282883000
H	6.245153000	-1.734147000	-0.130218000
C	-5.729508000	2.948827000	-1.035513000
H	-6.509461000	3.665594000	-1.280133000
C	-4.402431000	3.369403000	-0.930952000
H	-4.144149000	4.412468000	-1.092768000
C	-3.397484000	2.450087000	-0.613938000
H	-2.365322000	2.780988000	-0.531434000
C	7.806837000	-0.450123000	0.633597000
H	8.591214000	-1.183573000	0.471755000
C	-6.059048000	1.604744000	-0.823043000
H	-7.092574000	1.277651000	-0.903685000
C	1.431700000	-2.454572000	-2.557778000
H	2.416522000	-2.840126000	-2.798567000
C	-3.591659000	-3.204536000	2.409145000
H	-3.581567000	-4.291028000	2.372036000
C	-4.101711000	-2.547609000	3.531332000
H	-4.484402000	-3.121186000	4.371626000
C	-4.123593000	-1.148934000	3.571193000
H	-4.526663000	-0.634434000	4.439712000

Table S8. B3LYP-D3/SDD, 6-31G* level optimized coordinates of the transition state species (**L5–TS1**).

0, 1

Zn	0.034057000	0.061889000	-0.434347000
P	2.440219000	-0.495202000	-0.166562000
N	-2.990573000	-0.629214000	-1.030376000
N	-4.018185000	-0.802339000	-0.198141000
N	-1.911858000	-0.822432000	-0.327143000

N	0.066525000	-0.983061000	1.405061000
N	2.434566000	-0.992450000	1.434266000
C	-5.345722000	-0.515572000	-0.639713000
C	-5.544926000	0.612957000	-1.439035000
H	-4.696822000	1.246835000	-1.688410000
C	-7.914012000	0.086699000	-1.466282000
H	-8.923034000	0.324252000	-1.791495000
C	1.256114000	-1.235945000	2.026520000
C	4.290995000	1.366917000	0.829392000
H	4.357714000	0.692785000	1.678224000
C	1.189189000	-1.784707000	3.352571000
H	2.120169000	-1.945948000	3.885015000
C	3.453752000	-1.722830000	-1.070083000
C	3.424473000	1.044528000	-0.224494000
C	4.012024000	-1.412953000	-2.319294000
H	3.897843000	-0.414100000	-2.732907000
C	3.628882000	-3.002810000	-0.528028000
H	3.214959000	-3.222070000	0.451707000
C	-6.845290000	0.901248000	-1.855038000
H	-7.022886000	1.775893000	-2.473739000
C	-0.030378000	-2.113988000	3.900632000
H	-0.070571000	-2.541374000	4.899516000
C	-3.598350000	-1.119785000	1.061846000
H	-4.287604000	-1.247453000	1.880685000
C	-2.224680000	-1.134175000	0.977177000
C	-1.123327000	-1.366782000	1.921299000
C	-6.395317000	-1.343841000	-0.240866000
H	-6.197206000	-2.222531000	0.366428000
C	4.918480000	3.409380000	-0.311661000
H	5.495647000	4.329787000	-0.343331000
C	4.048387000	3.094908000	-1.359410000
H	3.939605000	3.772228000	-2.202044000

C	3.293583000	1.921040000	-1.309922000
H	2.582581000	1.704014000	-2.103131000
C	-7.690188000	-1.031315000	-0.656997000
H	-8.519005000	-1.666533000	-0.358227000
C	5.032725000	2.548797000	0.784860000
H	5.700030000	2.799485000	1.605462000
C	-1.235164000	-1.934494000	3.175570000
H	-2.194504000	-2.244582000	3.575002000
C	4.352820000	-3.966605000	-1.234421000
H	4.491421000	-4.956905000	-0.808076000
C	4.903829000	-3.657728000	-2.480504000
H	5.467206000	-4.408581000	-3.028325000
C	4.735030000	-2.378295000	-3.020477000
H	5.170941000	-2.131466000	-3.985018000
Cl	-2.276865000	2.479642000	-1.117552000
O	0.324165000	2.028984000	-0.013039000
C	0.677440000	2.436675000	1.337066000
H	1.422171000	1.704738000	1.666214000
C	1.314410000	3.818272000	1.270988000
H	0.588838000	4.547057000	0.888282000
H	1.631737000	4.135145000	2.272409000
H	2.186829000	3.800315000	0.610912000
C	-0.552715000	2.379866000	2.238273000
H	-0.934411000	1.355741000	2.307267000
H	-0.295090000	2.724505000	3.247326000
H	-1.345326000	3.018486000	1.831081000
H	-0.548551000	2.465535000	-0.324769000

Table S9. B3LYP-D3/SDD, 6-31G* level optimized coordinates of the intermediate state (**L5**–**Int1**).

0, 1

Zn	0.167627000	0.487860000	-0.211639000

P	2.542475000	-0.247781000	-0.024935000
N	-3.045962000	-0.052309000	-0.909678000
N	-4.059863000	-0.507949000	-0.153166000
N	-1.946132000	-0.351795000	-0.279096000
N	0.083842000	-0.966244000	1.343965000
N	2.462220000	-1.117758000	1.415101000
C	-5.412051000	-0.336492000	-0.570727000
C	-5.701621000	-0.241498000	-1.934636000
H	-4.895504000	-0.293968000	-2.657124000
C	-8.051969000	-0.020963000	-1.381698000
H	-9.083243000	0.101660000	-1.699320000
C	1.257852000	-1.411053000	1.906603000
C	5.049637000	0.906408000	0.521413000
H	5.419540000	-0.114732000	0.552982000
C	1.144365000	-2.247910000	3.075900000
H	2.064868000	-2.552526000	3.561845000
C	3.469836000	-1.331375000	-1.174607000
C	3.693376000	1.145366000	0.243884000
C	4.009762000	-0.801212000	-2.357320000
H	3.921443000	0.263191000	-2.562367000
C	3.607536000	-2.698679000	-0.903620000
H	3.205965000	-3.092285000	0.025576000
C	-7.027994000	-0.077581000	-2.332068000
H	-7.260576000	-0.001197000	-3.390087000
C	-0.086763000	-2.660834000	3.521797000
H	-0.157359000	-3.306330000	4.393938000
C	-3.595207000	-1.104062000	0.981701000
H	-4.250439000	-1.551016000	1.710784000
C	-2.223819000	-0.998319000	0.898526000
C	-1.117182000	-1.435325000	1.755948000
C	-6.422075000	-0.267701000	0.392090000
H	-6.175598000	-0.307920000	1.448364000

C	5.430341000	3.288754000	0.698956000
H	6.106757000	4.122037000	0.873802000
C	4.082962000	3.528162000	0.422428000
H	3.707909000	4.547723000	0.380887000
C	3.207686000	2.460678000	0.193806000
H	2.154318000	2.643228000	-0.022035000
C	-7.745861000	-0.116863000	-0.021847000
H	-8.534744000	-0.061417000	0.722414000
C	5.914268000	1.975748000	0.749169000
H	6.963623000	1.789210000	0.963877000
C	-1.269386000	-2.278270000	2.838559000
H	-2.246091000	-2.644578000	3.136276000
C	4.276582000	-3.528056000	-1.808519000
H	4.386176000	-4.587559000	-1.590310000
C	4.809855000	-2.997810000	-2.985592000
H	5.330436000	-3.643899000	-3.687946000
C	4.676951000	-1.631533000	-3.257771000
H	5.097394000	-1.213632000	-4.168991000
O	0.049201000	2.356795000	-0.415704000
C	-0.945342000	3.212694000	0.076822000
H	-0.485639000	4.204326000	0.245218000
C	-2.077518000	3.392970000	-0.943677000
H	-2.586305000	2.435773000	-1.113106000
H	-2.817868000	4.128033000	-0.596201000
H	-1.663022000	3.735561000	-1.899092000
C	-1.503434000	2.736722000	1.428134000
H	-0.682711000	2.588056000	2.141256000
H	-2.212790000	3.459646000	1.854591000
H	-2.029533000	1.779770000	1.301800000

Table S10. B3LYP-D3/SDD, 6-31G* level optimized coordinates of the transition state species (**L5**–**TS2**).

0, 1

Zn	0.057378000	-0.397742000	-0.348588000
P	2.417967000	0.362095000	-0.053840000
N	-3.224259000	-0.618298000	0.035229000
N	-4.240176000	0.262314000	-0.031604000
N	-2.126792000	0.071511000	-0.083754000
N	-0.079082000	1.773908000	-0.349708000
N	2.298012000	2.007987000	-0.370918000
C	-5.591617000	-0.178710000	0.063426000
C	-5.921323000	-1.473240000	-0.347912000
H	-5.145406000	-2.126482000	-0.729886000
C	-8.234182000	-1.028470000	0.228248000
H	-9.266206000	-1.360746000	0.291525000
C	1.070214000	2.525478000	-0.452285000
C	4.089753000	0.470955000	-2.304346000
H	3.557678000	1.390913000	-2.528337000
C	0.914883000	3.944190000	-0.657064000
H	1.820668000	4.531910000	-0.759298000
C	3.114440000	0.187311000	1.630856000
C	3.785958000	-0.216940000	-1.122247000
C	2.761672000	-0.923552000	2.410656000
H	2.035843000	-1.638287000	2.029402000
C	4.004504000	1.147421000	2.135773000
H	4.243831000	2.015699000	1.528071000
C	-7.247726000	-1.893086000	-0.255910000
H	-7.510637000	-2.898065000	-0.572690000
C	-0.332875000	4.514089000	-0.700522000
H	-0.434482000	5.587145000	-0.844225000
C	-3.775425000	1.533322000	-0.195995000
H	-4.433010000	2.380397000	-0.300157000
C	-2.403216000	1.403727000	-0.229355000
C	-1.300298000	2.356954000	-0.387495000

C	-6.563549000	0.692647000	0.561538000
H	-6.284533000	1.682965000	0.907313000
C	5.775306000	-1.184379000	-2.843848000
H	6.546833000	-1.559169000	-3.511695000
C	5.478546000	-1.870231000	-1.661601000
H	6.022704000	-2.775724000	-1.404868000
C	4.489142000	-1.388805000	-0.803247000
H	4.274179000	-1.910474000	0.126340000
C	-7.889003000	0.262966000	0.634490000
H	-8.647873000	0.936430000	1.021789000
C	5.082297000	-0.012858000	-3.160397000
H	5.317971000	0.528523000	-4.073438000
C	-1.493204000	3.714812000	-0.552913000
H	-2.489463000	4.144079000	-0.567785000
C	4.551993000	0.986520000	3.408370000
H	5.240991000	1.730490000	3.801006000
C	4.215051000	-0.131906000	4.180521000
H	4.643989000	-0.255230000	5.172056000
C	3.320298000	-1.082247000	3.683571000
H	3.046148000	-1.942150000	4.289796000
O	0.042079000	-2.150920000	0.896307000
C	-0.010960000	-2.851511000	-0.171389000
C	-1.318685000	-3.532293000	-0.528884000
C	1.259964000	-3.523919000	-0.659101000
H	-0.073598000	-1.685668000	-1.539564000
H	-2.159911000	-2.870238000	-0.311258000
H	-1.337146000	-3.844096000	-1.577604000
H	-1.403953000	-4.426463000	0.109253000
H	2.101106000	-2.826474000	-0.619421000
H	1.470854000	-4.362501000	0.022938000
H	1.150259000	-3.910013000	-1.676845000

Table S11. B3LYP-D3/SDD, 6-31G* level optimized coordinates of the intermediate state (**L5**–**Int2**).

0, 1

Zn	-0.013638000	-0.945919000	-0.101957000
P	-2.389471000	-0.010888000	0.078477000
N	3.242333000	-0.740988000	0.715159000
N	4.262153000	-0.085201000	0.127589000
N	2.145134000	-0.209082000	0.258376000
N	0.108076000	0.989833000	-1.024319000
N	-2.259153000	1.298289000	-0.970376000
C	5.613533000	-0.430934000	0.417698000
C	5.918130000	-1.737089000	0.811326000
H	5.122625000	-2.468475000	0.894847000
C	8.255174000	-1.107378000	0.960558000
H	9.286912000	-1.372891000	1.171700000
C	-1.040997000	1.674688000	-1.357408000
C	-3.479325000	1.996144000	1.718680000
H	-2.999792000	2.680138000	1.024584000
C	-0.890244000	2.868267000	-2.152407000
H	-1.797649000	3.368836000	-2.472075000
C	-3.541655000	-1.179219000	-0.737411000
C	-3.393247000	0.618460000	1.481127000
C	-3.461340000	-2.549560000	-0.455723000
H	-2.682862000	-2.920701000	0.206628000
C	-4.514156000	-0.708379000	-1.632800000
H	-4.545551000	0.352903000	-1.861676000
C	7.244776000	-2.065630000	1.087491000
H	7.488995000	-3.078360000	1.394420000
C	0.356506000	3.359409000	-2.447648000
H	0.456512000	4.271806000	-3.030628000
C	3.801366000	0.876029000	-0.722077000
H	4.460590000	1.485076000	-1.318315000

C	2.428297000	0.791466000	-0.635081000
C	1.329407000	1.533886000	-1.258380000
C	6.610017000	0.541262000	0.298645000
H	6.350506000	1.558550000	0.022901000
C	-4.831252000	1.580245000	3.685922000
H	-5.389335000	1.953101000	4.541059000
C	-4.750685000	0.203854000	3.448458000
H	-5.250417000	-0.494643000	4.115025000
C	-4.034487000	-0.275887000	2.351579000
H	-3.988405000	-1.345328000	2.159028000
C	7.934798000	0.193730000	0.564889000
H	8.712876000	0.945952000	0.474122000
C	-4.197390000	2.473390000	2.818529000
H	-4.266176000	3.544198000	2.994549000
C	1.517150000	2.704802000	-1.965791000
H	2.510134000	3.112659000	-2.121905000
C	-5.407824000	-1.601307000	-2.223963000
H	-6.160765000	-1.235089000	-2.917623000
C	-5.336914000	-2.967295000	-1.926346000
H	-6.034274000	-3.660907000	-2.389548000
C	-4.363140000	-3.441356000	-1.044580000
H	-4.295457000	-4.503732000	-0.824879000
H	0.183966000	-2.531762000	-0.437382000

Table S12. B3LYP-D3/SDD, 6-31G* level optimized coordinates of the transition state species (**L5**–**TS3**).

0,1

Zn	0.245034000	0.045104000	-0.253204000
P	-2.021395000	1.062846000	-0.009999000
N	3.500157000	-0.623736000	-0.219222000
N	4.616986000	0.122254000	-0.124661000
N	2.496728000	0.203715000	-0.170924000

N	0.671596000	2.157854000	0.008226000
N	-1.656874000	2.701994000	0.087834000
C	5.903570000	-0.489083000	-0.137161000
C	6.048038000	-1.793939000	0.342500000
H	5.179636000	-2.325336000	0.714380000
C	8.420735000	-1.668937000	-0.141573000
H	9.403931000	-2.130304000	-0.141762000
C	-0.371751000	3.056035000	0.081353000
C	-4.303930000	0.426201000	1.578850000
H	-4.899133000	0.551710000	0.679811000
C	-0.033730000	4.456886000	0.159510000
H	-0.857244000	5.160733000	0.210371000
C	-3.286365000	0.917621000	-1.317668000
C	-2.919835000	0.634922000	1.529401000
C	-3.652859000	-0.357829000	-1.774422000
H	-3.178014000	-1.241962000	-1.363112000
C	-3.892501000	2.056074000	-1.865641000
H	-3.586412000	3.034518000	-1.507090000
C	7.313176000	-2.380011000	0.330572000
H	7.433430000	-3.393816000	0.700975000
C	1.275698000	4.864341000	0.175143000
H	1.514368000	5.923338000	0.238387000
C	4.312619000	1.446671000	-0.018371000
H	5.068730000	2.205445000	0.097998000
C	2.934802000	1.493296000	-0.051126000
C	1.957765000	2.583387000	0.026132000
C	6.998086000	0.229926000	-0.624099000
H	6.860419000	1.230176000	-1.022571000
C	-4.150687000	-0.136713000	3.930251000
H	-4.626949000	-0.441798000	4.858613000
C	-2.768183000	0.075556000	3.888443000
H	-2.166585000	-0.068671000	4.782171000

C	-2.156223000	0.454281000	2.694008000
H	-1.076840000	0.575783000	2.655744000
C	8.260167000	-0.364782000	-0.616509000
H	9.114194000	0.189569000	-0.994351000
C	-4.915918000	0.040676000	2.774963000
H	-5.990968000	-0.120165000	2.803272000
C	2.323310000	3.912375000	0.110444000
H	3.367034000	4.208233000	0.124400000
C	-4.865960000	1.916976000	-2.858469000
H	-5.334582000	2.801197000	-3.283775000
C	-5.239036000	0.645303000	-3.303892000
H	-5.996879000	0.540450000	-4.076558000
C	-4.631161000	-0.491134000	-2.760310000
H	-4.911110000	-1.483277000	-3.105209000
O	0.178247000	-1.540316000	1.160934000
H	0.118944000	-1.372068000	-1.302520000
C	-0.001316000	-2.356520000	0.189237000
C	1.147737000	-3.272784000	-0.193679000
H	1.006129000	-3.739170000	-1.171933000
H	2.083139000	-2.709750000	-0.181549000
H	1.196430000	-4.065078000	0.569165000
C	-1.400760000	-2.845023000	-0.077109000
C	-1.742006000	-3.554539000	-1.238860000
C	-2.390092000	-2.584856000	0.879505000
C	-3.048606000	-3.996109000	-1.437217000
H	-0.990160000	-3.725852000	-2.003193000
C	-3.700331000	-3.028678000	0.682312000
H	-2.121860000	-2.026651000	1.767696000
C	-4.032922000	-3.735341000	-0.474300000
H	-3.304697000	-4.535143000	-2.345810000
H	-4.457096000	-2.801002000	1.427331000
H	-5.053254000	-4.074452000	-0.634298000

Table S13. B3LYP-D3/SDD, 6-31G* level optimized coordinates of the intermediate state (**L5**–**Int3**).

0, 1

Zn	-0.353145000	-0.243409000	0.095928000
P	-2.827019000	-0.439406000	0.022137000
N	2.748421000	-0.874905000	0.843705000
N	3.638759000	-1.668022000	0.227170000
N	1.568161000	-1.328145000	0.534980000
N	-0.637975000	-2.215282000	-0.677041000
N	-3.005068000	-1.928158000	-0.729522000
C	5.031225000	-1.369927000	0.296441000
C	5.432635000	-0.031204000	0.288057000
H	4.690174000	0.756967000	0.223596000
C	7.738180000	-0.774311000	0.394495000
H	8.798318000	-0.540818000	0.432142000
C	-1.907606000	-2.655350000	-0.963170000
C	-4.860154000	1.114804000	-1.197183000
H	-5.555001000	0.582221000	-0.554566000
C	-2.032132000	-3.971536000	-1.534526000
H	-3.027615000	-4.305587000	-1.805692000
C	-4.018090000	-0.439903000	1.405668000
C	-3.485580000	0.845079000	-1.108211000
C	-4.249612000	0.743210000	2.126115000
H	-3.753221000	1.664553000	1.829516000
C	-4.669706000	-1.620711000	1.782941000
H	-4.489352000	-2.523825000	1.207391000
C	6.795508000	0.257814000	0.345342000
H	7.117969000	1.294914000	0.336995000
C	-0.924629000	-4.766273000	-1.703841000
H	-1.033879000	-5.762111000	-2.126505000
C	3.014507000	-2.649758000	-0.484588000

H	3.558785000	-3.355635000	-1.090779000
C	1.669314000	-2.420623000	-0.287395000
C	0.436526000	-3.033233000	-0.795628000
C	5.956502000	-2.413545000	0.350517000
H	5.614286000	-3.443843000	0.378092000
C	-4.436627000	2.757814000	-2.924112000
H	-4.806120000	3.502251000	-3.624920000
C	-3.067378000	2.493010000	-2.841051000
H	-2.366328000	3.031562000	-3.473329000
C	-2.589827000	1.542766000	-1.935364000
H	-1.520114000	1.359977000	-1.858817000
C	7.317686000	-2.107238000	0.393198000
H	8.046580000	-2.911186000	0.436759000
C	-5.332130000	2.067897000	-2.100697000
H	-6.398016000	2.272499000	-2.162803000
C	0.358631000	-4.312698000	-1.307952000
H	1.237183000	-4.944910000	-1.378739000
C	-5.547166000	-1.616856000	2.871263000
H	-6.054955000	-2.534373000	3.158010000
C	-5.775581000	-0.438803000	3.586098000
H	-6.457401000	-0.438472000	4.432679000
C	-5.125976000	0.742813000	3.210852000
H	-5.304012000	1.662198000	3.762683000
O	0.506355000	1.255458000	-0.661772000
C	0.347523000	2.614422000	-0.407259000
H	-0.066156000	3.121540000	-1.301556000
C	-0.641332000	2.885618000	0.745970000
H	-0.264947000	2.410226000	1.663607000
H	-0.759971000	3.959532000	0.939607000
H	-1.622468000	2.461940000	0.496898000
C	1.680834000	3.285099000	-0.085166000
C	1.918137000	4.615492000	-0.446958000

C	2.667896000	2.596065000	0.630979000
C	3.113616000	5.252280000	-0.101222000
H	1.158180000	5.154739000	-1.010258000
C	3.861757000	3.229870000	0.984264000
H	2.492840000	1.559099000	0.895420000
C	4.091287000	4.560550000	0.618512000
H	3.282858000	6.285176000	-0.396771000
H	4.613764000	2.684110000	1.551483000
H	5.021914000	5.052714000	0.890763000

Table S14. B3LYP-D3/SDD, 6-31G* level optimized coordinates of the reactant species (**L3**–**R**).

0,1

Zn	1.902589000	-1.268148000	0.079863000
Cl	2.281701000	-2.089693000	-1.977509000
N	-1.322870000	-0.813430000	0.124368000
N	-2.133114000	0.257477000	0.024040000
N	-0.106398000	-0.361630000	0.086789000
N	2.272589000	0.928962000	-0.069172000
C	-3.551311000	0.098012000	0.022293000
C	-4.104107000	-1.081550000	-0.482756000
H	-3.452287000	-1.860540000	-0.861346000
C	-6.310982000	-0.200513000	-0.001187000
H	-7.390507000	-0.318113000	-0.010987000
C	3.484236000	1.491693000	-0.121309000
C	3.664555000	2.872126000	-0.215183000
H	4.665257000	3.288555000	-0.256014000
C	-5.491142000	-1.224724000	-0.484908000
H	-5.930649000	-2.138138000	-0.874102000
C	2.533827000	3.689717000	-0.253344000
H	2.634534000	4.768722000	-0.325383000
C	-1.414033000	1.408515000	-0.077136000

H	-1.882395000	2.371766000	-0.196490000
C	-0.097900000	1.000037000	-0.034208000
C	1.177121000	1.715924000	-0.103186000
C	-4.354473000	1.125813000	0.521640000
H	-3.903446000	2.018920000	0.943005000
C	-5.741002000	0.972774000	0.499926000
H	-6.372479000	1.766207000	0.888282000
C	1.268748000	3.107043000	-0.195410000
H	0.369091000	3.713862000	-0.218464000
Cl	2.571577000	-1.810507000	2.153221000
H	4.326811000	0.807743000	-0.085058000

Table S15. B3LYP-D3/SDD, 6-31G* level optimized coordinates of the transition state species (**L3**–**TS1**).

0,1

Zn	1.567588000	-0.390040000	0.812965000
N	-1.627528000	-0.452354000	0.864014000
N	-2.560096000	0.319501000	0.282364000
N	-0.501840000	0.188696000	0.752189000
N	1.667346000	1.669668000	0.138839000
C	-3.918308000	-0.110084000	0.213634000
C	-4.196911000	-1.474539000	0.104872000
H	-3.380166000	-2.186472000	0.072255000
C	-6.561243000	-0.940775000	0.054169000
H	-7.595216000	-1.266808000	-0.009664000
C	2.793416000	2.363710000	-0.048589000
C	2.790415000	3.646559000	-0.596374000
H	3.724841000	4.176505000	-0.745976000
C	-5.528108000	-1.882904000	0.032069000
H	-5.756207000	-2.941040000	-0.053848000
C	1.565555000	4.219724000	-0.941022000
H	1.524908000	5.216266000	-1.370898000

C	-2.017930000	1.470363000	-0.202962000
H	-2.598113000	2.192515000	-0.753204000
C	-0.679586000	1.375845000	0.098539000
C	0.478994000	2.222675000	-0.181707000
C	-4.937514000	0.843943000	0.247654000
H	-4.697326000	1.896534000	0.362276000
C	-6.263946000	0.420531000	0.159481000
H	-7.063046000	1.155357000	0.185772000
C	0.388376000	3.505070000	-0.721106000
H	-0.580928000	3.927745000	-0.964383000
Cl	0.692652000	-0.387610000	-2.329742000
O	1.498587000	-2.159668000	-0.183463000
C	2.727073000	-2.901996000	-0.440279000
H	3.033122000	-3.276741000	0.540681000
C	2.397139000	-4.054779000	-1.380790000
H	2.055116000	-3.659668000	-2.345497000
H	3.288326000	-4.670965000	-1.551179000
H	1.606619000	-4.683203000	-0.955989000
C	3.795116000	-1.967157000	-1.004285000
H	4.059642000	-1.202691000	-0.262294000
H	4.704240000	-2.531510000	-1.246110000
H	3.418512000	-1.480176000	-1.911347000
H	1.147196000	-1.799489000	-1.070982000
H	3.709057000	1.866236000	0.257139000
Cl	3.103978000	-0.450599000	2.463879000

Table S16. B3LYP-D3/SDD, 6-31G* level optimized coordinates of the intermediate species (**L3**–**Int1**).

0,1

Zn	1.862604000	-1.070842000	0.564725000
N	-1.382533000	-0.659038000	0.245277000
N	-2.198410000	0.398754000	0.065127000

N	-0.168382000	-0.202740000	0.208378000
N	2.202626000	1.114592000	0.111905000
C	-3.614943000	0.231437000	0.062127000
C	-4.179789000	-0.810685000	0.802014000
H	-3.537155000	-1.478096000	1.364656000
C	-6.373982000	-0.082364000	0.071345000
H	-7.452945000	-0.205541000	0.075825000
C	3.409036000	1.685057000	0.043469000
C	3.581081000	3.046047000	-0.213165000
H	4.578405000	3.470402000	-0.258222000
C	-5.565675000	-0.964035000	0.795474000
H	-6.013713000	-1.771713000	1.366396000
C	2.445635000	3.834595000	-0.407016000
H	2.539017000	4.897801000	-0.608442000
C	-1.482907000	1.545631000	-0.090674000
H	-1.954638000	2.506534000	-0.215435000
C	-0.165670000	1.148410000	0.001972000
C	1.104140000	1.872113000	-0.078559000
C	-4.406527000	1.113404000	-0.677300000
H	-3.946159000	1.895257000	-1.273519000
C	-5.792563000	0.955113000	-0.662279000
H	-6.414447000	1.635842000	-1.235949000
C	1.185530000	3.242323000	-0.341541000
H	0.282425000	3.825401000	-0.492535000
O	2.650785000	-2.057584000	-0.820696000
C	2.024661000	-2.296389000	-2.045140000
H	2.716875000	-2.884739000	-2.676295000
C	0.739986000	-3.123434000	-1.874055000
H	0.001707000	-2.552313000	-1.292088000
H	0.285886000	-3.384509000	-2.841074000
H	0.966026000	-4.046739000	-1.328037000
C	1.717956000	-0.990062000	-2.800607000

H	2.631743000	-0.391111000	-2.898937000
H	1.310398000	-1.182108000	-3.803488000
H	0.978629000	-0.399703000	-2.239291000
H	4.255521000	1.023141000	0.201230000
Cl	2.044653000	-1.139752000	2.814578000

Table S17. B3LYP-D3/SDD, 6-31G* level optimized coordinates of the transition state species (**L3**–**TS2**).

0,1

Zn	1.705115000	-0.876283000	0.380905000
N	-1.651224000	-0.846136000	-0.142161000
N	-2.584635000	0.131927000	-0.171593000
N	-0.496038000	-0.259936000	-0.115573000
N	1.716933000	1.312163000	-0.020878000
C	-3.972907000	-0.188190000	-0.211041000
C	-4.378370000	-1.404269000	-0.767976000
H	-3.633176000	-2.090381000	-1.153294000
C	-6.682003000	-0.802055000	-0.310083000
H	-7.740318000	-1.042684000	-0.349047000
C	2.854876000	2.020587000	-0.016107000
C	2.861780000	3.414722000	-0.084333000
H	3.804036000	3.952396000	-0.074458000
C	-5.738968000	-1.706176000	-0.808156000
H	-6.061535000	-2.650294000	-1.236978000
C	1.642132000	4.088443000	-0.160180000
H	1.610225000	5.173160000	-0.211173000
C	-1.999969000	1.360235000	-0.162196000
H	-2.572379000	2.272352000	-0.204039000
C	-0.646693000	1.097445000	-0.123444000
C	0.534595000	1.958790000	-0.102642000
C	-4.901539000	0.719406000	0.304671000
H	-4.566721000	1.641989000	0.768439000

C	-6.260375000	0.408933000	0.244819000
H	-6.986411000	1.109725000	0.646214000
C	0.458582000	3.352343000	-0.173818000
H	-0.507655000	3.842642000	-0.239745000
O	3.916393000	-0.736884000	0.008234000
C	3.707646000	-1.552027000	-0.950209000
C	4.143156000	-2.998528000	-0.776276000
C	3.754525000	-1.017993000	-2.376877000
H	2.043201000	-1.914465000	-0.985655000
H	3.892259000	-3.343553000	0.230294000
H	3.688213000	-3.655002000	-1.524741000
H	5.237959000	-3.026606000	-0.890791000
H	3.248718000	-0.049282000	-2.431198000
H	4.813462000	-0.872059000	-2.641066000
H	3.302324000	-1.714965000	-3.089306000
H	3.755617000	1.415986000	0.033562000
Cl	1.354913000	-1.278914000	2.579676000

Table S18. B3LYP-D3/SDD, 6-31G* level optimized coordinates of the intermediate species (**L3**–**Int2**).

0,1

Zn	-2.048596000	-1.697860000	-0.538465000
N	1.171072000	-0.916153000	-0.398296000
N	1.876076000	0.203442000	-0.130791000
N	-0.079512000	-0.571769000	-0.427225000
N	-2.568935000	0.536055000	-0.401398000
C	3.297882000	0.162673000	-0.032931000
C	4.005370000	-0.804083000	-0.752398000
H	3.465762000	-1.513370000	-1.369221000
C	6.069850000	0.097659000	0.144046000
H	7.153353000	0.071410000	0.212799000
C	-3.817458000	1.012007000	-0.385922000

C	-4.110464000	2.353198000	-0.135647000
H	-5.140019000	2.695100000	-0.131245000
C	5.395883000	-0.832755000	-0.652878000
H	5.953260000	-1.582366000	-1.206608000
C	-3.051576000	3.228694000	0.111348000
H	-3.237940000	4.279613000	0.312937000
C	1.050543000	1.275324000	0.011869000
H	1.422849000	2.268191000	0.204179000
C	-0.216457000	0.765802000	-0.179484000
C	-1.544933000	1.378367000	-0.158531000
C	3.954872000	1.090502000	0.778918000
H	3.385890000	1.809701000	1.359754000
C	5.347387000	1.057537000	0.857499000
H	5.863886000	1.774358000	1.488895000
C	-1.747666000	2.737586000	0.100844000
H	-0.901482000	3.389502000	0.294377000
H	-2.433390000	-2.386771000	-1.962823000
H	-4.603650000	0.286654000	-0.575753000
Cl	-2.356525000	-2.120724000	1.693542000

Table S19. B3LYP-D3/SDD, 6-31G* level optimized coordinates of the transition state species (**L3**–**TS3**).

0,1

Zn	1.057488000	0.203366000	0.394120000
N	-2.093356000	-0.948156000	-0.099855000
N	-3.308841000	-0.360070000	-0.167780000
N	-1.216849000	0.006087000	-0.083955000
N	0.305359000	2.250457000	-0.031418000
C	-4.496507000	-1.147135000	-0.209207000
C	-4.441868000	-2.438969000	-0.739702000
H	-3.497915000	-2.828511000	-1.102772000
C	-6.817460000	-2.672615000	-0.313688000

H	-7.723893000	-3.269374000	-0.354796000
C	1.128095000	3.308331000	-0.044807000
C	0.652579000	4.615905000	-0.157265000
H	1.349902000	5.447009000	-0.161268000
C	-5.610084000	-3.198921000	-0.782843000
H	-5.575147000	-4.204579000	-1.191131000
C	-0.723740000	4.822440000	-0.260076000
H	-1.128277000	5.826955000	-0.346676000
C	-3.191225000	0.995078000	-0.193964000
H	-4.045752000	1.647346000	-0.269759000
C	-1.832567000	1.224209000	-0.137136000
C	-1.026166000	2.443927000	-0.138525000
C	-5.691739000	-0.612077000	0.277642000
H	-5.708113000	0.378532000	0.721299000
C	-6.854930000	-1.379946000	0.215237000
H	-7.786380000	-0.969926000	0.594223000
C	-1.579310000	3.721906000	-0.254644000
H	-2.654424000	3.845023000	-0.340335000
O	3.053377000	1.063199000	0.054895000
H	1.752483000	-0.656178000	-0.986010000
C	3.205492000	0.178296000	-0.863530000
C	3.183227000	0.661896000	-2.308882000
H	2.970107000	-0.140487000	-3.020236000
H	2.424563000	1.443532000	-2.403889000
H	4.167792000	1.095263000	-2.538745000
C	4.047884000	-1.029523000	-0.538286000
C	4.645454000	-1.823488000	-1.526552000
C	4.256698000	-1.344573000	0.813100000
C	5.441501000	-2.914576000	-1.171028000
H	4.495110000	-1.594263000	-2.576832000
C	5.042148000	-2.439815000	1.166565000
H	3.784076000	-0.728162000	1.570870000

C	5.639833000	-3.226922000	0.176068000
H	5.904535000	-3.520237000	-1.946165000
H	5.188069000	-2.680534000	2.216385000
H	6.255156000	-4.079469000	0.452938000
H	2.181857000	3.056040000	0.026557000
Cl	0.930973000	-0.339607000	2.589636000

Table S20. B3LYP-D3/SDD, 6-31G* level optimized coordinates of the intermediate species (**L3**–**Int3**).

0,1

Zn	1.940895000	-0.420484000	0.415580000
N	-1.238685000	0.250713000	0.549416000
N	-2.001606000	1.284070000	0.143204000
N	-0.005071000	0.625787000	0.414732000
N	2.425380000	1.695593000	-0.120043000
C	-3.423401000	1.170906000	0.138741000
C	-3.999925000	-0.089986000	-0.035801000
H	-3.363046000	-0.959795000	-0.158777000
C	-6.188777000	0.947875000	0.102242000
H	-7.271190000	0.859522000	0.087470000
C	3.661783000	2.166609000	-0.308571000
C	3.910099000	3.478658000	-0.714393000
H	4.929412000	3.820841000	-0.857851000
C	-5.390654000	-0.190772000	-0.046606000
H	-5.850951000	-1.165376000	-0.180607000
C	2.821259000	4.325936000	-0.926227000
H	2.974456000	5.354113000	-1.241176000
C	-1.232826000	2.335074000	-0.253667000
H	-1.657730000	3.244489000	-0.646197000
C	0.063412000	1.900874000	-0.074668000
C	1.370419000	2.512651000	-0.319665000
C	-4.203155000	2.317984000	0.301804000

H	-3.732768000	3.282018000	0.470212000
C	-5.593226000	2.200175000	0.275028000
H	-6.207791000	3.086378000	0.402728000
C	1.530199000	3.840706000	-0.724304000
H	0.661900000	4.475323000	-0.871312000
O	2.115414000	-1.235330000	-1.278043000
C	1.711317000	-2.550988000	-1.529047000
H	1.584556000	-2.675597000	-2.620867000
C	2.779311000	-3.557796000	-1.071609000
H	2.939285000	-3.478592000	0.011286000
H	2.494877000	-4.592163000	-1.309961000
H	3.726310000	-3.321549000	-1.570281000
C	0.351001000	-2.846912000	-0.895065000
C	-0.805942000	-2.901521000	-1.680929000
C	0.217925000	-2.999284000	0.495543000
C	-2.061954000	-3.114562000	-1.104307000
H	-0.713346000	-2.782998000	-2.758685000
C	-1.033928000	-3.196922000	1.079800000
H	1.100851000	-2.971732000	1.131334000
C	-2.179658000	-3.263796000	0.280711000
H	-2.946119000	-3.169396000	-1.736606000
H	-1.112562000	-3.310513000	2.157950000
H	-3.153392000	-3.434973000	0.734302000
H	4.469011000	1.464031000	-0.124022000
Cl	2.817547000	-0.772321000	2.470163000

Refrences-

1. L. Radhakrishna, B. S. Kote, H. S. Kunchur, M. K. Pandey, D. Mondal and M. S. Balakrishna, *Dalton Trans.*, **2022**, *51*, 5480-5493.
2. S. Sheokand and M. S. Balakrishna, *Inorg. Chem.*, **2023**, *62*, 12317-12328.
3. Z. Li, C. Brouwer and C. He, *Chem. Rev.*, **2008**, *108*, 3239-3265.
4. O. V. Dolomanov, L. J. Bourhis, R. J. Gildea, J. A. K. Howard and H. Puschmann, *J. Appl. Cryst.*, **2009**, *42*, 339-341.
5. G. Sheldrick, *Acta Cryst.*, **2015**, *71*, 3-8.
6. a) A. D. Becke, *J. Chem. Phys.* , **1997**, *107*, 8554-8560; b) J. Antony and S. Grimme, *Phys. Chem. Chem. Phys.*, **2006**, *8*, 5287-5293; c) M. J. Frisch, G. W. Trucks, H. B. Schlegel, G. E. Scuseria, M. A. Robb, J. R. Cheeseman, G. Scalmani, V. Barone, B. Mennucci and G. Petersson, *See also: URL: http://www. gaussian. com*, **2009**.
7. a) L. E. Roy, P. J. Hay and R. L. Martin, *J. Chem. Theory Comput.*, **2008**, *4*, 1029-1031; b) A. V. Mitin, J. Baker and P. Pulay, *J. Chem. Phys.* , **2003**, *118*, 7775-7782; c) A. D. Becke, *J. Chem. Phys.*, **1997**, *107*, 8554-8560; d) A. D. Becke, *Phys. Rev. A*, **1988**, *38*, 3098-3100.
8. M. R. Silva-Junior, M. Schreiber, S. P. A. Sauer and W. Thiel, *J. Chem. Phys.*, **2010**, *133*.
9. J. Tomasi, B. Mennucci and R. Cammi, *Chem. Rev.*, **2005**, *105*, 2999-3094.
10. R. Dennington, T. Keith and J. Millam, *Shawnee Mission, KS*, **2009**.
11. a) E. D. Glendening, C. R. Landis and F. Weinhold, *J. Comput. Chem.*, **2013**, *34*, 1429-1437; b) I. Mayer, *Theor. Chim. Acta*, **1985**, *67*, 315-322.
12. a) S. Kozuch, S. E. Lee and S. Shaik, *Organometallics*, **2009**, *28*, 1303-1308; b) S. Kozuch and S. Shaik, *Acc. Chem. Res.*, **2011**, *44*, 101-110.
13. D. Baidilov, D. Hayrapetyan and A. Y. Khalimon, *Tetrahedron*, **2021**, *98*, 132435.